Molecular mechanisms underlying light-modulated leaf nastic responses in Arabidopsis

Michaud Olivier

Michaud Olivier, 2018, Molecular mechanisms underlying light-modulated leaf nastic responses in Arabidopsis

Originally published at : Thesis, University of Lausanne

Posted at the University of Lausanne Open Archive http://serval.unil.ch
Document URN : urn:nbn:ch:serval-BIB_0C6F1E2B97239

UNIL | Université de Lausanne
Faculté de biologie
et de médecine

Centre Intégratif de Génomique

Molecular mechanisms underlying light-modulated leaf nastic responses in Arabidopsis

Thèse de doctorat ès sciences de la vie (PhD)

présentée à la
Faculté de biologie et de médecine
de l'Université de Lausanne
par

Olivier MICHAUD

Master de l'Université de Lausanne

Jury

Prof. Jérôme Goudet, Président
Prof. Christian Fankhauser, Directeur de thèse
Prof. Ioannis Xenarios, Co-directeur de thèse
Prof. Edward Farmer, Expert
Prof. François Tardieu, Expert

Lausanne 2018

UNIL | Université de Lausanne
Faculté de biologie
et de médecine

Ecole Doctorale
Doctorat ès sciences de la vie

Imprimatur

Vu le rapport présenté par le jury d'examen, composé de

Président·e	Monsieur	Prof.	Jérôme **Goudet**
Directeur·trice de thèse	Monsieur	Prof.	Christian **Fankhauser**
Co-directeur·trice	Monsieur	Prof.	Ioannis **Xenarios**
Expert·e·s	Monsieur	Prof.	Edward **Farmer**
	Monsieur	Prof.	François **Tardieu**

le Conseil de Faculté autorise l'impression de la thèse de

Monsieur Olivier Michaud

Maîtrise universitaire ès Sciences en sciences moléculaires du vivant Université de Lausanne

intitulée

Molecular mechanisms underlying light-modulated leaf nastic responses in Arabidopsis

Lausanne, le 20 juillet 2018

pour le Doyen
de la Faculté de biologie et de médecine

Prof. Jérôme Goudet

“ There must be something behind the energy ”

Einstein

Remerciements

Tout d'abord, je tiens à remercier sincèrement Christian Fankhauser, mon superviseur de thèse, pour avoir accepté de me superviser tout au long de mes travaux de recherche, et ce, depuis ma maîtrise. Les qualités de superviseur, de scientifique et de conseiller que tu possèdes forment un cocktail qui est sans doute à la base de cette réussite qu'est ton groupe. Merci pour ta confiance en nos projets et pour nos discussions riches et stimulantes sur ces mécanismes fascinants qui permettent aux plantes de donner le meilleur d'elles-mêmes.

Je tiens également à remercier Ioannis Xenarios, mon co-superviseur de thèse, pour ses conseils avisés et pour le soutien qu'il nous a fourni, à l'aide de toute son équipe, tout au long de ces années passées à modéliser nos plantules d'Arabette. Je garderai particulièrement en mémoire la confiance que tu m'as accordée lors du passage de ma maîtrise à ma thèse, lorsque tu m'as demandé si je voulais continuer sur ce projet. Merci aussi pour ta personnalité et ta sympathie qui touchent.

Merci aux professeurs Jérôme Goudet, Edward Farmer et François Tardieu pour avoir accepté de faire partie de mon comité de thèse. Vos conseils et vos encouragements ont été précieux dans l'accomplissement de ce travail.

Un merci spécial à Tino Dornbusch, mon superviseur de projet de Master, pour le soutien qu'il a été dans le suivi de mon travail et dans le développement de cette plateforme de phénotypage. Merci pour cette belle collaboration que l'on a eu en début de doctorat et qui a porté ses fruits.

Bien évidemment, merci à tous les membres passés et présents du lab Fankhauser dont j'ai eu le plaisir de croiser la route: Séverine, Emilie, Tim, Tobias, Anupama, Bogna, Mieke, Markus, Perrine, Antoine, Cécile, Paolo, Yetkin, Prashant, Emanuel, Martial, Ana, Ganesh, Isabelle. Merci pour votre aide, vos conseils et pour l'ambiance de travail. Merci à Martine et Laure pour le soutien que vous apportez dans le fonctionnement du lab. Merci à Gilles Boss pour toutes les réalisations que tu as faites concernant nos projets quotidiens au labo. Merci à Corinne et Nathalie

qui font un travail de l'ombre impeccable. Un gros merci à Alessandra, Martina et Vinicius pour votre aide particulière dans les dernières étapes de cette thèse et pour l'élaboration de ce document. Une pensée spéciale à Fabien pour les superbes moments passés entre nos deux familles et qu'on doit absolument renouveler. A toi Anne-So, j'adresse un merci tout particulier pour ta collaboration, ta sympathie, ton efficacité et ton aide sans faille qui ont contribué à notre publication et à ce document. Finalement, une pensée à tous les gens du CIG, du DBMV, spécialement à Andrzej pour ton aide, à ceux de l'Eprouvette et à ceux que j'ai oubliés.

A côté du travail, il y a bien évidemment tout le reste. Je tiens à remercier profondément tous ceux qui m'ont soutenu, de près ou de loin, dans l'accomplissement de cette thèse et dans le quotidien en général.

A ma famille, frères, sœur, belle-sœur, nièces, futur(e) neveu ou nièce et grands-parents.

A ma belle-famille.

A mes amis, avec une pensée spéciale à Tim pour nos trips sur les atomes jusqu'à pas d'heure et pour ta curiosité sans pareille pour la nature qui nous entoure.

A mes parents, le fruit de mes études est avant tout le fruit de vos sacrifices.

A Chant, ma moitié, mon tout.

A notre rayon de soleil, Sofia.

Finalement, à Toi qui nous guide.

Table of contents

List of abbreviations

AAO	Abscisic aldehyde oxidase
ABA	*hormone:* Abscisic acid
ABA	*gene/protein:* ABA-deficient
ABC	ATP-binding cassette
ACC	1-aminocyclopropane-1-carboxylic acid
ACO	ACC oxidase
AFB	Auxin signaling F-box
AP2	Apetala 2
AQP	Aquaporin
Aux	Auxin-inducible
AUX1	Auxin resistant 1
ARF	Auxin response factor
BCH	β-carotenoid hydroxylase
BG	β-glucosidase
bHLH	Basic helix-loop-helix
BL	Blue light
BLUS1	Blue light signaling 1
BR	Brassinosteroid
BSC	Bundle sheath tissues
CMT	Cortical microtubule
cry	Cryptochrome
CYP707A	Cytochrome P450 707 A
d	Day
2,4-D	2,4-dichlorophenoxyacetic acid
DR5	Synthetic auxin-responsive promoter
E	Transpiration flow
EMS	Ethyl methanesulfonate
ERF	Ethylene responsive factor
FKF1	Flavin-binding kelch F-box 1
FR	Far-red light
GA	Gibberellin

GC	Stomata
GE	Glucosyl ester
Glc	Glucose
GUS	β-glucoronidase
GWAS	Genome-wide association study
HFR1	Long hypocotyl in far-red 1
HSD	Honestly significant difference
HY5	Elongated hypocotyl 5
IAA	*hormone:* Indole acetic acid
IAA	*gene/protein:* Indole-3-acetic acid-inducible
IPA	Indole-3-pyruvate
K^+	Potassium ion
K_{leaf}	Leaf hydraulic conductance
LAX	Like auxin resistant
LD	Long day (16-hour light period and 8-hour night period)
LKP2	LOV kelch protein 2
LOV	Light, oxygen and voltage sensing
L_{pr}	Root hydraulic conductance
MC	Mesophyll tissues
MoCo	Molybdenum cofactor
msg2	*massugu2*
n	Number of individuals
1-NAA	1-Naphthaleneacetic acid
NCED	9-cis-epoxycarotenoid dioxygenase
NPA	1-N-naphthylphthalamic acid
PAR	Photosynthetically active radiation
PAT	Polar auxin transport
PGP	P-glycoprotein
phot	Phototropin
phy	Phytochrome
Pfr	Far-red sensing phytochrome (active form)
PHR	Photolyase homology region
PIF	Phytochrome-interacting factor

PIL	Pin-like
PIP	Plasma membrane intrinsic protein
PKS4	Phytochrome kinase substrate 4
PP2C	Protein phosphatase 2C
Pr	Red sensing phytochrome (inactive form)
PYL	PYR1-like
PYR1	Pyrabactin resistance 1
RCAR	Regulatory component of ABA receptor
R:FR	Ratio between red light and far-red light
RL	Red light
ROS	Reactive oxygen species
SAS	Shade avoidance syndrome
SAV3	Shade avoidance 3
SDR	Short-chain dehydrogenase reductase
SHYG	Speedy hyponastic growth
SnRK2	SNF1-related protein kinase 2
t	Time
TAA1	Tryptophan aminotransferase of Arabidopsis 1
TIP	Tonoplast intrinsic protein
TIR1	Transport inhibitor response 1
Trp	Tryptophan
UGT	Uridine diphosphate glucosyltransferase
UVR8	UV-B resistance 8
VDE	Violaxanthin de-epoxidase
XTH	Xyloglucan endotransglucosylase/hydrolase
YUC	Yucca
ZEP	Zeaxanthin epoxidase
ZT	Zeitgeber (ZT0/ZT16 = start/end of the 16-hour light period)
ZTL	Zeitlupe

Résumé

La lumière est essentielle pour les plantes car elle leur permet non seulement de faire la photosynthèse mais aussi de s'informer sur leur environnement. Par exemple, la présence de compétiteurs induit des changements dans la qualité de l'environnement lumineux qui sont perçus par la plante grâce à des photorécepteurs appelés phytochromes. En cas de compétition, la plante déclenche une série de réponses physiologiques (appelées «syndrome d'évitement de l'ombre») telles que l'hyponastie foliaire qui consiste à réorienter ses feuilles vers le haut afin de favoriser l'accès à la lumière. Les acteurs clés de ce syndrome comme les PIF (Phytochrome Interacting Factors) et l'auxine sont connus, contrairement à la façon dont les événements de signalisation se succèdent jusqu'à l'hyponastie. De plus, un environnement compétitif est souvent caractérisé par des conditions de lumière hétérogènes pouvant entraîner un ombrage partiel de la plante et donc des réponses locales, mais les mécanismes à l'origine de ces réponses locales demeurent inconnus.

Dans ce travail, nous développons une approche se basant sur la technique à balayage laser qui permet d'analyser de façon non invasive la croissance et le mouvement des organes foliaires chez *Arabidopsis thaliana*. Cette approche nous a permis de décrire ces traits dans différentes conditions lumineuses et ainsi d'observer un découplage, dans certains cas, entre la croissance et le mouvement. Ensuite, nous explorons en détail les mécanismes impliqués dans la réponse hyponastique à l'ombre. Nous montrons d'abord que la perception de l'ombre se fait spécifiquement à la pointe de la feuille, là où est induite une production accrue d'auxine. L'auxine est ensuite transportée principalement dans les tissus vasculaires et ce, jusqu'au pétiole, où elle déclenche une suite d'évènements menant à l'hyponastie. Nous rapportons aussi le caractère local de l'hyponastie induite par l'ombre qui peut être expliqué par une restriction des signaux d'auxine à la feuille qui perçoit le signal. Finalement, nous observons également une augmentation de la production d'acide abscissique régulée par les PIF dans ces conditions et nous lui attribuons un nouveau rôle, potentiellement en aval de l'auxine, en montrant que sa biosynthèse et sa signalisation sont essentielles lors de la réponse hyponastique.

Summary

Light is essential for plants not only because it fuels photosynthesis but also because it acts as a signal informing plants about their surrounding environment. In presence of competitors, changes in light quality are sensed by the phytochrome photoreceptors and trigger a suite of plant adaptive responses known as the “shade-avoidance syndrome” (SAS). These responses include leaf hyponasty (upwards leaf reorientation) which allows to enhance plant access to sunlight. Several key SAS players such as the PIFs (phytochrome-interacting factors) and auxin have been studied in detail. Nevertheless, how SAS signaling events are integrated and lead to leaf hyponasty is still unknown. Moreover, competitive environments are often characterized by heterogeneous light conditions potentially leading to partial plant shading. Although it is well known that such a situation can trigger local plant adaptive responses, the mechanisms involved in these processes have remained elusive so far.

In this work we first develop a laser-scanning approach allowing the non-invasive monitoring of growth and movement in Arabidopsis leaf organs. We then report the patterns of leaf growth and movement in plants grown under different light regimes and conclude that, in certain conditions, these two processes are uncoupled. Afterwards, we explore the mechanisms leading to shade-induced leaf hyponasty. We find that shade signals are specifically perceived at the leaf tip where they trigger an increase in auxin production. Newly produced auxin is transported through vascular tissues down to the petiole where it induces downstream signaling events leading to hyponasty. We further demonstrate the local nature of the shade-induced leaf hyponasty and propose that this can be explained by auxin dynamics being restricted to the leaf perceiving the signal. Finally, we investigate abscisic acid (ABA) physiology during leaf adaptation to shade and show that shade signals induce an increase in ABA levels in a PIF4,5,7-dependent manner. In addition we establish a new role for ABA, potentially downstream of auxin, in shade-induced leaf hyponasty by highlighting the importance for ABA biosynthesis and signaling in the process.

General introduction

Perception of light signals is essential for plant survival

Light as a source of information and energy in plants

The survival of every living organism on earth depends on its ability to adapt to the conditions in its surrounding environment. Plants are sessile organisms and, contrary to most animals, they spend their whole life cycle at the unique location where they first germinated. Plants possess a remarkable developmental feature called phenotypic plasticity which allows them to optimize their growth in ever-changing environmental conditions imposed by their specific location. Such a trait enables plants to deal with important and fluctuating environmental biotic and abiotic factors like humidity, temperature and light. Mechanisms have evolved in plants for perceiving even slight variations in the quality, quantity and duration of those abiotic factors thereby permitting plants to adapt their growth consequently. For instance, being informed about the presence of competitors through the perception of changes in light quality in their surrounding environment allows plants to trigger physiological adaptations that might reduce the negative impact of future shade on their growth (1). Among the above-mentioned abiotic factors, light is particularly important as it is not only a factor influencing growth but also a direct source of energy fueling it. Indeed, a certain range of the solar spectrum called photosynthetically active radiation (PAR, $\lambda = 400$ - 700 nm) is absorbed by chlorophyll and other photosynthetic pigments located in the chloroplasts of aerial plant parts to enable the conversion of water and carbon dioxide into sugars and oxygen. This process happens mostly in leaves where sugar can be either used locally, exported as sucrose for plant biomass production or stocked as starch for the following night period (2). Excessive light incidence can however lead to irreversible damages of the photosynthetic apparatus and plants therefore need to continuously optimize light harvesting while avoiding photodamage (3).

Role of photoreceptors in plant adaptation and development

At a given location and throughout the life cycle of a plant, the quality, intensity and periodicity of natural light conditions can be highly variable and can change according to the time of the day and year but also to the potential development of nearby vegetation (4). In order to track such changes in light conditions plants have evolved multiple photoreceptors whose role is to transduce light cues into biological signals. Interpretation of the light signals by the plant further leads to adaptive developmental responses which are known as photomorphogenesis. As previous studies mainly focused on *Arabidopsis thaliana* as a plant model, we will therefore concentrate on what is known is this species. Several families of plant photoreceptors have been discovered so far comprising the UV-B sensing UV-B RESISTANCE 8 (UVR8), the blue/UV-A sensing Zeitlupe, cryptochrome and phototropin families as well as the red/far-red sensing phytochrome family (Fig. 1).

UVR8 is the only known plant photoreceptor allowing UV-B (λ = 280-315 nm) specific perception (Fig. 1A). Once activated by perception of UV-B, UVR8 modulates expression of target genes involved in a suite of photoprotective strategies such as production of reflective waxes and phenolic compounds in the leaf epidermal tissues serving as a “sun-screen” preventing the plant from suffering deleterious effects of UV-B on its organic components (Fig. 1B) (5, 6). In addition, UVR8 has recently been shown to play a role in other plant adaptations to light including hypocotyl bending during phototropism (organ bending towards a directional blue light signal) and stomatal movements in leaves (Fig. 1B,D) (7, 8).

UV-A/blue light (λ = 390-500 nm) perception in plants is confined to three photoreceptor families (Fig. 1A). The first one is the Zeitlupe family which comprises three members: Zeitlupe (ZTL), Flavin-binding Kelch F-box 1 (FKF1) and LOV Kelch Protein 2 (LKP2). Structurally Zeitlupes are characterized by the presence of one single photosensory LOV (Light, Oxygen and Voltage sensing) domain in their N-terminal region. Concerning their role in plant physiology, they are especially important in the control of biological timing processes such as photoperiod-dependent flowering (Fig. 1C) (9). The second family corresponds to the phototropins and is composed of two members, phot1 and phot2, each of them containing two LOV domains in their N-terminal part as well as a protein kinase

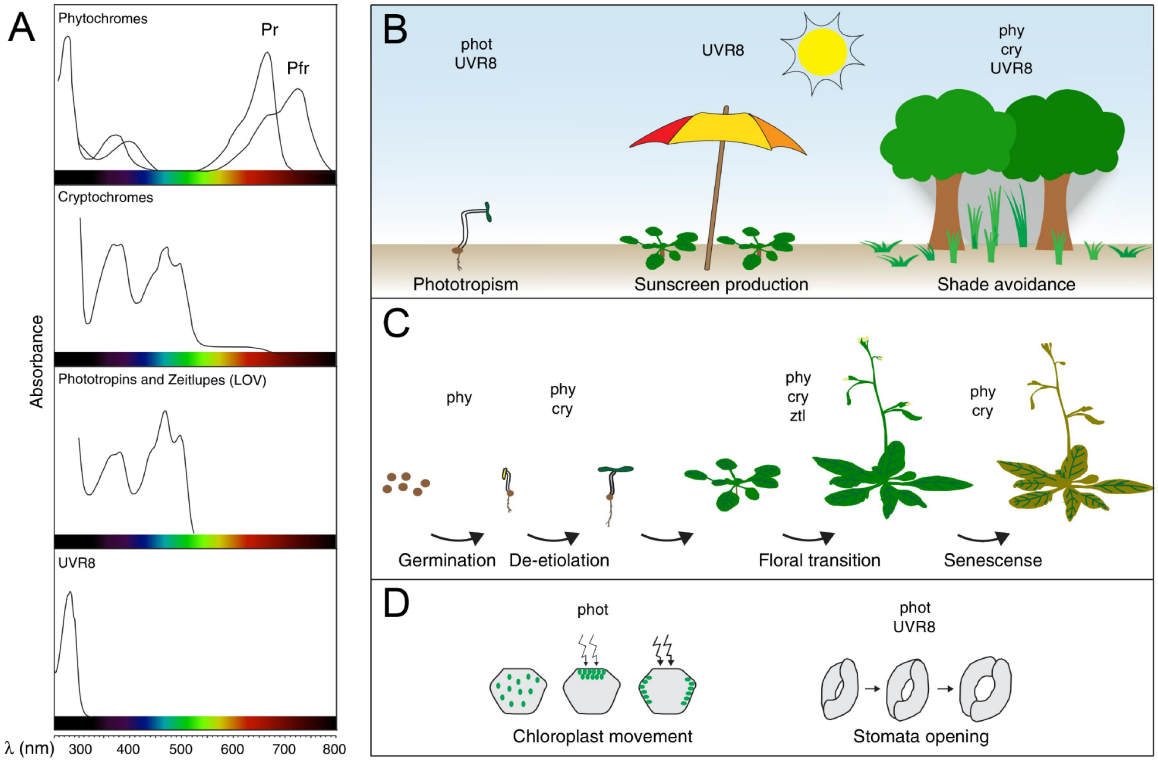

Figure 1. Light absorption spectrum of plant photoreceptors and their role in plant development and adaptation to the light environment

(adapted from Galvao and Fankhauser, 2015, Current Opinion in Neurobiology)

(A) Detailed absorption spectra for the different classes of plant photoreceptors. **(B)** The participation of photoreceptors in three major situations of plant adaptation to stressful light environmental conditions. Left: phototropic response in seedlings. Middle: adaptation to harmful UV-B emissions in rosette leaves. Right: competitive conditions triggering adaptive shade avoidance responses. **(C)** Life cycle of an Arabidopsis plant with illustrations of the major developmental transitions and the photoreceptors involved in those processes. From left to right: seed germination, seedling de-etiolation, vegetative growth of the rosette, induction of flowering, transition to senescence. **(D)** Two examples of cellular processes mediated by photoreceptors. Left: movement of chloroplasts towards light to favor light capture in limited light conditions (small arrows) and movement of chloroplasts away from strong light irradiance (large arrows) to avoid photodamage. Right: movement of the guard cells (increasing turgor) which results in the opening of the stomata.

domain in the C-terminal part. Blue light (BL) induces a conformational change in phototropins which triggers their autophosphorylation as well as phosphorylation of downstream signaling targets. Phototropins have important roles in plant adaptation responses leading to optimization of photosynthesis such as chloroplast and stomatal movement or promotion of differential growth such as phototropism (Fig. 1B,D) (10, 11). A role for phototropins in BL-mediated leaf flattening and leaf movement was also highlighted (12, 13). Only three direct targets of phototropins have been identified so far: a positive mediator of stomatal opening named BLUE LIGHT SIGNALING 1 (BLUS1) (14), the auxin efflux carrier ATP-BINDING CASSETTE B19 (ABCB19) (15) and the PHYTOCHROME KINASE SUBSTRATE 4 (PKS4), the two latter being involved in phototropic bending of the hypocotyl. The two cryptochromes cry1 and cry2 form the third family of UV-A/blue sensing photoreceptors. Unlike previously cited blue-sensing families, cryptochromes use a photolyase homology region (PHR) domain located in their N-terminal part for light sensing (11). Blue light activation of cryptochromes can lead to diverse photomorphogenic responses (16) (Fig. 1B,C). For instance, cryptochromes were shown to play an important role in seedling de-etiolation and photoperiod-controlled flowering (11, 17). A role is also attributed to these photoreceptors in BL-mediated shade avoidance responses in young seedlings and leaves (18, 19, 20). For instance, *cry* mutants were shown to be affected in BL-mediated leaf repositioning during shade avoidance (21).

Phytochrome photoreceptors are particularly known for their major role as red light (RL) and far-red light (FR) sensing photoreceptors. Phytochromes exist under two different states in the plant: they are produced under their red-absorbing (λ =~670 nm) inactive form but perception of red light rapidly switches them to their far red-absorbing (λ =~730 nm) active form, and inversely (22). This results in a permanent photoequilibrium in the plant where the amounts of active and inactive forms reflect the current red:far-red (R:FR) ratio in the plant surroundings. Mechanisms for degradation and thermal reversion of the active form of phytochromes allow the plant to avoid excessive active signaling in response to light cues (23). The phytochrome family comprises five members (phyA, phyB, phyC, phyD, phyE) which have both overlapping and distinct roles in many processes during plant development and adaptation like germination, seedling establishment, stomatal development,

flowering transition and shade avoidance (Fig. 1) (24, 25). While phyA and phyB are the most studied phytochromes, phyB is especially known for its predominant role in R:FR-mediated photomorphogenesis. The photolabile phyA has an antagonistic function to phyB but its role is mainly limited to early stages of seedling development (22). Phytochromes act as homo- or heterodimers. Their photosensory domain is located in the N-terminal region while their C-terminal region is essential for dimerization and interaction with downstream signaling targets. Among these targets, the PHYTOCHROME INTERACTING FACTORS (PIFs) are well known basic helix-loop-helix (bHLH) transcription factors involved in massive transcriptomic remodulation during many plant developmental processes such as adaptation to shade (26).

Shade avoidance response

Light perception and strategies in competitive environments

As green plant tissues absorb BL and RL (λ_{BL}=~400-500nm, λ_{RL}=~600-700nm) for photosynthesis and reflect FR (λ =700nm-800nm), the presence of competitors triggers a reduction of the R:FR ratio in the direct vicinity of a plant individual (Fig. 2A, left and middle) (27). R- and FR-sensing phytochromes are therefore excellent sensors for neighbor detection, with phyB playing a predominant role in the process in de-etiolated plants. Phytochrome photoequilibrium varies according to the R:FR ratio and it was observed that low R:FR-induced stem elongation inversely correlates with active phyB levels (4). Neighbor-detecting mechanisms are particularly important in environments where plants are growing at high densities such as agricultural systems. In natural environments, reduction in R:FR rather represents an early step in the development of a canopy when no change in global light intensity has happened yet (27). Later when canopy cover further develops, a general reduction in photosynthetically active radiation is observed and affects both light signaling and photosynthetic activity (Fig. 2A, right). The late lowering in RL and BL intensities are additional signals perceived by phytochromes and cryptochromes, respectively. Combination of these signals enhance early low R:FR-triggered adaptive responses (18, 20, 21, 28). Interestingly, recent observations indicate that low BL signals perceived by cryptochromes enhance low R:FR-induced responses

through inhibition of negative regulators of the R:FR responses (18). Signal convergence between phytochromes and phototropins is also established. Indeed, phytochrome-mediated growth enhancement in low R:FR reinforce BL-regulated phototropic response in hypocotyls, suggesting a mechanism for optimization of light capture in poor light conditions (29).

It is important to note that a developing canopy is a heterogeneous light environment where sunflecks and canopy gaps may offer transient access to unfiltered sunlight and thereby inhibit shade-initiated responses (30). Indeed, unfiltered UV-B emissions through the canopy negatively impact low R:FR-induced traits like stem elongation or upwards leaf movement in an UVR8-dependent manner (31, 32). In addition, such light environments may trigger heterogeneous light perception among distant organs within the same plant individual. While the existence of reciprocal communication between distant organs has been observed, some shade-induced responses are restricted to the shaded organs (33, 34, 35, 36).

Two major strategies have been observed among plant species facing stressful shade conditions in their natural environment: shade tolerance and shade avoidance. On the one hand, the shade tolerance strategy favors the ability of plants to deal with limited light conditions. For instance, some species have developed ways to manipulate photosynthetic efficiency and readjust leaf morphology to increase light capture (37). Interestingly, shade-tolerant responses are rather regulated by a decrease of PAR than a decrease in R:FR ratio (38). On the other hand, shade avoidance, a widespread strategy among plants (including Arabidopsis), comprises a suite of developmental adaptations mostly resulting in increased vertical growth thereby favoring overtopping of competitors and better light interception (27). Moreover, there is increasing evidence for other important aspects of shade avoidance such as readjustments in nutrient uptake, structural acclimation or in regulation of plant hydraulics (38). As a counterpart, reallocation of resources in shade avoidance may imply reduction in energy-costly processes like biomass production or defenses against predators (39, 40). Typical shade avoidance responses triggered by low R:FR are increased stem elongation, upwards leaf movement (hyponasty), inhibition of branching or acceleration of flowering, all these responses constituting the Shade Avoidance Syndrome (SAS) (41).

Importance of PIF-mediated auxin signaling in neighbor detection

Phytochromes are synthesized under their inactive form (Pr) in the cytoplasm (Fig. 2B). Upon red light perception active phytochromes (Pfr) migrate to the nucleus where they interact with PIFs, a family of bHLH transcription factors which form a central hub in the coordination of external and internal signals influencing plant growth (42). Interaction between active phytochromes and PIFs leads to phosphorylation and subsequent degradation of PIFs, except for PIF7 which subsists under its inactive phosphorylated form (43). A decrease in environmental R:FR shifts phytochromes to their inactive state. Phytochromes can then no longer inhibit the activity of PIFs which, in turn, induce massive remodulation in gene expression overall acting positively on SAS (43, 44, 45). Among the seven PIFs interacting with phyB, only three (PIF4, PIF5, PIF7) seem to be involved in shade responses (43, 46). While PIF7 seems to be restricted to low R:FR responses, PIF4 and PIF5 play a crucial role in the convergence between low R:FR and BL/UV-B signaling pathways at late stages of canopy development (20, 21, 31, 43). Other members of the bHLH family such as LONG HYPOCOTYL IN FAR-RED 1 (HFR1) play a negative role in SAS through direct inhibition of PIFs, preventing the plant from an excessive response (47).

A significant amount of PIF-targeted genes are involved in regulation of the auxin phytohormone, well known for its role in plant growth and key actor in SAS (Fig. 2B, top panel). Auxin production is enhanced in shade conditions (48, 49). In leaves, auxin production takes place mainly at leaf margins (50) and shade enhances auxin production specifically at this site although increase in auxin levels have been recorded simultaneously in blade and petiole organs (51). The burst in auxin biosynthesis seems to happen during the first 24 hours of shade, auxin levels getting back to normal after this period (51, 52). Therefore, changes in auxin levels cannot fully explain long-term low R:FR-induced responses. The major route of auxin biosynthesis relies on two sequential enzymatic steps: first the enzyme TRYPTOPHAN AMINOTRANSFERASE OF ARABIDOPSIS 1/SHAVE AVOIDANCE 3 (TAA1/SAV3) catalyzes the conversion of tryptophan to indole-3-pyruvate (IPA); then enzymes of the YUCCA family mediate the conversion of IPA to indole acetic acid (IAA), the natural auxin (49, 53). The latter step is rate-limiting in the process (53). Four *YUCCA* genes (*YUC2*, *YUC5*, *YUC8*, *YUC9*) are specifically induced in

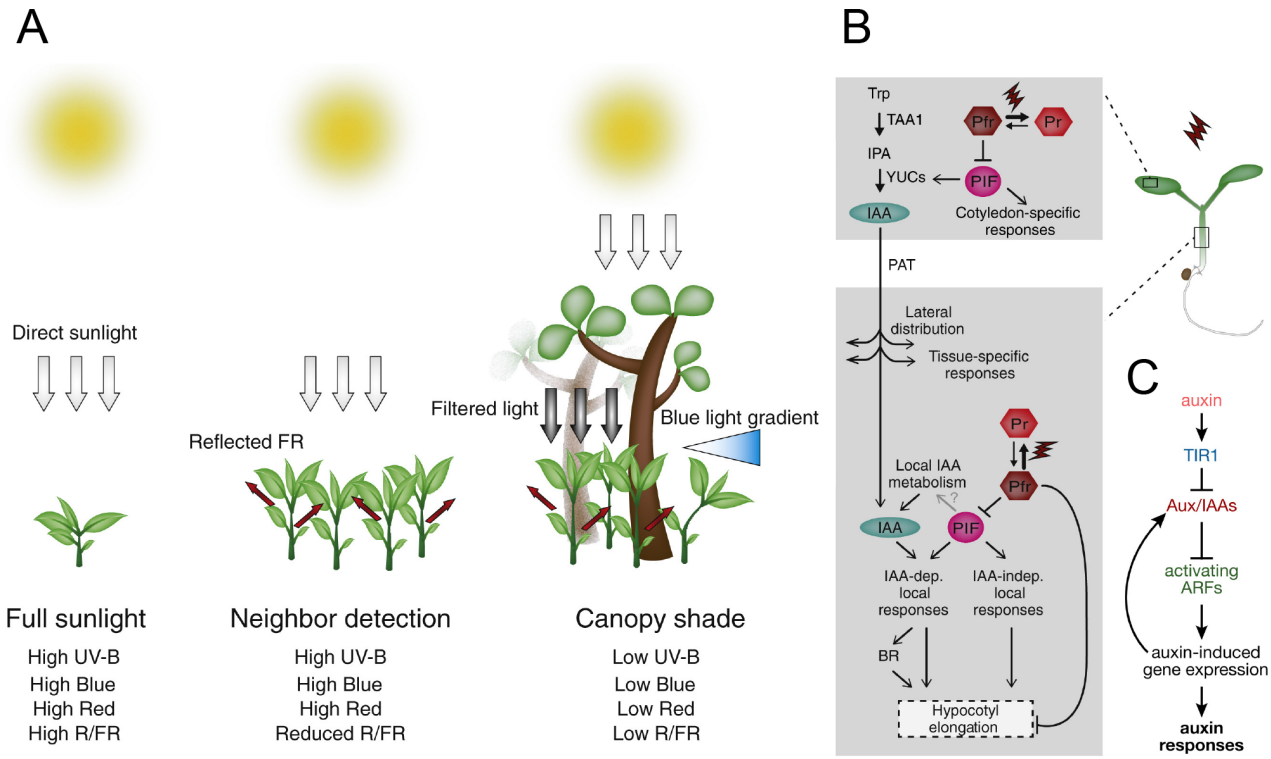

Figure 2. Shade perception and signaling in competitive environments

(A-B adapted from Fiorucci and Fankhauser, 2017, Current Biology; C from Woodward and Bartel, 2005, Plant Cell)

(A) Consecutive steps during the development of a canopy. Left: direct sunlight (white arrows) conditions with full amounts of UV-B, blue and red light. Absence of neighbors results in a high R:FR ratio in the environment. Middle: presence of neighbors which reflect FR light (red arrows) without masking direct sunlight. Reflected FR triggers a decrease in the R:FR ratio while amounts of UV-B, blue and red light remain intact. Right: plants at the top of the canopy get direct sunlight while plants under the canopy perceive only filtered sunlight (grey arrows) and reflected FR. Not only R:FR ratio but also UV-B, blue and red light are decreased. Canopy gaps create blue light gradients indicating direction of phototropic bending. **(B)** Signaling in seedlings during neighbor detection. Top panel: perception of FR signals (red lightning symbols) in cotyledons inactivates phys thereby triggering PIF-mediated responses like YUC-mediated increased auxin production. Lower panel: auxin is polarly transported to the hypocotyl while redistributed laterally where it triggers tissue-specific and elongation responses. FR perception in the hypocotyl may also lead to IAA-dependent and independent responses involved in hypocotyl elongation. **(C)** Signaling pathway downstream of auxin in the nucleus. Auxin interaction with TIR1/AFBs leads to degradation of the Aux/IAAs negative regulators. This releases activity of ARFs which trigger expression of auxin-responsive genes (including Aux/IAAs: negative feedback loop) thereby activating auxin responses.

low R:FR while *TAA1* expression seems to be slightly repressed in these conditions (43, 45, 54). Overall, mutants impaired in auxin biosynthesis display significant defects in shade responses (43, 44, 51), the quadruple *yuc2yuc5yuc8yuc9* mutant even displaying fully disrupted shade-induced elongation responses (45, 54). Inversely, auxin treatments mimic the effects of shade on gene expression and elongation responses (43, 45, 49, 51, 55). While PIF4, PIF5, PIF7 bind to promoters of the four low R:FR-induced *YUC* genes, PIF7 seems to play a prominent role in *YUC* expression, auxin biosynthesis and stem elongation in such conditions (43, 44). PIF4 and PIF5 appear to be rather involved in auxin sensitivity at later stages of canopy formation when blue light decreases (19, 21, 56). Indeed, auxin levels are decreased in canopy situations and it was suggested that PIF4 and PIF5 would allow the plant to respond better to weaker auxin signals in such conditions (56). In addition, low BL signals do not seem to trigger significant changes in the regulation of genes related to auxin production, supporting the idea that canopy shade signals affect auxin signaling rather than auxin biosynthesis (20).

A proper shade response not only requires intact auxin production but also intact polar auxin transport (PAT) (Fig. 2B, lower panel) (48, 49, 51, 57, 58, 59). Entering cells is relatively easy for auxin as the low pH of extracellular compartments converts it to its protonated form. Auxin internalization is also facilitated by the auxin influx carriers from the AUXIN RESISTANT 1/LIKE AUXIN RESISTANT (AUX1/LAX) family comprising AUX1, LAX1, LAX2 and LAX3 (60, 61). Once in the cell, auxin becomes deprotonated and requires efflux transporters to continue its cell-to-cell polar migration. Auxin efflux carriers belong to three families: the members of the PIN family which localize polarly in the cells; the ATP-BINDING CASSETTE/P-GLYCOPROTEIN (ABC/PGP) family whose members contribute mainly to efflux but also to uptake of auxin in the cells; and finally, the PIN-LIKE (PIL) family (60). In parallel to the main PAT, a study recently suggested the existence of a secondary connective transport allowing auxin to spread radially from the main stream to surrounding tissues, PIN3, PIN4 and PIN7 being the main actors of this process (62). Interestingly, low R:FR induces expression of several auxin transporter coding genes among which are *PIN3*, *PIN4* and *PIN7* (45, 48). Along with this hypothesis, the significant shade-induced decrease in *PIN1* expression, which seems to be crucial for the main polar stream through the vasculature, supports the idea that maintaining high auxin in the stem is favored in such conditions at the expense of downwards

transport to the roots (62, 63, 64). It is interesting to note that many of the above-mentioned auxin carriers are involved in BL-responses (20). For instance, some of them were shown to mediate phototropism where they probably help in the formation of the asymmetrical auxin gradient leading to organ bending (65). There is a long standing debate about the nature of the moving signal which connects shade sensing and consecutive auxin production in cotyledon and blade with shade-induced elongation in hypocotyl and petiole, respectively (66). Nowadays, there is increasing evidence for auxin being this long-distance signal (34, 45, 51, 58, 67). This being said, Kohnen *et al.* (2016) observed upregulation of many auxin-regulated genes simultaneously in cotyledons and hypocotyl (45). In addition, they also showed that some auxin responsive genes were induced in hypocotyl in absence of functional auxin biosynthesis or transport. This points toward the importance of local auxin metabolism at the site of elongation responses which can happen independently of auxin produced in upper parts (68). Recently, the ELONGATED HYPOCOTYL 5 (HY5) transcription factor which plays a negative role in shade response was observed as a mobile signal allowing communication between aerial parts and roots (35, 69). Further investigations are required to shed light on the potential existence of additional signals to auxin that would allow inter-organ communication in shade conditions.

Signaling downstream of auxin is crucial during shade avoidance and auxin has been shown to rapidly modulate the expression of many transcription factors as well as genes involved in cell elongation (45, 70, 71). In the nucleus, auxin binds to a co-receptor complex formed by a member of the TRANSPORT INHIBITOR RESPONSE1/AUXIN SIGNALING F-BOX (TIR1/AFB) family and a member of the AUXIN- OR INDOLE-3-ACETIC ACID-INDUCIBLE (Aux/IAA) family (Fig. 2C) (72). This interaction leads to the degradation of the Aux/IAAs which act as repressors of auxin-induced gene expression. Degradation of Aux/IAAs releases the activity of AUXIN-RESPONSE FACTORs (ARFs) which then trigger expression of auxin-induced genes. Some Aux/IAAs including IAA19 and IAA29, whose promoter regions are bound by PIFs, are rapidly induced in low R:FR conditions and this is proposed to constitute a negative feedback loop to avoid excessive auxin responses (44, 73). Interestingly, combination of low BL and low R:FR shade signals display additive effects on *IAA19* expression (18).

In addition to auxin, cortical microtubules (CMTs) which are part of the cytoskeleton as well as cell wall-modifying enzymes are additional key elements involved in shade-regulated growth processes (45, 74, 75). The expression and/or activity of cell wall modifying XYLOGLUCAN ENDOTRANSGLUCOSYLASE/HYDROLASE (XTH) and expansin families was shown to be modulated by shade in a PIF-dependent and/or auxin-dependent manner (45, 47, 74, 75). In addition, plants mutated in some members of the XTH family displayed defects in shade-induced organ elongation (75). CMTs are essential for the anisotropic aspect of shade-induced growth leading to organ extension. Reorganization of CMTs was observed in shaded hypocotyls and petioles and disruption of CMT organization through genetic and pharmacological approaches prevented proper responses in shade (74, 76). Interestingly, it was recently proposed that shade-induced CMT reorganization could modulate *XTH* expression in an auxin-dependent manner and thereby influence organ elongation response (74). In general, all these observations tend to support the widespread acid-induced growth theory suggesting that auxin triggers increased activity of membrane proton pumps which leads to acidification of the apoplast and further activation of cell wall modifying enzymes (77). The importance of the different plant tissues for auxin transport and auxin-induced growth is still not clear. The outermost epidermal tissues are currently thought to drive organ expansion (78). However, auxin signaling seems to be required not only in the epidermis but also in internal tissues for a proper shade elongation response to happen (79).

Other phytohormones involved in neighbor detection

Although auxin plays a major role in shade avoidance, other phytohormones influence the shade physiological outputs. First, brassinosteroids (BRs) are a class of plant hormones involved in many plant processes including growth. While BR levels do not seem to increase in low R:FR conditions, gene expression and mutant analyses have clearly underlined the importance of rapid BR-responses in shade-induced hypocotyl and petiole growth (19, 45, 52, 58, 79). Identification of common candidates between auxin- and BR-responsive genes also suggest partial overlapping functions between the two hormones (45). Indeed, auxin seems to modulate hypocotyl growth in shade through both BR-dependent and independent signaling pathways (79). Secondly, gibberellins (GA) are a class of phytohormones

that was shown to act positively on hypocotyl and petiole shade elongation responses. These positive effects are partly due to their role in the degradation of the DELLAs which are repressors of PIF activity (52, 80, 81). GA levels are significantly induced in low R:FR but, compared to auxin, the increase seems to happen later (52, 82). Thirdly, an increase in the levels of the gaseous ethylene hormone, which plays a pivotal role in stress responses during submergence, has been previously detected in low light and low R:FR conditions (83, 84). Analysis of mutants impaired in ethylene sensitivity highlighted the role of this hormone in low R:FR-induced elongation of petioles (83). However, the importance of ethylene in shade avoidance seems to be restricted to later stages of plant development as the ethylene mutants retained wild type responses in hypocotyl of young seedlings (85). Finally, the biosynthesis of abscisic acid, a key hormone in the plant adaptation to water deprivation, is also stimulated by low R:FR in different species and may negatively influence growth processes such as axillary bud development or stem elongation (86, 87, 88, 89). Recently, low R:FR-induced expression of some members of the 9-cis-epoxycarotenoid dioxygenase (NCED) family was observed in hypocotyl and petioles, the NCED family being considered as the rate-limiting step of stress-induced ABA biosynthesis in vegetative tissues (45, 58, 90). Interestingly, a co-working mechanism between auxin and ABA has recently been proposed in postgerminative embryonic axis growth during which ABA potentiates auxin effects through repressed expression of the *Aux/IAAs* negative regulators (91).

Leaf hyponasty: an essential trait during shade avoidance

Types of movement and underlying mechanisms in plants

Movements are ubiquitous in plants and have fascinated scientists at least since the 4th century before Christ. At this time, Androsthenes reported the existence of rhythmic leaf movements matching day and night cycles (nyctinastic movements) (92). Plants evolved their ability to move organs probably as a strategy to offset disadvantages linked to their sessile nature, strategy allowing a repositioning of organs in more favorable conditions. Plants display a great diversity of movements that can be dissected in different subjective categories depending if one considers

the directionality of the movement, the nature of the stimulus or the underlying cellular mechanisms (93).

Considering their directionality, plant movements are divided in three main categories: tropisms, nasties and nutations. Tropisms are movements allowing a reorientation of the organ towards the direction of the exogenous stimulus. Although tropic responses can be induced by a wide range of stimuli, they are mostly studied in response to light (phototropism), gravity (gravitropism) and, more recently, humidity (hydrotropism). Tropisms are considered as growth-mediated responses requiring asymmetrical growth between the two opposite sides of the organ leading to bending (94). Gravitropisms rely on amyloplasts (organelles involved in starch storage and gravity sensing) at the root tip as well as in hypocotyl and shoot endodermis to perceive gravity and trigger downstream signaling involved in organ bending (95, 96, 97). Although early signaling steps between photo- and gravitropisms differ, their signaling pathways converge at the level of auxin signaling where the formation of local auxin gradients, which is dependent on a functional auxin transport, has been frequently observed (94). Higher auxin levels are localized in the faster or slower extending side of shoot and root organs, respectively, and are probably mediating their growth response in a dose-dependent manner (98). Plants mutated in genes of the *TIR1/AFB* and *AUX/IAAs* auxin-signaling or *PIN* auxin-transport families show defect in both photo- and gravitropic responses (95). However auxin transport and signaling do not seem to be essential for hydrotropic responses which rely rather on ABA signaling in specific inner tissues (99, 100). Although ABA is generally thought to have negative effects on plant growth processes, it is now clear that such effects are dose-dependent, similarly to other growth hormones like auxin and ethylene, and may even become positive at low concentrations (98, 100, 101, 102, 103, 104, 105). The slow growth-mediated tropic movements rely on turgor-driven anisotropic cell expansion and therefore find their limitation in the capacity of cells to extend their walls (93). Rearrangement of cytoskeletal components like microtubules as well as function of cell wall-modifying proteins like XTHs have been shown to be important in tropic responses but the link between hormone signaling and these processes is still missing (95). However, increasing evidence points toward a role for hormones in tissue-specific modulation of proton pumps and apoplastic pH which in turn would affect cell wall properties and growth, thereby supporting the widespread acid growth theory (106, 107, 108, 109).

In contrast with tropisms, nasties are movements whose direction is not affected by the localization of the stimulus. They are mainly reported in leaf organs which possess two anatomically different sides (abaxial and adaxial) responsible for the predefined directionality of the movement. A nastic movement in the adaxial direction (upward) is termed hyponastic while if it happens in the abaxial direction (downward) it is named epinastic. Nastic movements are further divided into two different subcategories: the first one consists in the nastic movements occurring in absence of a direct environmental stimulus and being mostly regulated by the circadian clock such as the rhythmic Arabidopsis leaf movements as well as the nyctinastic sleep movements in legumes (110, 111); the second subcategory comprises the nastic movements being induced by a non-directional stimulus such as light (photonasty), temperature (thermonasty) and physical contact (thigmonasty) which are particularly important for escaping abiotic stresses such as shade, flooding or elevated temperature (112). The cellular mechanisms supporting nastic responses diverge between plant species. Some species possess a specialized motor organ at the base of the leaf petiole called the pulvinus, which supports the whole leaf movement (113, 114). The pulvinus consists in separate extensor and flexor tissues located on the abaxial and adaxial sides of the pulvinus organ, respectively, that orchestrate leaf movement by alternative reversible swelling and shrinking of cells. The pulvinus functions in a similar way as stomata which also rely on small and reversible turgor changes within the elastic boundaries of cell wall deformation (115, 116). Leaves of other plant species such as Arabidopsis or Tobacco while lacking a pulvinus are still capable of movement. In this case, it is widely assumed that nastic movement is due to differential growth rates between ab- and adaxial sides of the petiole organs (117, 118, 119, 120). Intriguingly, it was reported that not only the petiole but also the blade take part in some hyponastic responses, although no detailed analysis is available (119). The mechanisms underlying differential growth processes in nastic movements are probably related to the ones involved in tropic responses, but further research is required to understand to which extent these processes overlap or differ. Finally, nutations are short-period autonomous and helical movements often related to periods of growth and require gravity sensing as well as the presence of endodermal tissues (121, 122, 123). Relatively to tropisms and nasties, much less attention has been given to nutational movements which are generally seen as

residues of growth waves especially detectable in the absence of an environmental stimulus (124, 125).

Leaf hyponasty in response to abiotic stresses

In environments characterized by an alternation of day and night periods, the position of Arabidopsis leaves oscillate between high and low in a 24-hour interval: leaves start elevating (hyponasty) a few hours after dawn to reach maximal elevation angle at night and then initiate a downward movement (epinasty) to reach minimal elevation angles a few hours after dawn (110, 126). This circadian-regulated pattern in leaf elevation angle is called leaf diurnal hyponasty and is widespread among pulvinus-lacking plant species. In Arabidopsis, it has been suggested that this diurnal rhythmicity in leaf elevation angle results from a trade-off between maximizing light interception in the morning when temperature and humidity are optimal for photosynthesis and minimizing water loss in the afternoon to avoid overheating of the photosynthetic apparatus (112, 127). However, when leaves are exposed to certain environmental stresses, they initiate a significant increase in leaf elevation angle, called stress-induced leaf hyponasty, which overlaps with leaf diurnal hyponasty and probably allows the leaf to escape unfavorable conditions (Fig. 3). Many species are able to trigger such modifications in the circadian-regulated leaf angle in response to environmental stimuli. In crop species, this is an important trait during competition which favors photosynthetic efficiency and yield (128). Stress-induced leaf hyponasty also seems to be dependent on the clock, as the amplitude of the response was shown to depend on the time at which the stress signal was applied (129). Interestingly, hormone signaling may also be gated by the circadian clock and this might have a direct involvement in gated stress-induced hyponastic responses (130, 131).

The effects of three main abiotic factors have been explored in the context of stress-induced hyponasties: submergence, elevated temperature and shade (low light in particular) (21, 132, 133). *Arabidopsis thaliana* is not found in submerged environments but in open and warm habitats where it has to compete for light with similarly-sized plants while adjusting leaf positioning to avoid overheating (112). Although hyponasty may have therefore primarily been useful to escape shade and elevated temperature, all three factors (submergence, shade and high temperature)

induce very close hyponastic responses with similar kinetics (112, 119). Moreover, in the case of submergence-induced hyponasty many studies have also focused on semi-aquatic species such as *Rumex palustris* where hyponasty allows leaf emergence from floods (112).

Submergence-induced hyponasty

Submergence is stressful for plant species living in flooded environments because gas exchanges are dramatically reduced in water, which therefore affects respiration of plant tissues and photosynthesis (112). In submerged plant tissues, ethylene gets trapped within tissues and this causes a rapid increase in the concentration of the hormone (134). In *Rumex palustris*, increased ethylene first triggers elevation of leaves until a certain angle before it induces subsequent petiole elongation reestablishing air contact (135). In Arabidopsis, a rapid (7 hours) hyponastic response is induced but without consecutive petiole elongation (119). Ethylene biosynthesis and signaling play a central role in submergence-induced hyponasty both in Rumex and Arabidopsis species (119, 136). However, inhibition of ethylene production leads to dramatic although not complete reduction of submergence-induced hyponasty in *R. palustris*, highlighting the existence of other signaling pathways (137). Compared to ethylene, the role of auxin is far less clear during submergence-induced hyponasty. In *R. palustris*, although a rapid increase in auxin levels is observed in petioles, blocking PAT only triggers a slight delay without preventing the response (136). In Arabidopsis, auxin and PAT are apparently not required during ethylene-induced hyponasty (138). Indeed, pharmacological or genetic inhibition of PAT and auxin signaling did not affect the response but rather enhanced it (138). Concerning ABA, a rapid reduction in ABA concentration happens in submerged petioles in *R. palustris* through decreased expression of ABA biosynthetic *NCED* genes and increased degradation of ABA to phaseic acid (136, 139). Pharmacological and genetic approaches also clearly established the inhibitory role of this hormone in the hyponastic response induced by ethylene and submergence conditions (136, 140). This negative function was proposed to be acting through parallel inhibition of GA accumulation but inhibiting GA biosynthesis only triggers a delay in the response (136). It is important to note that ABA is already

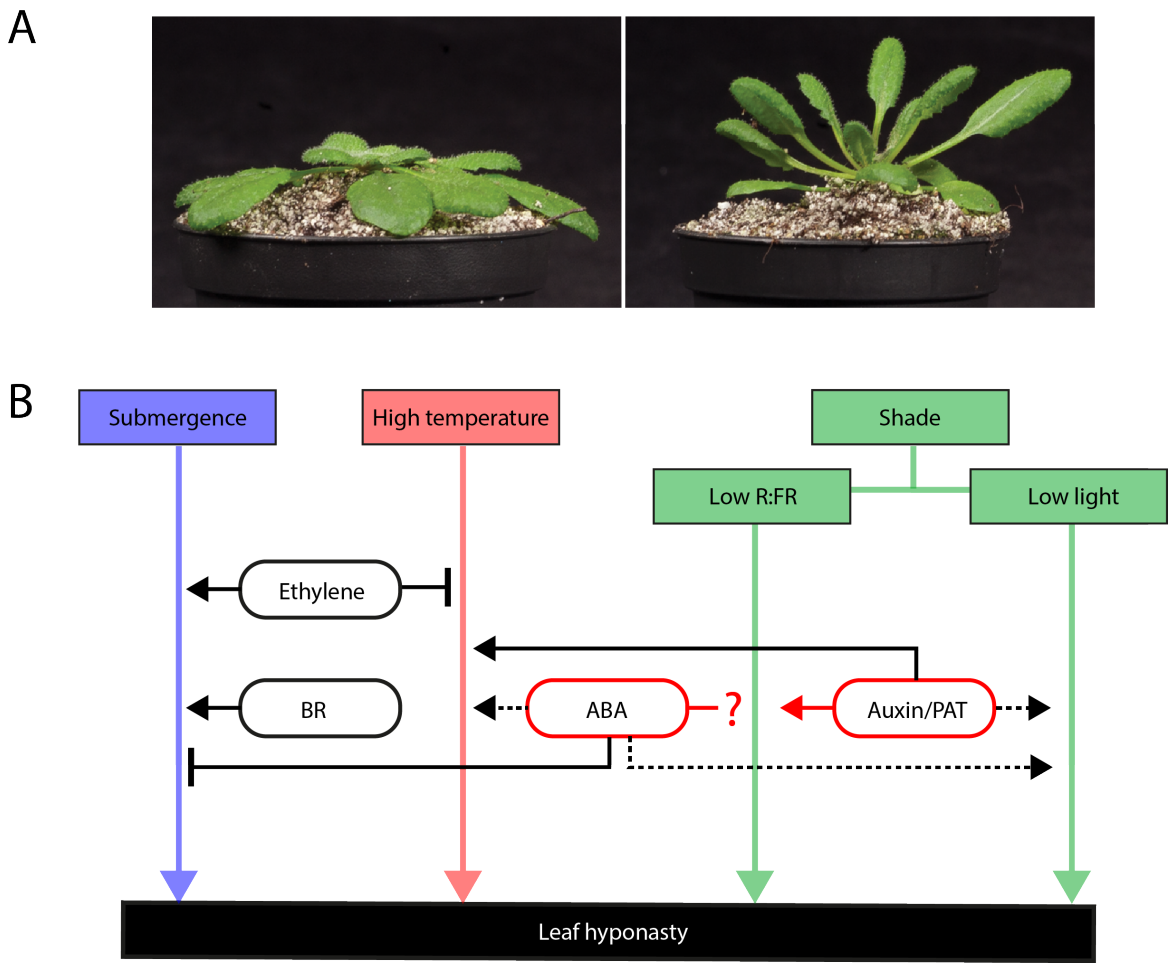

Figure 3. Illustration of abiotic stress-induced leaf hyponasty and model of the involvement of hormonal pathways in the response

(A from Sasidharan *et al.*, 2014, PLOS ONE)

(A) Illustration of a shade-induced hyponasty in a four-week-old Arabidopsis rosette. Left: rosette after 24 h in standard white light conditions. Right: rosette after 24 h in green shade conditions. A strong hyponastic response is visible in most leaves.

(B) Schematic model of the three main abiotic stimuli as well as the involvement of hormones in the downstream signaling pathways leading to hyponastic response in leaves of the *Arabidopsis thaliana* plant model. Submergence is positively regulated by both ethylene and brassinosteroids while it is negatively regulated by abscisic acid. High temperature triggers hyponasty through auxin and polar auxin transport while abscisic acid also seems to be required in the response. Low R:FR, the early step in developing shade, requires auxin and polar auxin transport to induce hyponastic response while the involvement of abscisic acid in the response has not been considered so far. Low light conditions induce hyponastic response presumably through auxin, polar auxin transport and abscisic acid. Arrow-headed and bar-headed lines represent positive and negative impact, respectively, of an hormone on a pathway. Full lines indicate a relationship which is supported by converging studies while dotted lines indicate a probable relationship which still needs to be clarified. Red colored lines highlight the hormones and relationships which have been investigated in the present study.

known to have a negative impact on leaf positioning in absence of stressful conditions (129, 140). For instance, simultaneous treatment of shoots and roots with ABA inhibits the diurnal leaf hyponastic response in wild type plants (140). Finally, BRs also play a positive role in ethylene-induced hyponasty as pharmacological or genetic inhibition of BR biosynthesis affected the response (141).

In addition to hormones, several genes, some of them coding for transcription factors, are involved in hyponastic responses mediated by ethylene (112, 118, 142). First, the extensive family of APETALA 2/ETHYLENE RESPONSIVE FACTOR (AP2/ERF) plant-specific transcription factors involved in abiotic responses was suggested to play a role in ethylene-induced hyponasty since lines overexpressing such factors displayed affected responses (112, 143). Then, *ERECTA*, known to be involved in plant organ embryogenesis, positively controls ethylene-induced hyponasty as well as general leaf positioning independently of ethylene signaling (117, 144). Finally, a new actor called *SPEEDY HYPONASTIC GROWTH* (*SHYG)*, which encodes a transcription factor of the NAC family associated to plant stress responses, was shown to be induced by ethylene and essential for the consecutive hyponastic response (118, 145). Rauf *et al.* further demonstrated that SHYG plays a positive role in hyponasty through the upregulation of the ethylene biosynthetic gene *ACC OXIDASE 5* (*ACO5)* which suggests the existence of positive feedback loops in the response. Moreover, SHYG enhances the expression of several genes of the *XTH* and expansin families involved in cell elongation. These findings are supported by previous studies which reported ethylene-mediated rapid apoplastic acidification and induction of expansin expression in both Arabidopsis and Rumex species (120, 136, 146). In addition, induction of expansins was specifically observed at the abaxial and shoot-proximal part of petiole organs, which is generally considered as the site responsible for leaf movement where differential elongation happens (118, 120, 135). In Arabidopsis, reorganization of the CMT was also observed specifically in abaxial petiole side and disruption of CMT network by oryzalin affected the hyponastic response (120).

Heat-induced hyponasty

Elevating leaves in response to environmental heat is thought to allow plants minimizing the risks of overheating through decreased light incidence and increased

contact with refreshing wind (112). However, much fewer studies have focused on the mechanisms regulating hyponasty in response to heat compared to submergence. Still, phytochromes and cryptochromes appear to be involved in heat-induced hyponasty, phyB behaving as a negative regulator of the response (147). Interestingly, a role for phytochromes as plant thermosensors was recently highlighted in addition to their photoreceptor function (148, 149). Another study revealed a crucial positive function for PIF4 in temperature-induced hyponastic and elongation responses both in leaves and hypocotyl organs (132).

Three of the major growth-related hormones have been involved in heat-induced hyponasty so far: ethylene, auxin and ABA. First, ethylene was shown to be a negative player in the response and release of this hormone in the plant is reduced by heat signals (147). Second, contrary to submergence conditions heat-induced hyponasty requires auxin and PAT (147). PIF4-mediated induction of *Aux/IAAs* in petioles under elevated temperature also suggests that auxin sensitivity might be enhanced by heat and thereby impacting on elongation and hyponastic responses in leaves (132, 147). Finally, pharmacological and genetic studies attributed a positive role to ABA in heat-induced hyponasty even though mutants impaired at different steps of ABA biosynthesis display diverging responses (147).

Shade-induced hyponasty

Hyponasty is thought to be important for survival in shade-avoiding plants and especially for species forming a rosette like Arabidopsis which often have to compete with similarly-sized neighbors. In these species, hyponasty does not lead to optimal light interception as the blade organ moves to a more vertical position but this is probably outweighed by increased light harvesting in leaves reaching the canopy surface (112). A reduction in R:FR induces a significant hyponastic response and mutants with disrupted phyB display a constitutive hyponastic response (150, 151). A decrease of the PAR triggers a dose-dependent hyponastic response and this appears to be mediated by phytochrome- and cryptochrome-dependent perception of reduced R and BL signals (21, 152). In such conditions, the signaling routes downstream of phytochromes and cryptochromes seem to converge towards PIF4 and PIF5 which play a central role in the response (21). However, care must be taken when considering BL-mediated leaf movements as BL signals affect not only low

light-induced hyponasty but also general leaf positioning (12, 153). BL-mediated leaf positioning is mainly regulated by phototropins while they are not required *per se* in low light-induced hyponasty. Interestingly, phot1-dependent perception of side BL illumination triggers a rotation (twisting) of the blade organ towards the BL source (12, 13). Finally, total darkness also triggers upward movement of leaves (96, 97, 129).

There are conflicting data concerning the role of ethylene in low light-induced leaf hyponasty (112). A first study reported an increase in ethylene production in low light and showed that ethylene-insensitive mutants were defective in hyponastic response in such conditions (84). In parallel, ethylene sensitivity was shown to be required for low light-induced hyponasty in tobacco (154). In two later studies however, researchers reported an absence of defects during low light-induced hyponastic response in ethylene-insensitive Arabidopsis mutants and no increase in ethylene production could be detected in these conditions (138, 152). Considering low R:FR environments, ethylene does not seem to play a role in the leaf hyponastic response under such conditions (83, 84).

Concerning auxin, biosynthesis, transport and signaling are all essential to low R:FR-induced hyponastic responses in Arabidopsis while their role is less clear in low light conditions (21, 48, 49, 84, 152). For instance, SAV3-dependent auxin biosynthesis is required for hyponasty in low R:FR conditions but *sav3* mutants display a full hyponastic response in low light conditions (21, 49). Similarly, implication of PIN3-dependent auxin transport in hyponasty seems to be more important in earlier stages of shade avoidance although some results lead to contradictory interpretations (21, 48, 152). Interestingly, it was observed that disrupting PAT suppressed low BL-induced petiole elongation while maintaining a full hyponastic response (21). Such results point towards a diverging point in the regulation of hyponasty versus petiole elongation.

No data is available concerning the role of ABA in low R:FR-induced hyponasty (129). ABA seems to play a positive role in low light conditions but similarly to what has been observed under elevated temperature, mutants impaired at different steps of ABA biosynthesis displayed diverging hyponastic responses in low light conditions (155). Concerning gibberellins and BRs, no data has been published concerning their involvement in low R:FR-induced hyponasty (58, 83). However, in low blue light disruption of BR and GA signaling pathways does not affect hyponastic response

while it strongly reduces petiole elongation (21). Again, this underlies the existence of different mechanisms regulating these two responses in Arabidopsis leaves.
In addition to the major role of hormones during shade-induced hyponastic response, *ERECTA*, previously mentioned for its role in ethylene-induced hyponasty, is also involved in the regulation of the leaf hyponastic response in low light conditions (142). This is not surprising considering the importance of this gene for leaf positioning in general (117).

A role for leaf hydraulics in shade-induced hyponasty?

Water transport and hydraulic properties in plants

Vascular plants uptake water from the soil through their root system (Fig. 4). Water is then redistributed in the entire plant body up to the aerial plant parts, where most of it is finally released in the atmosphere through stomatal transpiration (156). Water can be transported in three different ways in plants including the transcellular path (via membrane water-channel proteins called aquaporins), the symplastic path (via plasmodesmata connections between cells) or the apoplastic path (via extracellular spaces and cell walls) (157, 158).
In order to access the root center from soil, water is forced by the casparian strip to use the transcellular route. Water is then axially transported along the dead xylem cells of the vasculature which spreads from the roots up to the extremities of aerial plant parts (Fig. 4A). Due to their lack of membranes, xylem dead vessels have low resistance to water flow and constitute an efficient way for apoplastic water transport. Once arrived at the exit point, water radially crosses living xylem parenchyma tissues in the vasculature to get in contact with bundle sheath tissues (BSC) (Fig. 4B). BSC are composed of a single parenchymatous cell layer which tightly enwraps the whole vasculature of the leaf, at the exception of the vascular ends located at the blade margins (called the hydathodes). BSC are considered as the leaf “dynamic control barrier” because they act as a water filter between vessels and extravascular tissues whose properties can be modulated by abiotic factors such as light and temperature (50, 158, 159, 160). Interestingly, symplastic continuum is absent between vascular tissues and BSC, reinforcing the role for BSC as a border guard between vascular apoplastic and extravascular symplastic routes (160, 161). Moreover, in some plant

species BSC display structural similarities, such as the presence of suberized cell walls, with the casparian strip of the root endodermis (158, 162). After crossing BSC, water travels in the mesophyll photosynthetic leaf tissues (MC), which are partly constituted of air spaces facilitating gas exchange for transpiration and photosynthesis, to finally evaporates into the atmosphere through stomatal apertures. When stomata close and transpiration is reduced at night, MC get flooded and hydraulic pressure increases in the xylem (160). This potentially leads to water being released through the hydathodes and constitute guttation drops at extremities. Overall, this long-distance water transport is regulated by differences in water potential, with water moving from high soil water potential to low atmospheric water potential (157, 158). While only a small proportion of the whole water flow is used to sustain expansion growth, the biggest part evaporates in the atmosphere thereby leading to a tension force pulling up water though the plant (156, 163). In general, transpiration rate in plants displays a rhythmic pattern, increasing during the day and being reduced at night (164, 165).

Water homeostasis in plants results from the interplay between interconnected hydraulic traits including water potential (driving force for water movement), transpiration rate and hydraulic conductance (how easily water can move through plant tissue) in roots (L_{pr}) and leaves (K_{leaf}) (158, 166). So far numerous techniques have been developed in order to monitor plant hydraulics but studying precise contributions of the internal tissues remains difficult (166, 167). For instance, although it is not known how exactly xylem and extra-xylem routes contribute to the whole K_{leaf}, there is a consensus idea that both are more or less contributing similar amounts (158). Vascular architecture as well as sap pH play important roles in the regulation of K_{leaf} relatively to the xylem route (158, 168, 169, 170). AHA1 and AHA2, two of the most abundant H^+-ATPase isoforms in Arabidopsis leaves, are crucial regulators of xylem sap pH (170, 171). AHA2 is especially abundant in vascular tissues and BSC-specific complementation rescues the pH decrease observed in the mutant (170, 172). Nowadays there is increasing evidence for vascular tissues and BSC exerting a major control on K_{leaf}, thereby also impacting on hydraulic status of roots, MC and stomata (159, 173, 174, 175). For instance, a reduction in MC turgor was observed in conditions of increased transpiration, underlying the role for BSC in limiting hydraulic distribution (159, 161). Still, MC tissues generally display a low

hydraulic conductivity and this also influences general leaf hydraulic conductance (157, 176).

Aquaporins (AQPs) are water channel proteins which play a crucial role in transcellular water transport across plant tissues (177). The aquaporin family consists of 35 genes in Arabidopsis and is divided into several subfamilies among which are the PIP subfamily (Plasma membrane Intrinsic Proteins) and the TIP subfamily (Tonoplast Intrinsic Proteins) (178). The PIP family further separates into the two PIP1 and PIP2 subfamilies, most of their members being expressed in vascular tissues and BSC, with PIP1;2, PIP2;1, PIP2;6 and PIP2;7 being the most abundant isoforms in leaves (167, 177, 179, 180). Aquaporins are essential through their role in the radial hydraulic conductivity in roots as well as for radial export from xylem parenchyma to BSC in the shoot (181). Indeed, previous studies reported defects in hydraulic conductance in roots and shoots in several *pip* mutants (176, 182, 183, 184). Recently, targeted silencing in the whole Arabidopsis plant of the whole PIP1 subfamily led to many defects in water homeostasis such as decreased K_{leaf}, transpiration and water permeability in BSC and MC (175).

Plants are generally separated in two categories when it comes to their strategy in water management: anisohydric and isohydric species (185). Anisohydric species adopt a risky behavior in water stress conditions by maintaining a high growth rate. Such strategy may be advantageous in moderate water stress but can potentially lead to water overdraft. Isohydric species, including Arabidopsis, adopt a “water-conserving” strategy and rapidly trigger hydraulic adaptations to limit water loss in case of water stress. The latter strategy is characterized by the development of ways for translating hydraulic signals into chemical information, typically ABA signaling (186, 187).

Light and hormonal regulation of leaf hydraulics

Among the abiotic factors triggering a modulation of leaf hydraulic properties in plants are light intensity and light quality (184, 188). An increase in light intensity generally goes with an increase in K_{leaf} and often associates with PIP and reactive oxygen species (ROS) activity (184, 188, 189, 190, 191). Inversely, darkness triggers a significant reduction in K_{leaf} except in Arabidopsis which, unlike the majority of

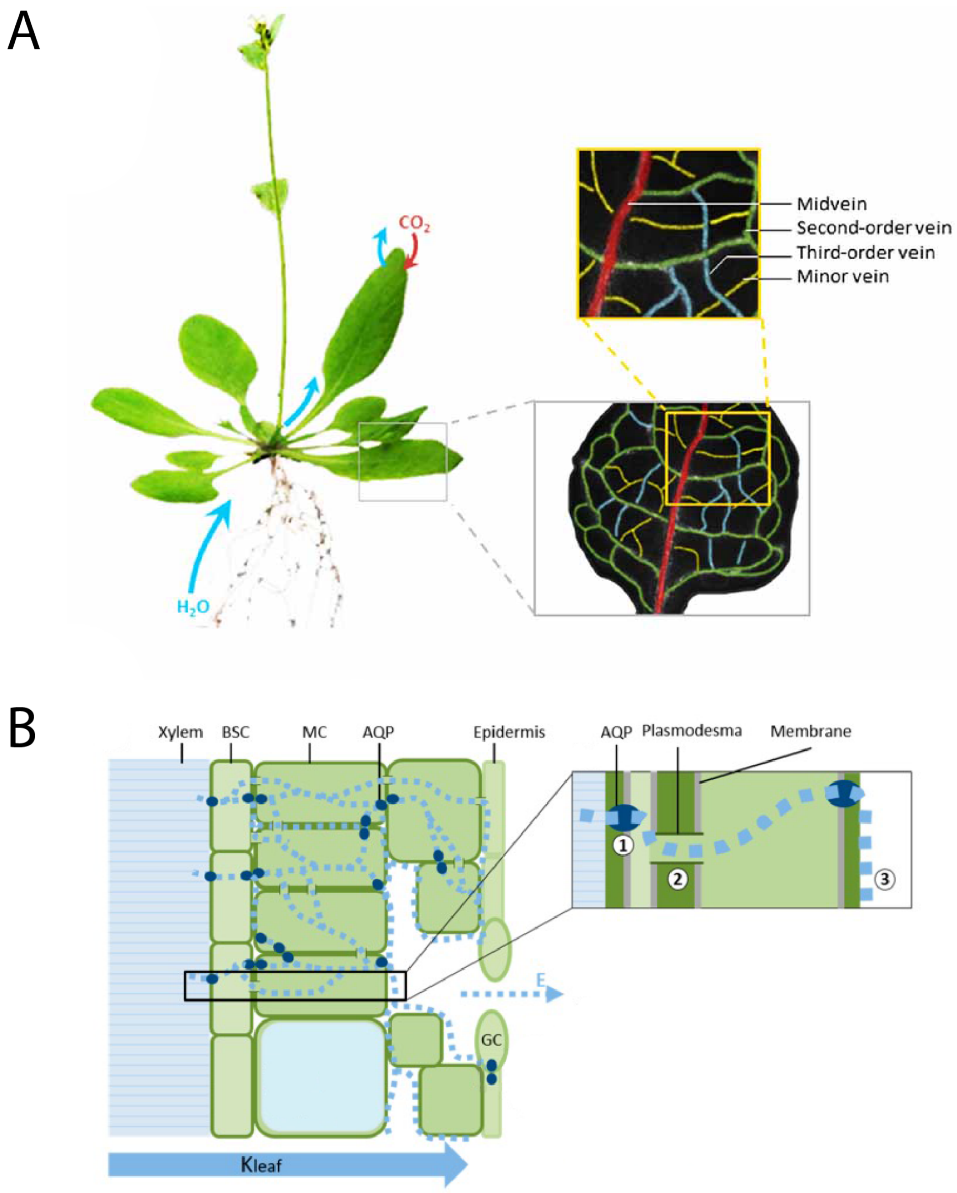

Figure 4. Models of vascular and extravascular pathways for water in Arabidopsis

(A from Prado and Maurel, 2013, Frontiers in Plant Science; B adapted from Yaaran and Moshelion, 2016, International Journal of Molecular Sciences)

(A) Illustration of the vascular pathway. After uptake by the roots, water is distributed to the aerial plant parts through the non-living xylem cells of the vascular pathway. In leaves, the vascular pathway comprises the midvein (going from the petiole base to the leaf tip) as well as several classes of sub-order veins (second-order, third-order and minor veins). All types of leaf veins form together a highly organized and hierarchical network allowing water distribution throughout the leaf.

(B) Illustration of the extravascular pathway. From xylem cells, the water enters the extravascular pathway through the BSC, this step being mediated by aquaporins (AQP). From BSC, water is then transported through the MC to finally reach the stomata (GC) depending on three different ways: 1) the transcellular way, 2) the symplastic way formed by plasmodesmata and 3) the apoplastic way. The amount of water delivered into the atmosphere through the GC constitutes the transpiration flow (*E*, dashed blue arrow).

species, displays an increased K_{leaf} in such conditions which is mediated by light-dependent post-translational modifications of PIPs in Arabidopsis veins (176, 184). In addition, as mentioned earlier alternations of day and night periods profoundly affect aquaporin activity and plant hydraulic properties like water content, water permeability and hydraulic conductance (192, 193, 194, 195). Concerning impact of light quality, BL and RL trigger an increase and decrease in K_{leaf} , respectively, in cucumber and birch tree (196, 197). Moreover, phyB was shown to be involved in long-term hydraulic adaptive responses to light signals and revealed to be important for water use efficiency, transpiration and stomata development (198, 199). Besides these aspects, light is also known to influence plant hydraulic properties through pH modulation and this is particularly interesting knowing that pH regulates dissociation states and therefore distribution of phytohormones like ABA and auxin (200).

ABA is a key hormone when it comes to the regulation of plant hydraulics in response to water limitation and light signals (201). Indeed, modulation of *NCED* genes, which regulate the committed step of ABA biosynthesis, is known to be important during plant adaptation to light-induced and water-induced stressful conditions (202, 203). Moreover, light-regulated changes in leaf water content and turgor in Arabidopsis were shown to be impaired in ABA signaling mutants (161). Effects of light on the regulation of ABA biosynthesis was previously proposed to be due to quick light-induced changes in plant turgor which in turn triggers modulation of ABA levels (203). Indeed, rapid turgor-dependent induction of ABA biosynthesis has been observed in several studies (204, 205, 206). Xylem parenchyma currently stands as the major site for ABA biosynthesis although autonomous ABA biosynthesis has also been reported in stomata (207, 208). ABA is highly mobile in plants and can travel long distances using xylem or phloem routes from roots to shoots and inversely finally leading to appropriate organ responses (186, 209, 210, 211, 212). Interestingly, in maize and tomato it was proposed that increased conductance in roots might serve shoot rehydration in case of drought conditions without involving stomatal transpiration (202, 211). Distribution of ABA seems to be crucial for appropriate local hydraulic responses in roots, BSC and stomata and might trigger positive or negative effects on hydraulic conductance depending on the species and organ considered (176, 202). However, ABA effects on plant hydraulics are concentration-dependent and it was proposed that opposite responses after ABA treatment might rather be due to inappropriate concentration usage (213). In Arabidopsis, xylem-fed ABA

reduced both K_{leaf} and transpiration while smearing ABA on blade only reduced transpiration (159). In addition, xylem-fed ABA specifically impacted on water permeability of BSC and not MC (159). All this points towards a specific responsiveness to ABA in BSC.

Many studies highlighted the importance of aquaporins in ABA-induced plant hydraulic changes. Strong evidence now exists for the involvement of ABA-dependent transcriptional and post-translational aquaporin changes in the regulation of plant hydraulic processes such as hydraulic conductance, water permeability and stomata movement (159, 174, 214, 215, 216, 217). Much less research has been conducted on the other phytohormones but evidence is now emerging concerning their role in plant hydraulic processes. For instance, an elegant study recently pointed towards a crucial role for auxin in lateral root emergence (218). In this case, auxin caused an overall decrease in aquaporin expression which led to a significant reduction in local water transport thereby facilitating the emergence of lateral roots. Salicylic acid, ethylene, GAs and BRs were also shown to interfere with plant hydraulic regulation but more research needs to be conducted to reveal their exact role in the process (181, 219).

Links between hydraulics and nastic movements in leaves

How abiotic signals and especially light induce leaf nastic movements is still not fully elucidated. Involvement of hormones in shade-induced hyponasty is well established but how signaling downstream of hormones triggers an active leaf movement remains unknown. However, there is increasing evidence suggesting a role for hormones in the reorganization of plant hydraulic properties leading to organ movement (100, 161). For instance, ABA signaling has been recently shown to play a key role during root hydrotropism (100). Interestingly, hydrotropic response in pea roots was proposed to be due to differential water conductance between the opposite sides of the organ (220).

In pulvinus-possessing plants like mimosa, bean and rain tree (*Albizia saman*), rhythmic changes in solute and ion (K^+ especially) content induce osmotic water fluxes between cells located at the two opposite sides of the pulvinus are responsible for leaf movement (113). These fluxes are strongly associated with cyclic expression of aquaporins and ion channels throughout the 24-hours period, displaying a peak

in the morning (114, 221). Literature covering the relationship between hydraulics and movement in pulvinus-lacking species remains much more scarce. However, a few studies indicate potential links between these two processes in tulip, tobacco and tomato species. First, the thermonastic movements of tulip petals involve aquaporin phosphorylation and reorganization in water transport (222, 223). Then, diurnal leaf nastic movements in tobacco associate with rhythmic aquaporin expression in the petiole (224). Expression of *PIP1* and cellular water permeability peaks in the morning in petioles at the same time when leaves go down, while these processes reach their minimum values at the end of the photoperiod when leaves go up. Moreover, Siefritz *et al.* (2004) reported that *pip1* tobacco mutants show defects in such movements (224). Finally, tomato lines overexpressing *NCED* genes and consequently having high ABA levels displayed reduced transpiration and increased root hydraulic conductivity (202). Moreover, these lines displayed increased petiole elongation and leaf elevation angles compared to wild type plants. Concerning Arabidopsis, no direct evidence between leaf hydraulics and nastic movements has been reported. However, ABA-mediated stomata closure reduced transpiration water loss but also maintained leaves in an erect position instead of wilting (208). Also, defects in leaf turgor were associated with defects in leaf movements in ABA signaling mutants (161). This was proposed to be due to constitutive transpiration in the mutant leading to loss of turgor in leaf rachis in turn causing leaf wilting.

Aim of the study

It is assumed that leaf nastic responses allow plants to enhance their access to sunlight in competitive environments and thereby increase their fitness. The whole cascade of signaling events from the perception of the shade signal to the achievement of the organ movement is still unclear. The aim of the present study is to improve our understanding of how such responses are regulated in plants. We started focusing on analysing with high spatial and temporal precision the macroscopic patterns of leaf growth and movements in the pulvinus-lacking model species *Arabidopsis thaliana*. Measurements of such patterns were achieved not only in standard light conditions but also in conditions mimicking competitive environments. In the latter case, additional far red radiation was supplemented to standard light conditions to decrease the R:FR ratio and thereby trigger increased hyponastic response. We then investigated in more detail the crucial role of the auxin phytohormone, well known for its involvement in plant growth, during diurnal and shade-induced leaf nastic responses. In addition, our study finally addressed the issue concerning the involvement of abscisic acid in shade-induced leaf nasty, this hormone being mostly studied for its roles in seed germination and responses to water-limiting conditions.

Results

Introduction to results

The results are presented in three main chapters.

In the first chapter, I present the development of a new method for analysis of growth and elevation angle in individual leaves of the Arabidopsis plant model. This method is based on the previous work from Dornbusch *et al.* (2012) where the authors developed a phenotyping pipeline for estimating these traits at the overall plant level (110). This chapter further presents detailed patterns of growth and movement in individual leaves grown in different light conditions. Particularly, it focuses on how these traits coordinate between petiole and blade organs and how they are integrated in the general leaf development. The new method and the consecutive results have been published in the journal The Plant Cell in 2014 (225).

In the second chapter, I monitor in detail the movements of individual Arabidopsis leaves in standard versus shade (low R:FR) conditions based on the technique developed in Dornbusch *et al.* (2014). I then investigate the role of auxin in these responses using a combination of pharmacological and molecular genetic approaches. This led to new aspects concerning the importance of auxin during plant adaptation to changes in light environment. These results were published in the Proceedings of the National Academy of Sciences of the United States of America (PNAS) in 2017.

In the third chapter, I focus on the function of abscisic acid in leaves under competitive conditions based on physiological, biochemical and genetic approaches. This led to exciting results highlighting a potential novel role for abscisic acid in shade-induced responses in leaves, especially concerning the leaf nastic response.

CHAPTER I

New laser-scanning methodology for investigation of growth and movement in individual leaves of Arabidopsis rosettes

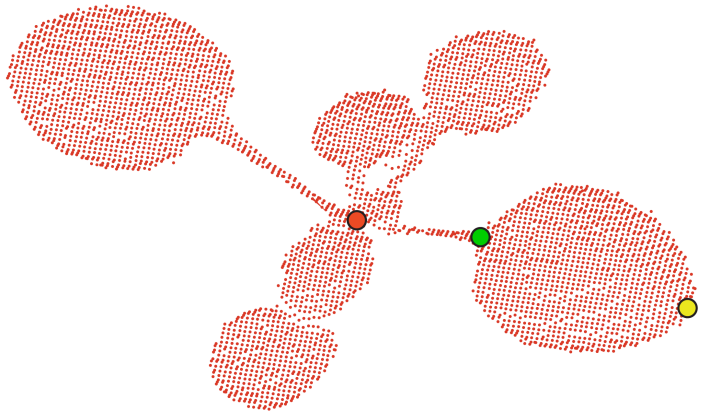

3D point cloud of an Arabidopsis rosette with detected positions for the leaf tip (yellow), petiole-blade junction (green) and shoot apical meristem (red).
2014. O. Michaud

Overview

During the first year of my thesis, I collaborated with Dr. Tino Dornbusch who was my former Master thesis supervisor in the Fankhauser group at the University of Lausanne. We worked towards finalizing and publishing the project that we developed during my Master thesis. This collaboration resulted in a publication in the journal The Plant Cell (225). In addition, the publication was highlighted through an In Brief article written by a Science Editor of the journal (226).

The objectives of this project were (1) to describe in detail the patterns of growth and movement in blade and petiole organs as well as at the overall leaf level, and (2) to understand how these two traits are related and regulated during leaf development. To this purpose, we implemented the pipeline of a pre-existing phenotyping methodology allowing non-invasive and high-throughput estimation of rosette growth and rosette elevation in Arabidopsis (110). Once our new method was implemented, we could then investigate how growth and movement coordinate at the leaf level and we finally reported novel aspects on the involvement of light, PIFs and circadian clock in these processes.

My involvement in this project was in a first time to contribute to the development of the new analytical tools, to conduct consecutive validation tests as well as to implement these tools in the pre-existing pipeline. In a second time, I designed and performed research experiments in an autonomous manner, dealing with all the successive steps of our phenotyping pipeline. Finally, I analyzed and interpreted data in collaboration with the authors of the publication.

The Plant Cell, Vol. 26: 3911–3921, October 2014, www.plantcell.org

LARGE-SCALE BIOLOGY ARTICLE

Differentially Phased Leaf Growth and Movements in *Arabidopsis* Depend on Coordinated Circadian and Light Regulation[W]

Tino Dornbusch,[a] Olivier Michaud,[a] Ioannis Xenarios,[b] and Christian Fankhauser[a,1]

[a] Center for Integrative Genomics, Faculty of Biology and Medicine, University of Lausanne, 1015 Lausanne, Switzerland
[b] SIB-Swiss Institute of Bioinformatics, University of Lausanne, 1015 Lausanne, Switzerland

In contrast to vastly studied hypocotyl growth, little is known about diel regulation of leaf growth and its coordination with movements such as changes in leaf elevation angle (hyponasty). We developed a 3D live-leaf growth analysis system enabling simultaneous monitoring of growth and movements. Leaf growth is maximal several hours after dawn, requires light, and is regulated by daylength, suggesting coupling between growth and metabolism. We identify both blade and petiole positioning as important components of leaf movements in *Arabidopsis thaliana* and reveal a temporal delay between growth and movements. In hypocotyls, the combination of circadian expression of *PHYTOCHROME INTERACTING FACTOR4* (*PIF4*) and *PIF5* and their light-regulated protein stability drives rhythmic hypocotyl elongation with peak growth at dawn. We find that PIF4 and PIF5 are not essential to sustain rhythmic leaf growth but influence their amplitude. Furthermore, EARLY FLOWERING3, a member of the evening complex (EC), is required to maintain the correct phase between growth and movement. Our study shows that the mechanisms underlying rhythmic hypocotyl and leaf growth differ. Moreover, we reveal the temporal relationship between leaf elongation and movements and demonstrate the importance of the EC for the coordination of these phenotypic traits.

INTRODUCTION

The survival of most organisms on Earth depends on plants using solar energy, water, nutrients, and CO_2 to fuel their own growth. The conversion of solar into chemical energy happens primarily in leaves, but surprisingly little is known about the regulation of the growth of leaves themselves. It has been shown that growth of leaves and other plant structures occurs with a diel (24-h) rhythm (Nozue et al., 2007; Wiese et al., 2007; Yazdanbakhsh et al., 2011; Farré, 2012; Ruts et al., 2012a), which is not entirely surprising given that the ever-occurring day-night alternations profoundly affect plant metabolic reactions. The circadian clock and leaf starch metabolism regulate the growth patterns of roots and leaves (Wiese et al., 2007; Yazdanbakhsh et al., 2011; Ruts et al., 2012b). However, detailed kinetics of diel leaf growth rhythms, a prerequisite to understand the molecular mechanisms underlying growth control, remain scarce (Wiese et al., 2007; Ruts et al., 2012b). This presumably results from leaf movements accompanying leaf growth, thereby complicating growth analysis in living plants (Wiese et al., 2007).

Growth rhythms are best understood in hypocotyls (one-dimensional) where they depend on coordinated regulation by light, the availability of carbon, and the circadian clock (Nozue et al., 2007; Nusinow et al., 2011; Stewart et al., 2011). In the presence of sufficient resources, rhythmic hypocotyl growth peaks at the dark-light transition (dawn). This rhythm depends on an external coincidence mechanism whereby circadian expression of *PHYTOCHROME INTERACTING FACTOR4* and *5* (*PIF4* and *PIF5*) and light-regulated degradation of these basic helix-loop-helix factors leads to their maximal activity around dawn (Nozue et al., 2007). Repression of *PIF4* and *PIF5* expression earlier in the night depends on the evening complex, which is composed of EARLY FLOWERING3 (ELF3) and ELF4 and LUX ARRHYTHMO, and prevents excessive growth earlier in the night (Nusinow et al., 2011).

Different types of movements accompany rhythmic leaf growth (Wiese et al., 2007; Whippo and Hangarter, 2009; Dornbusch et al., 2012). Diel leaf movements are a well-characterized output of the circadian clock (Farré, 2012). In addition, movements with much shorter periods known as circumnutations occur in many plant structures including growing leaves (Stolarz, 2009; Whippo and Hangarter, 2009). All these movements are known to be associated with growth and/or reversible cell enlargement at the level of the petiole (the structure connecting the leaf blade to the stem). In some plant species, such as *Mimosa pudica*, specialized cells at the base of the petiole form the pulvinus that allows for rapid reversible changes in leaf position (Whippo and Hangarter, 2009). Plants like *Arabidopsis thaliana*, which do not possess such pulvini, also undergo leaf movements that at least partially depend on differential growth of the adaxial and abaxial sides of the petiole (Polko et al., 2012; Rauf et al., 2013). However, the coordination and relationship between leaf movements and growth remain largely unknown.

[1] Address correspondence to christian.fankhauser@unil.ch.
The author responsible for distribution of materials integral to the findings presented in this article in accordance with the policy described in the Instructions for Authors (www.plantcell.org) is: Christian Fankhauser (christian.fankhauser@unil.ch).
[W] Online version contains Web-only data.
www.plantcell.org/cgi/doi/10.1105/tpc.114.129031

The movements accompanying rhythmic leaf growth render kinetic growth analyses challenging, prompting some authors to prevent leaf movements to measure growth (Wiese et al., 2007). Moreover, simultaneous analyses of leaf growth and movements have not been reported previously, thereby making it difficult to understand the relationship between these phenomena. Here, we used near-infrared laser scanning and developed imaging algorithms that allow us to follow growth, nutations, and movements of the same leaves with high spatial and temporal resolution. We found that leaves accelerate elongation growth several hours prior to upward movements of the leaves (leaf hyponasty). Proper phasing between elongation and hyponasty depends on ELF3, a member of the evening complex. As in hypocotyls, leaf growth rhythms in day-night conditions are coordinately regulated by the interplay between light and circadian signals. However, our results in leaves show that the underlying molecular mechanism differs from the one that was previously uncovered for the regulation of hypocotyl growth.

RESULTS

Development of a Method for Simultaneous Analysis of Leaf Growth and Movements

To analyze the relationship between leaf growth and leaf movements, we developed an image analysis algorithm to measure single leaves using a previously described laser scanning method (Dornbusch et al., 2012). *Arabidopsis* plants were imaged at intervals of 60 min and time-lapse images were analyzed to track points at the base (P_0), petiole-blade-junction (P_P), and the tip (P_T) of each individual leaf (Figure 1A; Supplemental Figure 1 and Supplemental Movie 1). The vector P_0P_T defines length l_{tip} and elevation angle Φ_{tip} of each leaf, while the analogous traits for the petiole vector and blade vector are l_{pet}, Φ_{pet} and l_{bl}, Φ_{bl}, respectively (Figure 1A). A more detailed geometric definition of these traits is given in the Supplemental Methods. The leaf-tracking algorithm was validated comparing data from the laser scanning system with measurements on simultaneously photographed plants (Figures 2A and 2B; Supplemental Movie 2). This analysis demonstrated the precision of our system (Figures 2C and 2D). Although l_{tip} is somewhat shorter than the precise leaf length (l_{leaf}; Figure 1A), we showed that diel leaf elongation rate (integrated over 24 h) and the growth rhythms were highly similar for both l_{tip} and l_{leaf} (Figure 1B). Therefore, in the following, we primarily used the leaf elongation rate computed from l_{tip} to discuss the diurnal pattern of growth. Note that leaf expansion in width is not captured here and may occur at different times or rates. For simplicity, we refer to elongation rates as growth and changes in elevation angles as movements (Supplemental Figures 2A and 2B). When imaged at 10-min intervals, we can also measure ultradian circumnutations (nutations) that are distinct from the diurnal leaf movements (Supplemental Figure 2C).

Due to geometric constraints from the measuring device, the entire leaf can be scanned with the most precision in plants with relatively horizontal leaves. This dictated our choice to start our analysis with plants grown in long days (L/D, 16/8 h) that were released into continuous days (L/L) where the leaf positions remain relatively horizontal. Both growth and movements followed a rhythmically oscillating pattern consistent with circadian regulation of growth and movement (Figure 3; Supplemental Figure 2). By simultaneously analyzing growth rates and movements, we observed that the phase of both peaks was distinct (Figure 3; Supplemental Figure 2). Growth was minimal during the subjective night around zeitgeber time 20 (ZT20) and peaked in the subjective morning around ZT3-4. Leaf elevation angle Φ_{tip}

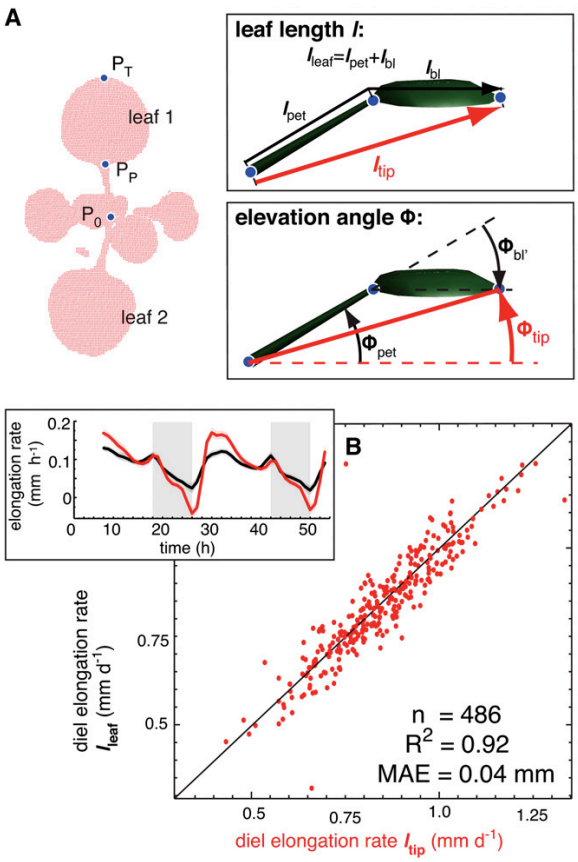

Figure 1. Definition of Measured Traits.

(A) Geometric definition of leaf length and elevation angle. *Arabidopsis* plant as a measured 3D point cloud (red dots) viewed from top down. The points P_0 (position of meristem), P_P (position of petiole-blade junction), and P_T (position of leaf tip) define length (l) and elevation angle (Φ) of the whole leaf (l_{tip}, Φ_{tip}), of the petiole (l_{pet}, Φ_{pet}), and of the blade (l_{bl}, Φ_{bl}) as illustrated in the insets.

(B) Comparison of diel (24 h) elongation rate using l_{tip} and elongation rate using l_{leaf} of leaf 1 and 2. One data point reflects one measurement per leaf per day. n = number of data points, R^2 = coefficient of determination, MAE = mean absolute error. Col-0 plants were grown for 14 d in long-day conditions (L/D, 16/8) before measurement in L/D; the inset shows time courses of elongation rate as moving average over 3 h using l_{leaf} (black line) or using l_{tip} (red line); vertical gray bars represent true night periods. The colored opaque band (same color as mean line) is the 95% confidence interval of mean estimate (solid line).

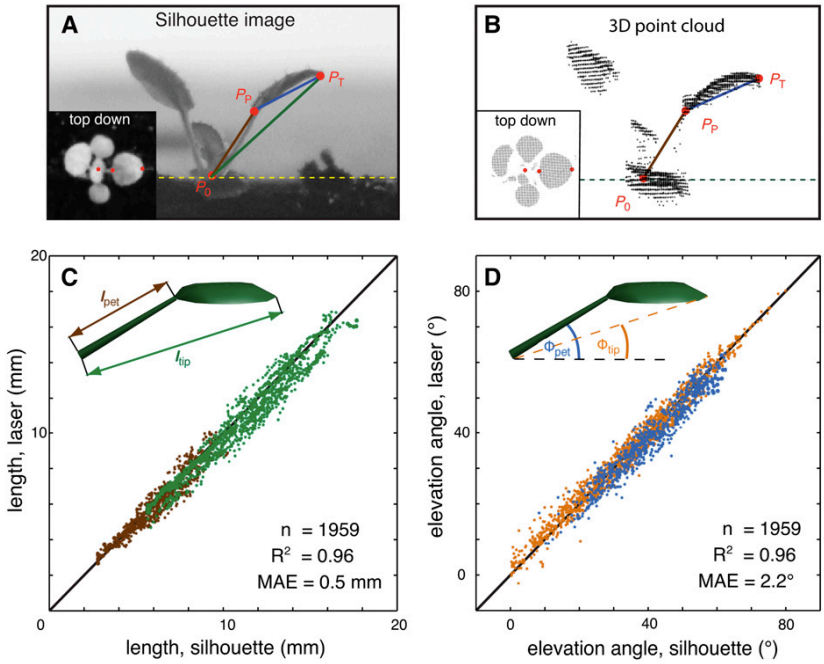

Figure 2. Development and Validation of a Method for Live Measurements of Leaf Growth and Leaf Movements.

(A) Silhouette image taken with an infrared-sensitive camera from the side and top-down (inset); three characteristic points define the dimension and orientation of each leaf and were manually selected: P_0, shoot apical meristem; P_P, blade-petiole junction; P_T, leaf tip.
(B) The laser scanner renders the plant surface as a 3D point cloud. The points P_0, P_P, and P_T are computed for each leaf using a semiautomated image analysis algorithm. We simultaneously photographed and scanned 27 individual leaves over 48 h and compared values for P_0, P_P, and P_T determined with each method.
(C) Length of petiole (brown dots) and leaf (green dots) measured from silhouette images (*x* axis) plotted against corresponding values computed with our algorithm (*y* axis).
(D) Petiole elevation angle (blue dots) and leaf elevation angle (orange dots) measured from silhouette images (*x* axis) plotted against corresponding values computed with our algorithm (*y* axis). One data point reflects one measurement per leaf per time step. Data of five different repeated control experiments were grouped together. Solid black line is the 1:1 line, *n* = number of data points, R^2 = coefficient of determination, and MAE = mean absolute error.

was minimal around ZT2 and reached a maximum in the subjective evening at ZT14 (Figure 3C; Supplemental Figure 2B). To better compare the growth rate with movement, we also plotted the rate of change of leaf position (in °h $^{-1}$) (Figures 3D and 4A). This method allows comparing acceleration of growth (slope in Figure 3B) with acceleration of up- and downward movement (slope in Figure 3D). It confirms a phase difference of ~3 h between acceleration of growth and movement (Figure 4A). Finally, we noticed that upward movement of leaves largely coincided with a phase of nutations that faded out around ZT16, when leaves started to move down (Supplemental Figure 2C).

Both Petiole and Blade Contribute to the Patterns of Leaf Growth and Hyponasty

By analyzing leaf growth and movement, we identified the temporal relationship between the phases of upward movement and acceleration of growth (Figures 3 and 4A). To uncover how blade and petiole contribute to these patterns, we measured them separately. Our measurements revealed that at ZT20 the leaf blade started to elongate several hours before the petiole (Figure 4B, arrows). This initial blade growth phase occurred at a time when both the petiole and the blade still moved down, explaining why the leaf tip moved downwards around subjective dawn (Figure 3C). The leaf blade accelerated its movement around ZT0 (Figure 4C) and moved upwards when it reached its maximal elongation rate (approximately ZT2), a time that also corresponded to an increase in petiole growth rate (Figure 4B). Petioles moved with similar amplitude as blades and accelerated their movement shortly after blades, but at a slower rate (Figure 4C). Similarly to the blades, they started to move upwards when reaching their maximal growth rate (Figures 4B to 4D). Finally, we noticed that while blade growth showed one growth peak shortly after subjective dawn, the petiole showed a morning growth peak and a second one before subjective dusk (Figure 4B). Petiole growth around ZT12 may explain the second growth peak observed in L/L conditions (Figures 3B and 4B). These experiments indicate that around subjective dawn both growth and movement first start in the blade and then in the

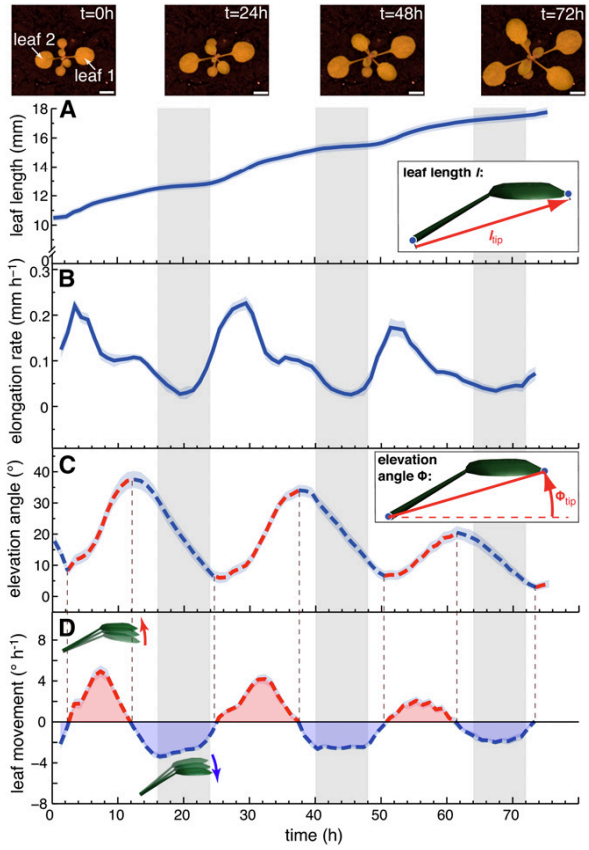

Figure 3. The Pattern of Leaf Growth and Movements in Constant Light.

Length **(A)**, elongation rate **(B)**, elevation angle **(C)**, and movements **(D)** (angular rate of change) of leaves 1 and 2 in continuous day (L/L) measured on 43 leaves (30 plants). l_{tip} **[A]** and **[B]**) and Φ_{tip} **[C]** and **[D]**) were used to compute the graphs. Images on top show a representative plant at times (t = 0, 24, 48, and 72 h) during the experiment (bar = 5 mm). Parts of the graph in **(C)** highlighted in red represent phases of upward and parts highlighted in blue phases of downward movement. Col-0 plants were grown for 14 d in standard L/D conditions. At time 0 h (ZT0), lights were switched on for imaging and kept on in L/L. Vertical gray bars represent subjective night periods. Leaf elongation rate was computed as mean moving average (3 h) of 43 individual curves. Leaf elevation angle and movement rates are mean values. The opaque band around the mean lines is the 95% confidence interval of mean estimate.

petiole. Moreover, in both parts of the leaf rapid upward movement starts significantly later than acceleration of growth (Figures 3 and 4).

To determine whether leaf blade position also contributes to leaf hyponasty in other growth conditions, we analyzed blade and petiole position in L/D-grown plants and in plants transferred into simulated shade, which is known to enhance leaf hyponasty (Moreno et al., 2009; Dornbusch et al., 2012). In both conditions, blade movement clearly contributed to overall leaf hyponasty (Supplemental Figures 3 and 4). Moreover, both in L/D conditions and in response to simulated shade, the blade started to move upwards prior to the petiole (Supplemental Figures 3 and 4, arrows).

Collectively, these experiments identify the movement of the blade as an important contributor to leaf hyponasty and show that blade movement precedes petiole movements.

Changes in the Light Environment Differentially Affect Leaf Growth and Movements

Earlier studies in *Arabidopsis* have identified a differential growth response between the adaxial and abaxial sides of the petiole as a mechanism underlying leaf hyponasty (Polko et al., 2012; Rauf

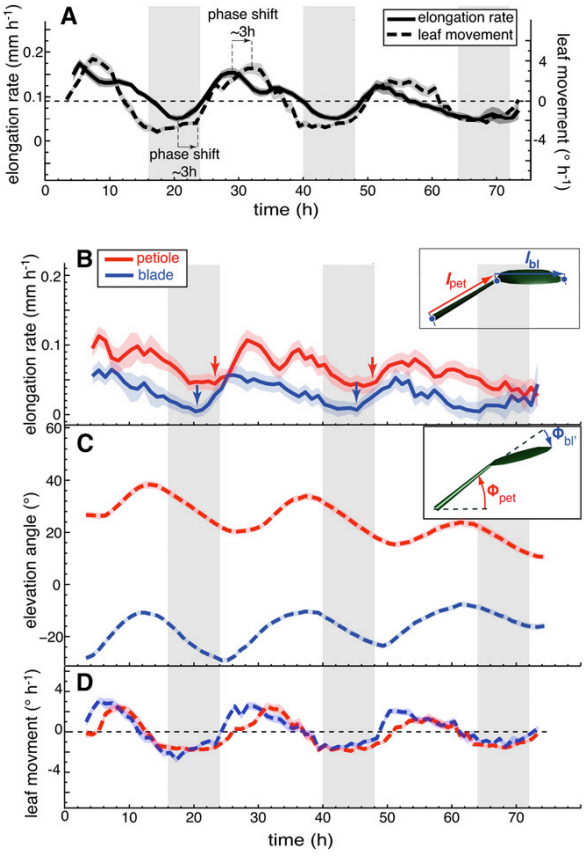

Figure 4. Blade and Petiole Movements Contribute to the Leaf Hyponastic Response.

(A) Leaf elongation rate and leaf movements (angular rate of change) of leaves 1 and 2 in continuous day were replotted from Figures 3B and 3D for better direct comparison.

(B) to **(D)** Leaf elongation rate **(B)**, leaf elevation angle **(C)**, and leaf movements **(D)** (angular rate of change) of petioles (in red) and blades (in blue) of leaves 1 and 2 in continuous day (L/L) measured on 32 leaves. Col-0 plants were grown for 14 d in standard L/D conditions. At time 0 h, lights were switched on for imaging and kept on in L/L. Vertical gray bars represent subjective night periods. Leaf elongation rate is computed as mean moving average (3 h) of 32 individual curves. Leaf elevation angle and movement rates are mean values. The opaque band around the mean lines is the 95% confidence interval of mean estimate. Arrows indicate acceleration of growth.

et al., 2013). This suggests that *Arabidopsis* leaf hyponasty is primarily a growth-driven process. Our work shows that there is a temporal shift between growth and movement (Figures 3 and 4; Supplemental Figures 3 and 4), suggesting a more complex relationship between these two processes. To test this further, we analyzed growth and movement in plants grown in different light regimes and plotted diel (24 h) growth rates and diel leaf movements (Figure 5). This comparison showed that a decrease in PAR and a decrease in daylength alter the relationship between growth and movements. In short-day conditions (S/D), diel leaf growth rate was decreased, whereas the magnitude of diel movements was similar in S/D compared with L/L or L/D (Figure 5). Low PAR-grown plants also showed decreased growth but increased diel leaf movements compared with L/L or L/D (Figure 5) consistent with other findings of low-PAR-induced hyponasty (Keller et al., 2011). These experiments suggest a partial uncoupling between the magnitude of growth and movement.

Light Is Required to Initiate Leaf Growth at Dawn

Rhythmic growth of hypocotyls is regulated by a combination of circadian and light cues (Nozue et al., 2007); we thus compared leaf growth and movements between plants maintained in day-night

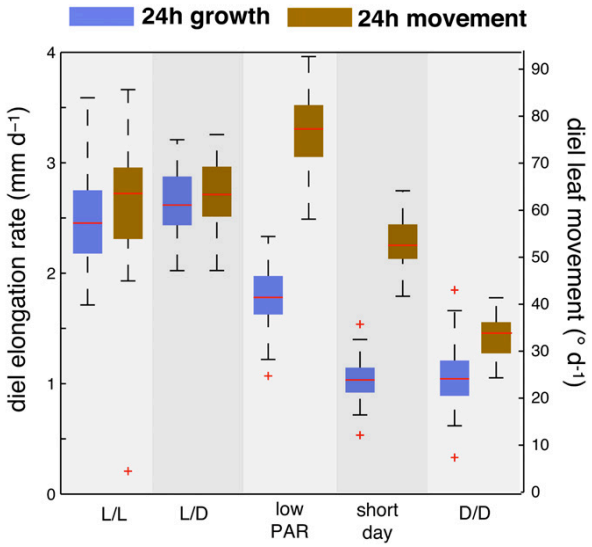

Figure 5. The Magnitude of Growth and Movements Is Differentially Affected by Decreasing Light Intensity and Daylength.

Diel leaf elongation rate and leaf movement of leaves 1 and 2 (24 h period). Diel elongation rates and leaf movements (absolute changes in leaf elevation angle) were computed by summing hourly rates over a period of 24 h starting from ZT2.25. Col-0 plants were grown for 14 d in standard L/D conditions (16/8 h). At time 0 h, plants were imaged for 24 h in constant light (L/L; n_{leaf} = 43), maintaining day-night cycles (L/D, n_{leaf} = 27), reducing the light intensity (low PAR) but maintaining L/D (PAR=35 µmol m^{-2} s^{-1}; n_{leaf} = 57) and in continuous darkness (D/D; n_{leaf} = 41). For the S/D experiment Col-0 was grown for 18 d in S/D (8/16 h) before imaging under the same conditions (n_{leaf} = 47). n_{leaf} = number of measured leaves.

and plants released into constant light (L/L). In L/L, growth rates started to rise several hours before the subjective dawn (ZT20), whereas in L/D, growth did not recover until dawn (ZT0). As light was given, the growth rate rose very quickly to reach the same rate as in LL (Figure 6A, arrows). In L/D-grown plants, the increase of the growth rate coincided with lights on but the timing of the morning peak was similar in L/D and L/L (Figure 6A). The second growth peak preceding dusk at ZT16 was more pronounced in L/D than L/L (Figure 6A). The diurnal pattern of the leaf elevation angle was similar in L/D and L/L. Minimum values for Φ_{tip} were observed at the time of the morning growth peak at ZT3 and maximum values around ZT13-14 (Figure 6B). Hence, similar phasing between growth and movements was maintained in both conditions (Figure 6B). In our growth chamber, light-dark transitions are abrupt. At dusk, this coincided with a transient upward movement (strong acceleration of movement) (Figures 6B and 6C). Downward movement accelerates in the second half of the night followed by a brief reacceleration of first downward then upwards movement at dawn (Figure 6C). Our data thus show that the circadian clock regulates both movement and growth rhythms and that day-night transitions influence these patterns.

When grown in day-night conditions, the leaf growth rate was at its minimum at the end of the night (ZT0) and rapidly increased after dawn (Figure 6). To test whether light is essential to induce growth in the morning, we entrained plants in L/D (16/8 h) and imaged them prolonging the night for 3 h before dusk ($L/_{+3}D$) or after dawn (L/D_{+3}). At L/D_{+3}, leaves did not start growing at ZT0 but at actual dawn ZT3 (Figure 7A; Supplemental Figure 5A). At $L/_{+3}D$, the first growth peak remained at ZT0, but the second growth peak was shifted to ZT13 (Figure 7B; Supplemental Figure 5B). To determine whether light is sufficient to trigger growth, we shortened the night by 3 h ($L/_{-3}D$). Early onset of the day ($L/_{-3}D$) triggered growth, although not as sharply as dawn in plants grown in L/D (Figure 7C; Supplemental Figure 5C). These experiments show that light at dawn has a profoundly different effect on growth of hypocotyls and leaves: In leaves it triggers growth (Figures 6 and 7), while in hypocotyls it inhibits it (Nozue et al., 2007).

The need for light at dawn to initiate leaf growth could result from the need for photosynthates. We decided to indirectly test this idea by growing plants in different light regimes. Plants partition more resources into starch when grown in short days (S/D) than in long days, suggesting that they may have more resources available to fuel growth early in the morning when grown in L/D (Stitt and Zeeman, 2012; Sulpice et al., 2014). We therefore compared growth and movements in S/D- and L/D-grown plants and found that in both conditions, growth in the morning required light and that the morning growth peak was reduced in S/D compared with L/D (Supplemental Figure 6A). In contrast to L/D conditions, we could not detect a second growth peak preceding dusk (ZT8), but rather a peak during the night at ZT12 (Supplemental Figure 6A). Overall growth was reduced in S/D-grown plants but more growth (in relative terms) occurred at night in S/D-grown plants than in L/D plants (Supplemental Figure 6A). As S/D-grown plants invest more resources into starch, this finding is compatible with a metabolic role of light in the regulation of growth patterns (Stitt and Zeeman, 2012; Sulpice et al., 2014). In contrast to diel growth rates, daylength moderately affected the pattern and the magnitude of diel leaf movements, except that dusk

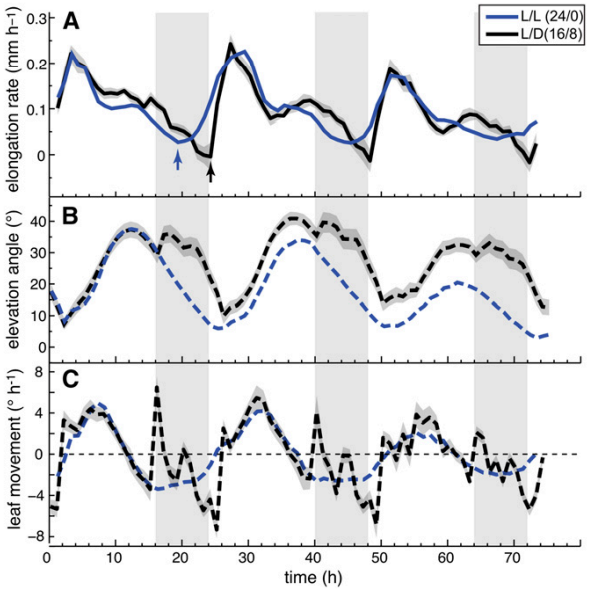

Figure 6. Day-Night Transitions Alter Rhythmic Growth and Movements.

Leaf elongation rate **(A)**, leaf elevation angle **(B)**, and leaf movements **(C)** (angular rate of change) of leaves 1 and 2 in continuous day (L/L; blue line; n_{leaf} = 43) and long-day conditions (L/D; 16/8; black line, n_{leaf} = 27). Col-0 plants were grown for 14 d in standard L/D conditions. Beginning from time 0 h, plants were imaged either in L/L or in L/D. Vertical gray bars represent subjective or true night periods. Leaf elongation rate was computed as mean moving average (3 h) of individual curves. Leaf elevation angle and movement rates are mean values. The opaque band around the mean lines is the 95% confidence interval of mean estimate. Arrows indicate acceleration of growth and n_{leaf} = number of measured leaves. l_{tip} and Φ_{tip} were used to compute the graphs.

altered leaf position in L/D but not in S/D (Figure 5; Supplemental Figure 6A).

Our results suggest that light-induced metabolism is required to promote leaf growth. To test this further, we compared growth of L/D-grown plants in either in high or low PAR and found that in low PAR the magnitude of leaf growth was reduced (Figure 5). We also transferred L/D-grown plants into D/D, which led to a decrease in the diel growth rate (Figure 5). Consistent with our night extension experiment (Figure 7A), there was no growth induction shortly after subjective dawn in D/D (Supplemental Figure 6B); however, there was a transient growth peak around ZT6-8 (Supplemental Figure 6B). Upon return into the light, the leaf growth rate increased rapidly (Supplemental Figure 6B, black arrow). Taken together, our results are consistent with a metabolic role of light to initiate leaf growth at dawn (Figures 5 to 7; Supplemental Figures 5 and 6).

The Phase Relationship between Leaf Growth and Movements Requires a Functional Evening Complex

Our results show that day-night cycles interplaying with the circadian clock orchestrate the diurnal patterns of growth and movement. Rhythmic hypocotyl growth is also coordinately controlled by the circadian clock and light cues that converge on the regulation of PIF4 and PIF5 (Nozue et al., 2007). We thus analyzed leaf growth and movements of *pif4 pif5* double mutants and found that, when grown in long days, this mutant displayed low amplitude growth and movement rhythms that were otherwise similar to those of the wild type (Figure 8A). Overexpression of PIF4 or PIF5 and photoreceptor mutants caused a reduction of the amplitude in hypocotyl growth rhythms (Nozue et al., 2007). The situation was different for leaf growth as PIF4 overexpression and *phyB* mutants maintained robust leaf growth rhythms, although in these mutant backgrounds, there was more leaf growth toward the end of the day (Supplemental Figure 7). High PIF4 and PIF5 activity is prevented early in the night by the evening complex that restricts the expression of *PIF4* and *PIF5* and hypocotyl growth during the night (Nozue et al., 2007; Nusinow et al., 2011). To investigate the role of the evening complex in rhythmic leaf growth,

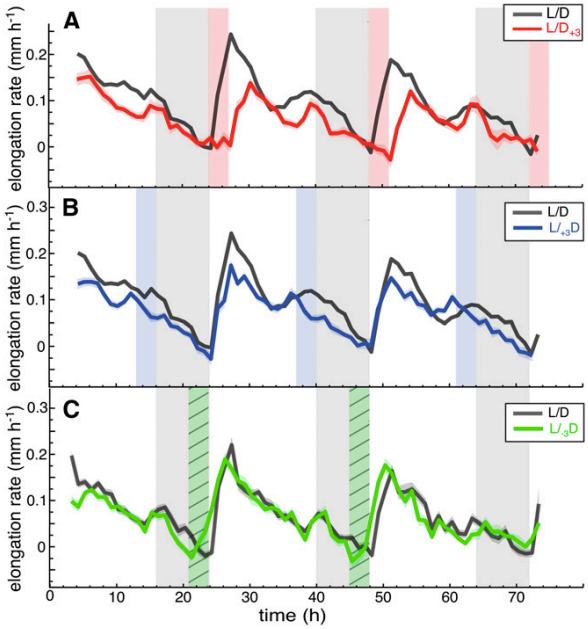

Figure 7. Light Is Required at Dawn to Trigger Leaf Growth.

(A) Leaf elongation rate of leaves 1 and 2 in long day (L/D, black line, n_{leaf} = 27) and in +3 h prolonged night period after dawn (L/D+3; red line n_{leaf} = 27).

(B) Leaf elongation rate in L/D (black line) and in +3 h prolonged night period before dusk (L/+3D; blue line, n_{leaf} = 54).

(C) Leaf elongation rate and leaf elevation angle of leaves 1 and 2 where night was shortened before dawn by −3 h (L/-3D; green line, n_{leaf} = 35; L/D control; black line, n_{leaf} = 42). Col-0 plants were grown for 14 d in standard L/D (16/8) conditions before measurement; vertical gray bars represent true night periods; vertical red/blue bars indicate prolonged night periods (**[A]** and **[B]**) and vertical hatched green bar shortened night period **(C)**. Leaf elongation rate was computed as mean moving average (3 h) of individual curves. The opaque band around the mean lines is the 95% confidence interval of mean estimate, and n_{leaf} = number of leaves. Day 1 of the experiment represents the first day when the plants were subjected to an abrupt change in night length. l_{tip} was used to compute the graphs.

we analyzed the *elf3* mutant. When grown in long days, the major growth peak of *elf3* was moved forward and was no longer dependent on light, indicating that the evening complex prevents leaf growth at night (Figure 8B, arrows) (Nozue et al., 2007). In addition, maximal growth rates in the *elf3* mutant coincided with maximal leaf angles, showing that ELF3 is needed to maintain the normal phase relationship between leaf growth and movement (Figure 8B, arrows). Analysis of *elf3* and *pif4 pif5* grown in constant light confirmed the importance of the circadian clock for rhythmic growth and movements and revealed a moderate phase phenotype in *pif4 pif5* (Figures 8C and 8D). Collectively, our data show that the mechanisms responsible for rhythmic growth in leaves and hypocotyls differ and reveal that ELF3 is required for normal phasing between leaf growth and movements.

DISCUSSION

Live measurements of leaf growth and/or leaf movements have been reported before (Wiese et al., 2007; Walter et al., 2009; Bours et al., 2012); our method is unique in that it simultaneously but separately reports on both growth and movements (Figure 3; Supplemental Figure 2). By imaging at sufficient frequency (every 10 min rather than hourly), we reduce the number of plants that we can simultaneously analyze, but this enables us to characterize circumnutations (Supplemental Figure 2C). Future work should allow us to better understand the mechanisms underlying this well-known form of "rapid" plant movements that have been discussed since the times of Charles Darwin but remain poorly understood (Whippo and Hangarter, 2009). The geometry of the laser scanning system is well suited for relatively flat and horizontally oriented objects like an *Arabidopsis* rosette. Imaging the entire leaf, in particular the blade-petiole junction, becomes difficult when leaves are erect, which is why we use l_{tip} rather than l_{leaf} (Figure 1). Importantly, our data show that l_{tip} is an excellent proxy to determine leaf elongation rates (Figure 1B). Moreover, our data correlate well with relative leaf surface growth rhythms (our own observations) and with previous publications (Wiese et al., 2007; Walter et al., 2009; Ruts et al., 2012b). However, in previous reports, in *Arabidopsis* rosettes grown in 12/12 cycles, they also identified growth peaks early in the morning and toward the end of the day similar to our data in long days (16/8; Figure 6) (Wiese et al., 2007; Ruts et al., 2012b).

By simultaneously tracking leaf movements and growth, we determined that elongation growth precedes upward movement of the leaf (Figures 3, 4, and 6, Supplemental Figures 5 and 6). This is true when analyzed at the level of the entire leaf, the blade, and the petiole (Figure 4). We thus conclude that a change in leaf hyponasty is consistent with differential petiole growth as determined before (Polko et al., 2012; Rauf et al., 2013), but in addition blade growth and elevation angle (relative to the petiole) also contribute to the overall leaf position (Figure 4). We demonstrate the importance of leaf blade position in leaf hyponasty in several growth conditions (L/L, L/D, and simulated shade), suggesting that this is a general feature of the leaf hyponastic response (Figure 4; Supplemental Figures 3 and 4). In all cases, the analyzed upward movements were initiated as the leaf (or part of it) reached its maximal elongation rate (Figures 4 and 6; Supplemental Figures 5 and 6), demonstrating a correlation between both processes (although with temporal delays). This finding is consistent with the fact that as leaves age both growth and movements decline (Mullen et al., 2006). However, our work also reveals that coupling between growth and movements is a regulated process as environmental stimuli differentially affect growth and movements (Figure 5). For example, when PAR was diminished, the leaf growth rate declined but the leaf movements increased (Figure 5). Moreover, in the *elf3* mutant, the phase relationship between the peak of growth and elevation angle was strongly altered (Figure 8B). Growth of different parts of the blade and petiole may contribute differentially to overall growth and changes in elevation angle and thereby explain the complex relationship between growth and movement reported here (Figure 4) (Wiese et al., 2007; Andriankaja et al., 2012; Polko et al., 2012; Remmler and Rolland-Lagan, 2012). In addition, reversible turgor pressure-driven changes in cell size may also contribute to changes in leaf hyponasty (Mullen et al., 2006; Barillot et al., 2010).

By separately analyzing growth and movement of blades and petioles, we observed that blades started to grow and move upwards 2 to 3 h before the petiole (Figure 4). One possibility is that this is regulated by the combined action of auxin and carbohydrates (Lilley et al., 2012). Interestingly, rhythms in auxin responsiveness and soluble carbohydrates correlate quite well (Covington and Harmer, 2007). As the leaf blade is considered as a major source of auxin production (Tao et al., 2008), we propose that blade growth occurs before petiole growth because auxin first needs to be transported to the petiole. Interestingly, in L/L conditions, a second growth peak occurred in petioles that we did not observe in the blade (Figure 4), indicating that the growth pattern is more complex in the petiole than the blade. Based on the analysis of overall leaf growth, we can also conclude that these patterns are environmentally regulated (Figure 5). To fully understand the relationship between growth and movements, our organ-level analysis needs to be combined with the determination of growth patterns with cellular resolution, which is very challenging at the level of expanded leaves (Ichihashi et al., 2011; Andriankaja et al., 2012; Polko et al., 2012).

By moving plants into constant darkness and performing night extension or shortening experiments, we showed the requirement for light to initiate growth at dawn (Figures 6 and 7; Supplemental Figure 6B). The earlier rise of the growth rate observed in plants entrained in L/D for which the night was shortened by 3 h is consistent with the rise in growth at ZT20 observed in plants transferred into L/L (compared with Figures 3 and 7C). Importantly, when the night is extended by 3 h before the dark phase, the timing of the morning growth-peak was unaffected (Figure 7B). By contrast, extending the night by 3 h in the morning delayed the acceleration of growth until the actual onset of light (Figure 7A). Plants precisely regulate starch degradation during the night and almost completely exhaust their reserves by dawn (Stitt and Zeeman, 2012). Starch metabolism is immediately adjusted if the night is extended due to an early onset but not if the night is extended beyond the subjective dawn. Moreover, exhaustion of starch resources at the end of the night limits *Arabidopsis* growth (Graf et al., 2010). These data together with our results suggest that light at dawn fuels leaf growth if growth repression by the circadian clock is released (Figures 6 and 7; Supplemental Figure 5). Performing growth experiments in a low CO_2 environment

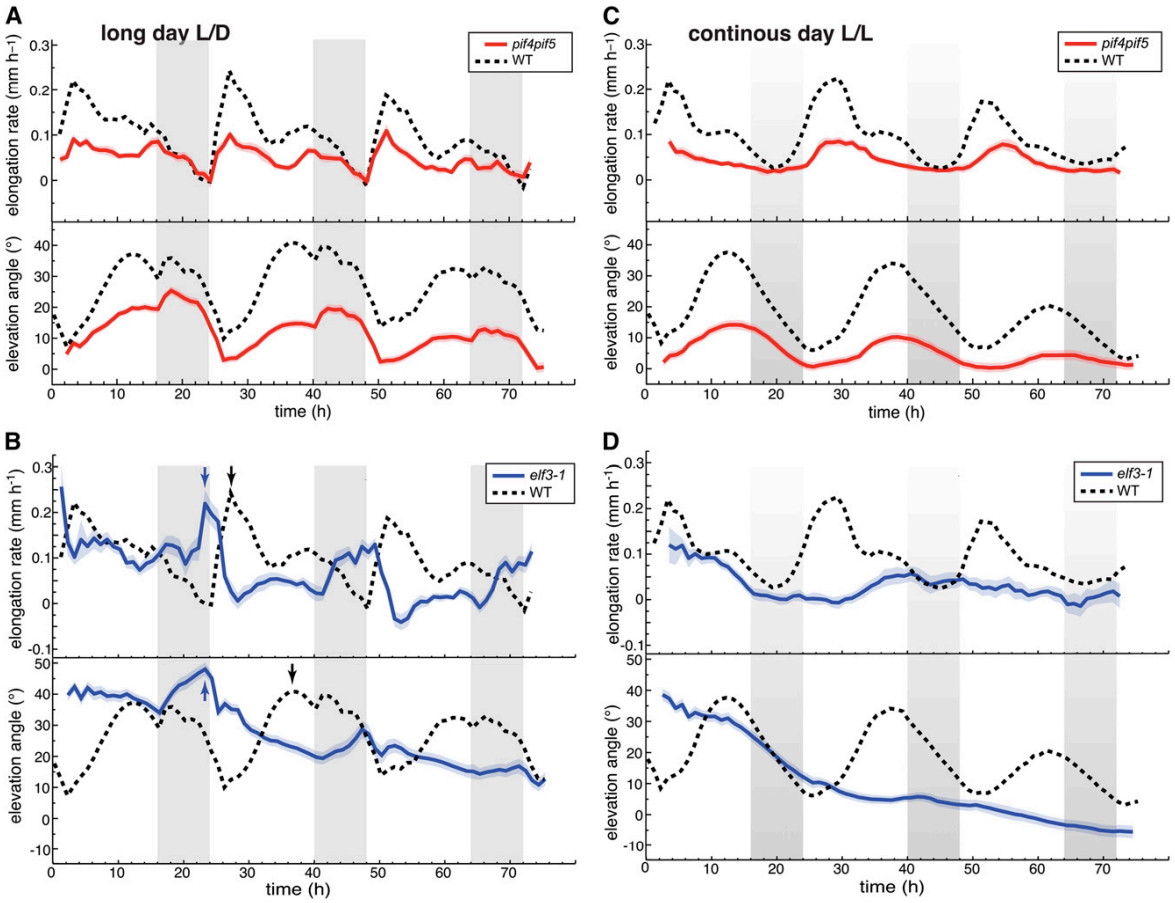

Figure 8. The Role of PIF4, PIF5, and ELF3 in Establishing Rhythmic Leaf Growth and Movement.

Leaf elongation rate and leaf elevation angle of leaves 1 and 2. Col-0, *elf3-1*, and *pif4 pif5* plants were grown for 14 d in standard L/D conditions. Beginning from time 0 h, plants were imaged either in L/D (**[A]** and **[B]**) or in L/L (**[C]** and **[D]**). Leaf elongation rate was computed as mean moving average (3 h) of individual curves. Leaf elevation angle are mean values. Vertical gray bars represent subjective or true night periods. The opaque band around the mean lines is the 95% confidence interval of mean estimate. n_{leaf} = number of measured leaves. I_{tip} and Φ_{tip} were used to compute the graphs.

(A) *pif4 pif5* double mutant grown and imaged in long-day conditions n_{leaf} = 48.

(B) Clock mutant *elf3-1* grown and imaged in long-day conditions n_{leaf} = 45. Note that in *elf3-1* the peaks of elevation angle and maximal growth coincide (blue arrows), while in the wild type there is a large phase shift between the two peaks (black arrows).

(C) *pif4 pif5* double mutant entrained in L/D and imaged in continuous light n_{leaf} = 46.

(D) *elf3-1* entrained in L/D and grown in continuous light n_{leaf} = 23.

or treating plants with photosynthesis inhibitors would be appropriate ways to further test this hypothesis. Short-day grown plants accumulate more starch during the day in order to have enough resources at night. In such conditions, fewer resources will be immediately available for growth in the morning (Stitt and Zeeman, 2012). Consistent with this idea, our data show that the morning growth peak in short-day grown plants is reduced compared with long-day-grown plants (Supplemental Figure 6A). Also consistent with this metabolic model is the relatively enhanced growth at night in short-day plants (Supplemental Figure 6A) (Sulpice et al., 2014), reduced growth in low PAR conditions (Figure 5), and the fact that starchless mutants invest more resources in growth during the day when solar energy is present (Wiese et al., 2007). It was recently reported that a long-term consequence of sugar starvation is a reduction of gibberellin biosynthesis that limits growth (Paparelli et al., 2013). However, it is unlikely that this gibberellin response can explain the immediate effect of light on growth in the morning reported here (Figures 6 and 7). Finally, we wish to point out that when wild-type plants are kept in darkness for extended periods of time a short pulse of growth occurs ~6 to 8 h after subjective dawn (Supplemental Figure 6B). This experiment indicates that alternative metabolic pathways (e.g., induction of autophagy) can be

activated to fuel growth under exceptional circumstances (Usadel et al., 2008; Suttangkakul et al., 2011; Izumi et al., 2013).

ELF3 regulates rhythmic growth of leaves, hypocotyls, and roots (Figure 8) (Nozue et al., 2007; Nusinow et al., 2011; Yazdanbakhsh et al., 2011). Our work identifies similarities and differences for ELF3 function in these different organs. In all organs, growth at night is restricted by ELF3 (Figures 8B and 8D) (Nozue et al., 2007; Nusinow et al., 2011; Yazdanbakhsh et al., 2011). The leaf growth peak toward the end of the night in *elf3* is surprising given that in the wild type, light in the morning is essential to trigger growth (Figures 6 and 7). A possible explanation for this observation is the incomplete starch degradation during the night in *elf3* (Yazdanbakhsh et al., 2011). This may explain how this mutant has sufficient resources at the end of the night to enhance leaf growth without the need for light (Figure 8). Interestingly, long-day-grown *elf3* mutants have reduced leaf growth, contrasting with enhanced rates of root and hypocotyl growth in this mutant (Figure 8) (Nozue et al., 2007; Nusinow et al., 2011; Yazdanbakhsh et al., 2011). These organ-specific effects on growth might be due to different partitioning of resources in *elf3* (Yazdanbakhsh et al., 2011).

In hypocotyls, the circadian expression of *PIF4* and *PIF5* in conjunction with light-induced PIF4 and PIF5 protein degradation explains a rhythmic growth pattern with a major peak at dawn (Nozue et al., 2007). The analysis of leaf growth in the wild type and *pif* mutants suggests that in leaves light does not shape growth rhythms primarily by influencing PIF4 and PIF5 abundance. First, the leaf growth peak occurs several hours after dawn, which is not consistent with light-induced degradation of growth-promoting PIFs explaining this pattern (Figure 6). Second, in leaves, the *pif4 pif5* mutant maintains a growth rhythm similar to the wild type but with a reduced amplitude (Figure 8). Third, PIF4-overexpressing plants and *phyB* mutants that show reduced PIF4 degradation (de Lucas et al., 2008) maintain leaf growth rhythms with a robust amplitude in contrast to hypocotyls where this leads to dampened growth rhythms (Supplemental Figure 7) (Nozue et al., 2007). Our night extension and day-length experiments suggest that the light regulation of leaf growth has a metabolic component (Figures 6 and 7; Supplemental Figures 5 and 6). However, leaf growth patterns in constant light and reduced growth in *pif4 pif5* clearly show the importance of PIF4, PIF5, and the circadian clock in regulating this process (Figures 6 and 8; Supplemental Figure 7). Thus, rhythmic leaf and hypocotyl growth are regulated by distinct mechanisms with a different role of light in shaping growth rhythms in both organs. It will be interesting to further contrast these growth rhythms in young leaves that largely rely on their own resources with those of roots or hypocotyls that depend on photosynthates exported from the leaves.

Finally, we would like to briefly speculate on the biological significance of diel rhythms of leaf growth rates and movements. A maximal peak of growth during the first few hours of the day matches with favorable conditions in terms of energetic requirements, water availability, and auxin responsiveness (Covington and Harmer, 2007; Nozue et al., 2007; Stitt and Zeeman, 2012). Availability of resources also explains why more growth is observed at night in short-day-grown plants than in long-day-grown plants and the larger growth peak at dawn when *Arabidopsis* is grown in long days (Figure 6; Supplemental Figure 6) (Sulpice et al., 2014). The temperature cycles that accompany day-night transitions also contribute to the growth pattern (Sidaway-Lee et al., 2010; Bours et al., 2013). We note that the maximal growth rate identified in our conditions corresponds to the early morning when temperature is typically relatively low (Figure 6). Interestingly, leaf elevation follows the typical daily temperature fluctuations with a peak in the late afternoon. Elevating leaves with this pattern is favorable to cool leaves during the warm hours of the day and diminishes the radiation load at times when it surpasses photosynthetic capacity (Bridge et al., 2013).

METHODS

Plant Material and Growth Conditions

The *Arabidopsis thaliana* ecotype Columbia-0 (Col-0), the *pif4 pif5* mutant (Nozue et al., 2007), and the *elf3-1* mutant (Liu et al., 2001) were grown on soil saturated with deionized water in a Percival CU-36L4 incubator (Percival Scientific) at 21°C, R_H = 85% relative humidity, and EP_{AR} = 180 µmol m^{-2} s^{-1} for 13 d under long-day (16/8 h) or 17 d under short-day (8/16 h) conditions. Plants were transferred to the ScanAlyzer HTS (Lemnatec) 24 h before scanning for adaptation maintaining the day-night cycles and light conditions in the incubator. At the beginning of the scanning (at time t = 0), conditions were adjusted according to experiment (e.g., L/L or low PAR). The light intensity in the measurement chamber was E_{PAR} = 165 µmol m^{-2} s^{-1} and reduced to E_{PAR} = 35 µmol m^{-2} s^{-1} for the low PAR treatment. The red/far-red ratio (R/FR) was decreased from R/FR = 5.59 to R/FR = 0.49 using far-red-emitting diodes. Further experimental details, spectral composition of light, computation of R/FR ratio, and technical specification of the phenotyping device are described in more detail by Dornbusch et al. (2012) and are available on our website (http://plantgrowth.vital-it.ch).

Analysis of Leaf Growth Rates and Elevation Angles

Plants were scanned at intervals of 10 and 60 min. In the time-lapse images, the distance of measured plant surface points from a reference plane was color-coded (Supplemental Figure 1). Images were transformed into 3D point clouds as described by Dornbusch et al. (2012), which yields a precise representation of plant surfaces over time (Supplemental Movie 1). A detailed description of the geometric definition of leaf length and elevation angle and image and data processing is presented in the Supplemental Methods.

Supplemental Data

The following materials are available in the online version of this article.

Supplemental Figure 1. Image Analysis Algorithm to Compute P_P and P_T from Time-Lapse Images.

Supplemental Figure 2. Definition of Principal Output.

Supplemental Figure 3. In Response to a Low R/FR Treatment the Blade Upward Movement Precedes the Petiole Upward Movement.

Supplemental Figure 4. In L/D Conditions the Blade Upward Movement Precedes the Petiole upward Movement.

Supplemental Figure 5. Light Is Required at Dawn to Trigger Leaf Growth.

Supplemental Figure 6. Growth and Movements Are Altered by Shortening Daylength or in Continuous Darkness.

Supplemental Figure 7. Plants with Elevated Levels of PIF4 Maintain Leaf Growth Rhythms Robust in Amplitude.

Supplemental Methods. Detailed Description of Geometric Definition of Leaf Length and Elevation Angle, Image Processing, and Data Processing.

Supplemental Movie 1. Semiautomated Leaf Tracking on Time-Lapse 3D Images of Growing *Arabidopsis* Plant.

Supplemental Movie 2. Comparison of Leaf Tracking on 3D Images with Manual Leaf Selection on Simultaneously Photographed Growing *Arabidopsis* Plant.

ACKNOWLEDGMENTS

This project was funded by grants from the Swiss SystemX.ch project ('SyBIT' to I.X. and 'Plant Growth in a Changing Environment' to I.X. and C.F.) and the University of Lausanne. T.D. benefitted from a Marie Curie Intra-European Fellowships (No. 275999). We thank the Department of Molecular Plant Biology of UNIL for access to their plant facilities. We thank Seth Davis for providing *elf3-1* seeds and Mieke de Wit, Tobias Preuten, and Samuel Zeeman (ETH, Zürich) for comments on the article. We thank Dmitry Kuznetsov, Arnaud Fortier, Hon Wai Wan, and Robin Liechti for their help in maintaining the knowledge and phenotyping resource (plantgrowth.vital-it.ch). The computations were performed at the Vital-IT Center (http://www.vital-it.ch) for high-performance computing of the SIB-Swiss Institute of Bioinformatics.

AUTHOR CONTRIBUTIONS

T.D. designed research, contributed new analytic computational tools, performed research, analyzed data, and wrote the article. O.M. designed research, contributed new analytic computational tools, performed research, and analyzed data. I.X. contributed new analytic computational tools. C.F. designed research, analyzed data, and wrote the article.

Received June 19, 2014; revised September 4, 2014; accepted September 19, 2014; published October 3, 2014.

REFERENCES

Andriankaja, M., Dhondt, S., De Bodt, S., Vanhaeren, H., Coppens, F., De Milde, L., Mühlenbock, P., Skirycz, A., Gonzalez, N., Beemster, G.T., and Inzé, D. (2012). Exit from proliferation during leaf development in *Arabidopsis thaliana*: a not-so-gradual process. Dev. Cell **22:** 64–78.

Barillot, R., Frak, E., Combes, D., Durand, J.L., and Escobar-Gutiérrez, A.J. (2010). What determines the complex kinetics of stomatal conductance under blueless PAR in *Festuca arundinacea*? Subsequent effects on leaf transpiration. J. Exp. Bot. **61:** 2795–2806.

Bours, R., Muthuraman, M., Bouwmeester, H., and van der Krol, A. (2012). OSCILLATOR: A system for analysis of diurnal leaf growth using infrared photography combined with wavelet transformation. Plant Methods **8:** 29.

Bours, R., van Zanten, M., Pierik, R., Bouwmeester, H., and van der Krol, A. (2013). Antiphase light and temperature cycles affect PHYTOCHROME B-controlled ethylene sensitivity and biosynthesis, limiting leaf movement and growth of Arabidopsis. Plant Physiol. **163:** 882–895.

Bridge, L.J., Franklin, K.A., and Homer, M.E. (2013). Impact of plant shoot architecture on leaf cooling: a coupled heat and mass transfer model. J. R. Soc. Interface **10:** 20130326.

Covington, M.F., and Harmer, S.L. (2007). The circadian clock regulates auxin signaling and responses in Arabidopsis. PLoS Biol. **5:** e222.

de Lucas, M., Davière, J.M., Rodríguez-Falcón, M., Pontin, M., Iglesias-Pedraz, J.M., Lorrain, S., Fankhauser, C., Blázquez, M.A., Titarenko, E., and Prat, S. (2008). A molecular framework for light and gibberellin control of cell elongation. Nature **451:** 480–484.

Dornbusch, T., Lorrain, S., Kuznetsov, D., Fortier, A., Liechti, R., Xenarios, I., and Fankhauser, C. (2012). Measuring the diurnal pattern of leaf hyponasty and growth in Arabidopsis - a novel phenotyping approach using laser scanning. Funct. Plant Biol. **39:** 860–869.

Farré, E.M. (2012). The regulation of plant growth by the circadian clock. Plant Biol. (Stuttg.) **14:** 401–410.

Graf, A., Schlereth, A., Stitt, M., and Smith, A.M. (2010). Circadian control of carbohydrate availability for growth in Arabidopsis plants at night. Proc. Natl. Acad. Sci. USA **107:** 9458–9463.

Ichihashi, Y., Kawade, K., Usami, T., Horiguchi, G., Takahashi, T., and Tsukaya, H. (2011). Key proliferative activity in the junction between the leaf blade and leaf petiole of Arabidopsis. Plant Physiol. **157:** 1151–1162.

Izumi, M., Hidema, J., Makino, A., and Ishida, H. (2013). Autophagy contributes to nighttime energy availability for growth in Arabidopsis. Plant Physiol. **161:** 1682–1693.

Keller, M.M., Jaillais, Y., Pedmale, U.V., Moreno, J.E., Chory, J., and Ballaré, C.L. (2011). Cryptochrome 1 and phytochrome B control shade-avoidance responses in Arabidopsis via partially independent hormonal cascades. Plant J. **67:** 195–207.

Lilley, J.L.S., Gee, C.W., Sairanen, I., Ljung, K., and Nemhauser, J.L. (2012). An endogenous carbon-sensing pathway triggers increased auxin flux and hypocotyl elongation. Plant Physiol. **160:** 2261–2270.

Liu, X.L., Covington, M.F., Fankhauser, C., Chory, J., and Wagner, D.R. (2001). ELF3 encodes a circadian clock-regulated nuclear protein that functions in an Arabidopsis PHYB signal transduction pathway. Plant Cell **13:** 1293–1304.

Moreno, J.E., Tao, Y., Chory, J., and Ballaré, C.L. (2009). Ecological modulation of plant defense via phytochrome control of jasmonate sensitivity. Proc. Natl. Acad. Sci. USA **106:** 4935–4940.

Mullen, J.L., Weinig, C., and Hangarter, R.P. (2006). Shade avoidance and the regulation of leaf inclination in Arabidopsis. Plant Cell Environ. **29:** 1099–1106.

Nozue, K., Covington, M.F., Duek, P.D., Lorrain, S., Fankhauser, C., Harmer, S.L., and Maloof, J.N. (2007). Rhythmic growth explained by coincidence between internal and external cues. Nature **448:** 358–361.

Nusinow, D.A., Helfer, A., Hamilton, E.E., King, J.J., Imaizumi, T., Schultz, T.F., Farré, E.M., and Kay, S.A. (2011). The ELF4-ELF3-LUX complex links the circadian clock to diurnal control of hypocotyl growth. Nature **475:** 398–402.

Paparelli, E., Parlanti, S., Gonzali, S., Novi, G., Mariotti, L., Ceccarelli, N., van Dongen, J.T., Kölling, K., Zeeman, S.C., and Perata, P. (2013). Nighttime sugar starvation orchestrates gibberellin biosynthesis and plant growth in Arabidopsis. Plant Cell **25:** 3760–3769.

Polko, J.K., van Zanten, M., van Rooij, J.A., Marée, A.F., Voesenek, L.A., Peeters, A.J., and Pierik, R. (2012). Ethylene-induced differential petiole growth in *Arabidopsis thaliana* involves local microtubule reorientation and cell expansion. New Phytol. **193:** 339–348.

Rauf, M., Arif, M., Fisahn, J., Xue, G.P., Balazadeh, S., and Mueller-Roeber, B. (2013). NAC transcription factor speedy hyponastic growth regulates flooding-induced leaf movement in Arabidopsis. Plant Cell **25:** 4941–4955.

Remmler, L., and Rolland-Lagan, A.G. (2012). Computational method for quantifying growth patterns at the adaxial leaf surface in three dimensions. Plant Physiol. **159:** 27–39.

Ruts, T., Matsubara, S., Wiese-Klinkenberg, A., and Walter, A. (2012a). Diel patterns of leaf and root growth: endogenous rhythmicity or environmental response? J. Exp. Bot. **63:** 3339–3351.

Ruts, T., Matsubara, S., Wiese-Klinkenberg, A., and Walter, A. (2012b). Aberrant temporal growth pattern and morphology of root

and shoot caused by a defective circadian clock in *Arabidopsis thaliana*. Plant J. **72:** 154–161.

Sidaway-Lee, K., Josse, E.M., Brown, A., Gan, Y., Halliday, K.J., Graham, I.A., and Penfield, S. (2010). SPATULA links daytime temperature and plant growth rate. Curr. Biol. **20:** 1493–1497.

Stewart, J.L., Maloof, J.N., and Nemhauser, J.L. (2011). PIF genes mediate the effect of sucrose on seedling growth dynamics. PLoS ONE **6:** e19894.

Stitt, M., and Zeeman, S.C. (2012). Starch turnover: pathways, regulation and role in growth. Curr. Opin. Plant Biol. **15:** 282–292.

Stolarz, M. (2009). Circumnutation as a visible plant action and reaction: physiological, cellular and molecular basis for circumnutations. Plant Signal. Behav. **4:** 380–387.

Sulpice, R., Flis, A., Ivakov, A.A., Apelt, F., Krohn, N., Encke, B., Abel, C., Feil, R., Lunn, J.E., and Stitt, M. (2014). Arabidopsis coordinates the diurnal regulation of carbon allocation and growth across a wide range of photoperiods. Mol. Plant **7:** 137–155.

Suttangkakul, A., Li, F., Chung, T., and Vierstra, R.D. (2011). The ATG1/ATG13 protein kinase complex is both a regulator and a target of autophagic recycling in Arabidopsis. Plant Cell **23:** 3761–3779.

Tao, Y., et al. (2008). Rapid synthesis of auxin via a new tryptophan-dependent pathway is required for shade avoidance in plants. Cell **133:** 164–176.

Usadel, B., Bläsing, O.E., Gibon, Y., Retzlaff, K., Höhne, M., Günther, M., and Stitt, M. (2008). Global transcript levels respond to small changes of the carbon status during progressive exhaustion of carbohydrates in Arabidopsis rosettes. Plant Physiol. **146:** 1834–1861.

Walter, A., Silk, W.K., and Schurr, U. (2009). Environmental effects on spatial and temporal patterns of leaf and root growth. Annu. Rev. Plant Biol. **60:** 279–304.

Whippo, C.W., and Hangarter, R.P. (2009). The "sensational" power of movement in plants: A Darwinian system for studying the evolution of behavior. Am. J. Bot. **96:** 2115–2127.

Wiese, A., Christ, M.M., Virnich, O., Schurr, U., and Walter, A. (2007). Spatio-temporal leaf growth patterns of Arabidopsis thaliana and evidence for sugar control of the diel leaf growth cycle. New Phytol. **174:** 752–761.

Yazdanbakhsh, N., Sulpice, R., Graf, A., Stitt, M., and Fisahn, J. (2011). Circadian control of root elongation and C partitioning in *Arabidopsis thaliana*. Plant Cell Environ. **34:** 877–894.

Supplemental Data. Dornbusch et al. (2014). Plant Cell 10.1105/tpc.114.129031

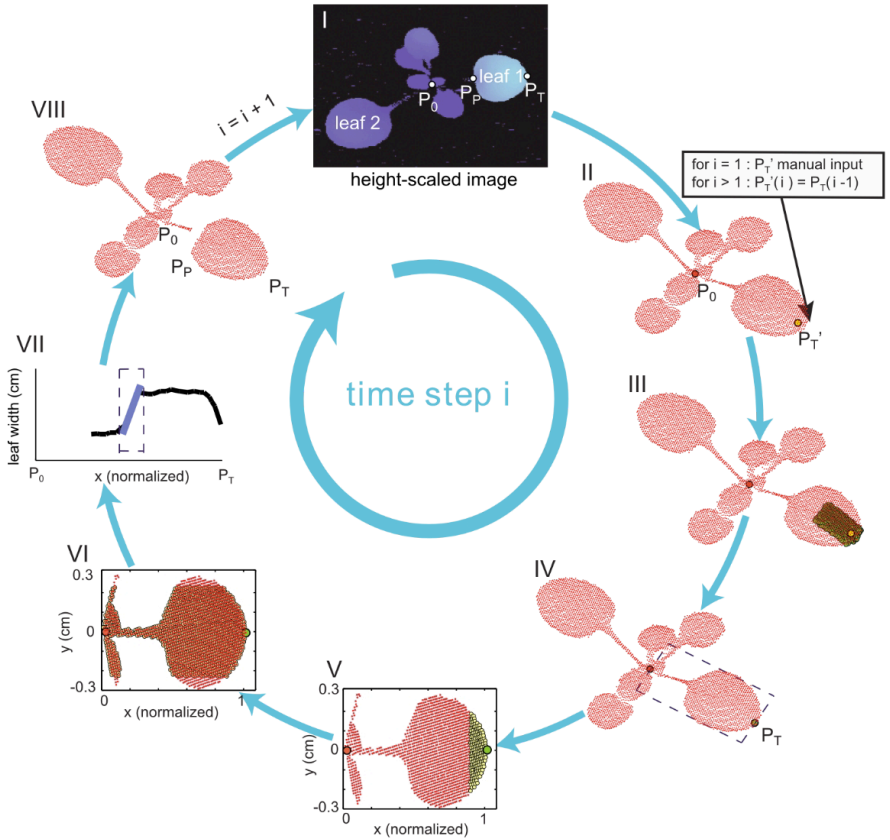

Supplemental Figure 1. Image analysis algorithm to compute P_P and P_T from time-lapse images.

Flow chart illustrating one time step *i* of the image analysis algorithm to compute the leaf tip point P_T and the petiole-blade intersection point P_P. I: Height-scaled image of a plant obtained with the laser scanner; II: point cloud representing the plant surface after 3D transformation; P_0 is manually selected each 24 h at zeitgeber time 3 (ZT3) or linearly interpolated for intermediate *i*; if *i*=1, the approximate leaf tip point P_T'(1) is manually selected; if *i* > 1 the leaf tip point of the previous time step is used to enter the calculation: P_T'(i) = P_T(i-1); III: filtering of points (in green) within a defined area around P_T'; IV: computation of P_T as the median of 10-20 leaf points with the largest distance to P_0; using P_0 and P_T, points are related to a leaf as highlighted by the dashed rectangle; V: selected points are rotated to the *x*-*y* plane and normalized such than P_0 = (0,0,0) and P_T = (0,1,0); approximated leaf width is computed using the highlighted points (in yellow) close to P_T; VI: highlighted points (in yellow) are filtered using the previously computed value for leaf width; VII: leaf width as a function of normalized axis position; the maximum of the first-order derivative is the approximate the position of P_P highlighted with a dashed rectangle; VIII: computation of P_P as is the centroid of selected points inside the dashed rectangle; in the subsequent iteration step *i*+1 the image of the same plant taken at the subsequent time step is processed and P_T and P_P computed for each leaf; the algorithm is automated and only needs user input at the first iteration step *i*=1.

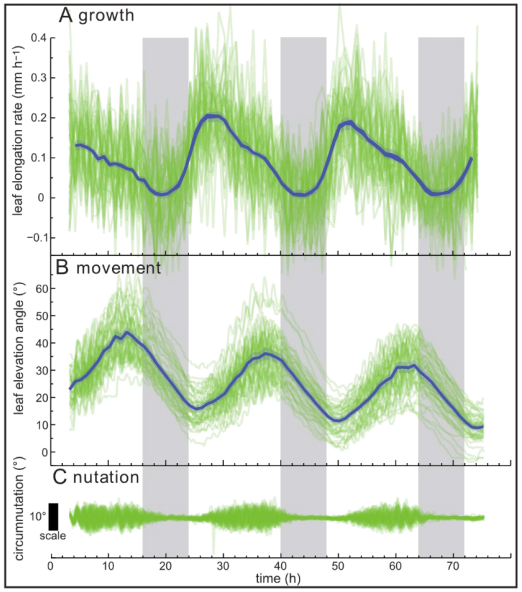

Supplemental Figure 2. Definition of principal output.
(A) Leaf elongation rate (growth), (B) leaf elevation angle (movement) and (C) circumnutations (nutations) of leaves 1 and 2 grown in continuous day (L/L) measured on 53 leaves (30 plants). Col-0 plants were grown for 14 d in standard L/D (16/8). At time t=0h (ZT0) lights were switched on for imaging and kept on in L/L; vertical gray bars represent subjective night periods. Opaque green lines represent data of 53 individual leaves. The solid blue line of leaf elongation rate is mean moving average (3 h) of individual curves. The blue line of leaf elevation angle represent mean value of data points each 60 min (conversely to raw data sampled each 10 min). The blue opaque band around the mean lines is the 95% confidence interval of mean estimate. Circumnutations are computed by detrending individual curves of leaf elevation angle. The trend line was computed using piecewise linear regression (regression parameter tau=0.7). l_{tip} and Φ_{tip} were used to compute the graphs.

Supplemental Data. Dornbusch et al. (2014). Plant Cell 10.1105/tpc.114.129031

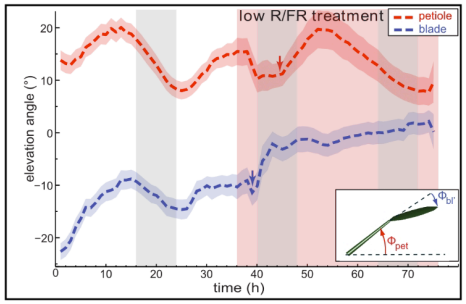

Supplemental Figure 3. In response to a low R/FR treatment the blade upward movement precedes the petiole upward movement.
Elevation angle of petioles (in red) and blades (in blue) of leaves 1 and 2 in continuous day measured on 28 leaves; Col-0 plants were grown for 14 d in standard long day (16/8) followed by 2 d continuous light (L/L). At time t = 0 plants were imaged in L/L (subjective nights are darkened); after 36 h the R/FR ratio was decreased to simulate shade (highlighted by the red rectangle). Leaf elevation angle are mean values. The opaque band around the mean lines is the 95% confidence interval of mean estimate. Arrows indicate the beginning of rapid upward movement.

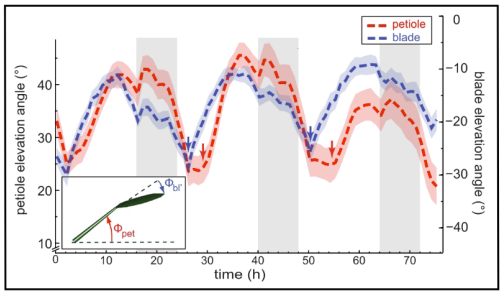

Supplemental Figure 4. In L/D conditions the blade upward movement precedes the petiole upward movement.
Elevation angle of petioles (in red; leaf scale) and blades (in blue, right scale) of leaves 1 and 2 in long day conditions (L/D; 16/8) measured on 19 leaves (30 plants); Col-0 plants were grown for 14 d in standard L/D conditions. Beginning from time t=0 plants were imaged in L/D. Vertical gray bars represent true night periods. Elevation angle are mean values. The opaque band around the mean lines is the 95% confidence interval of mean estimate. Arrows indicate the beginning of rapid upward movement.

Supplemental Data. Dornbusch et al. (2014). Plant Cell 10.1105/tpc.114.129031

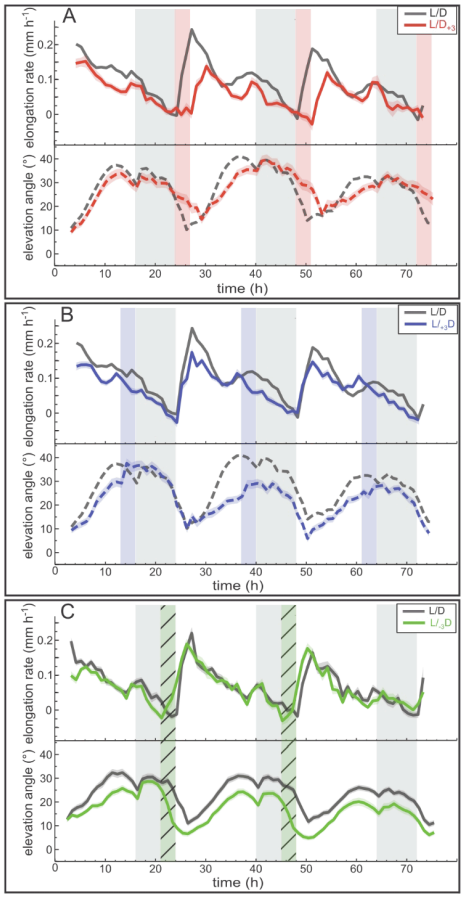

Supplemental Figure 5: Light is required at dawn to trigger leaf growth.
(A) This is the same growth data as plotted on Figure 7A, in addition we included leaf movement for those plants, night was prolonged after dawn by 3 h (L/D_{+3}; red line n_{leaf}=27), (B) This is the same growth data as plotted on Figure 7B, in addition we included leaf movement for those plants, night was prolonged before dusk by 3 h ($L/_{+3}D$; blue line, n_{leaf}=54).
(C) This is the same growth data as plotted on Figure 7C, in addition we included leaf movement for those plants, night was shortened before dawn by 3 h (L/D_{-3}; green line n_{leaf}=35)
Col-0 plants were grown for 14 d in standard L/D (16/8) conditions before measurement; vertical gray bars represent true night periods; vertical red/blue bars indicate prolonged night periods (A,B) and vertical hatched green bar shortened night period (C). Leaf elongation rate was computed as mean moving average (3 h) of individual curves. Leaf elevation angles are mean values. The opaque band around the mean lines is the 95% confidence interval of mean estimate, n_{leaf} = number of leaves. Day 1 of the experiment represents the 1st day when the plants were subjected to an abrupt change in night length. I_{tip} and Φ_{tip} were used to compute the graphs.

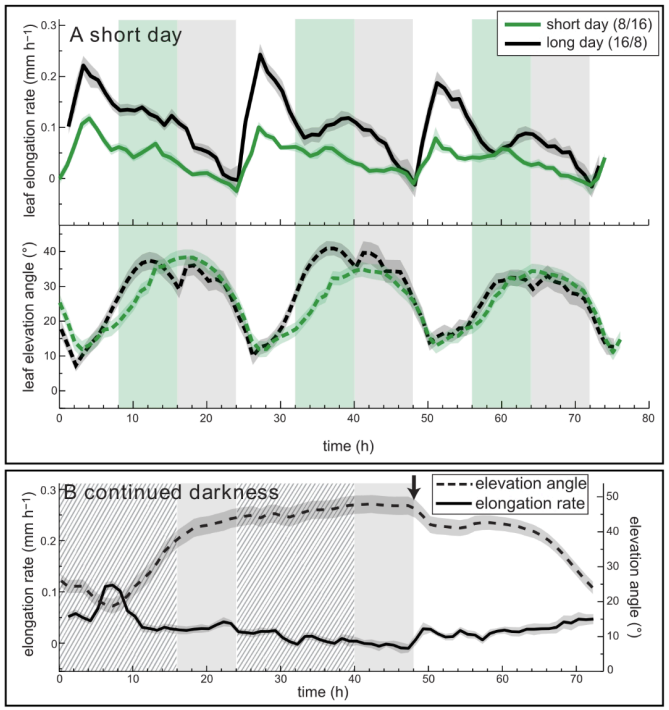

Supplemental Figure 6. Growth and movements are altered by shortening day length or in continuous darkness.

(A) Leaf elongation rate and leaf elevation angle of leaf 1, 2 in long day (black line, n_{leaf}=27) and short day (green line, n_{leaf}=47). Col-0 plants were grown for 14 days in standard long day (16/8h) or for 18 days under short day (8/16h) condition before measurement under the same conditions.

(B) Leaf elongation rate and leaf elevation angle of leaf 1, 2 in prolonged darkness (D/D, n_{leaf}=41). Col-0 plants were grown for 14 days in standard L/D (16/8) conditions before measurement. At time t=0 lights were not switched on and plants were imaged for 48h in darkness followed by 24h of light; vertical gray bars represent subjective night periods and the hatched part the subjective day; The arrow marks the time when light was switched on. Solid lines of leaf elongation rate are the mean moving average (3h) of individual curves. Solid lines of leaf elevation angle are mean values. The opaque band around the mean lines is the 95% confidence interval of mean estimate. n_{leaf} = number of measured leaves. l_{tip} and Φ_{tip} were used to compute the graphs.

Supplemental Data. Dornbusch et al. (2014). Plant Cell 10.1105/tpc.114.129031

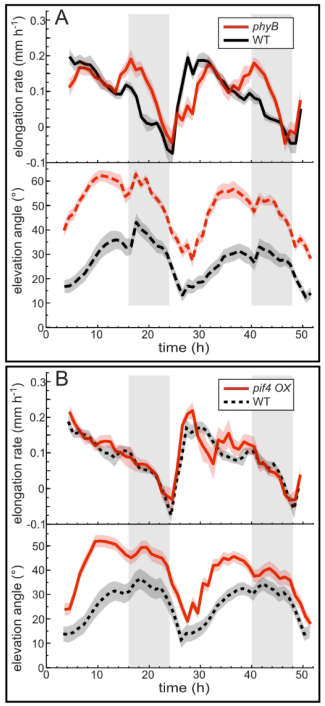

Supplemental Figure 7: Plants with elevated levels of PIF4 maintain leaf growth rhythms robust in amplitude.
(A) Leaf elongation rate and leaf elevation angle of leaves 1 and 2 in the *phyB* mutant (n_{leaf}=29) and Col-0 (n_{leaf}=30) grown in standard long-day conditions. **(B)** Leaf elongation rate and leaf elevation angle of leaves 1 and 2 in the *PIF4 overexpressor* line (n_{leaf}=30) and Col-0 (n_{leaf}=30) grown in L/D. Col-0, *phyB* and *PIF4 OX* plants were grown for 14 d in L/D prior to imaging in the same conditions. Vertical gray bars represent night periods. Solid lines of leaf elongation rate are the mean moving average (3 h) of individual curves. Leaf elevation angle are mean values. The opaque band around the mean lines is the 95% confidence interval of mean estimate. n_{leaf} = number of measured leaves. I_{tip} and Φ_{tip} were used to compute the graphs.

Supplemental Methods

Geometric definition of leaf length and elevation angle

In *Arabidopsis*, the basal end of leaves is located in the center of the plant, which we geometrically define as the point P_0 (Figure 1A). The distal end of leaves –the leaf tip– is defined by the point P_T. Hence the vector P_0P_T delineates length (l_{tip}) and elevation angle (Φ_{tip}) of a leaf (Figure 1A). A leaf is further subdivided into petiole and blade. The point P_P defines the junction between them (Figure 1A). Thus P_0P_P delineates length (l_{pet}) and elevation angle (Φ_{pet}) of the petiole, and P_PP_T length (l_{bl}) and elevation angle (Φ_{bl}) of the blade. In reality, the proximodistal axis of an *Arabidopsis* leaf is slightly curved. We approximate this curve by P_0, P_P and P_T (Figure 1A). In many cases petioles cannot be scanned and P_P not reliably be estimated. This is attributed to the measurement geometry of the laser and plant architecture (e.g. steep leaf angle). However, the vector P_0P_T is available in most cases and represent a simplified yet robust description of the leaf axis (Figure 1A). Geometrically, Φ_{tip} is a good estimate for mean leaf elevation angle of a slightly curved line, but l_{tip} is smaller than actual leaf length $l_{leaf}=l_{pet}+l_{bl}$ (Figure 1A). To estimate the degree of leaf curvature, we computed the elevation angle of the leaf blade relative to the petiole (Φ_{bl}') (Figure 1A). Realistic values for Φ_{bl}' for leaf 1 and 2 and in our experimental conditions were $-15° > \Phi_{bl}' > -30°$ (Figure 4C). Using these values (assuming $l_{pet}=l_{bl}$) and applying the law of cosines, l_{tip} is underestimated compared to l_{leaf} by 0.9% to 3.4%. The diel elongation rate computed from l_{tip} did not differ much from the one computed from l_{leaf} (Figure 1B). The elongation rate using l_{tip} is amplified compared to l_{leaf} around the night/day transition (Figure 1B, indent), which can mainly be attributed to relatively fast down- and upward movements of the leaf blade relative to the petiole (Supplemental Figure 4). Nevertheless the vector P_0P_T yields a simplified yet robust estimate of the diurnal pattern of leaf elongation rate (growth), and leaf elevation angle (movements) and nutations (Supplemental Figure 2).

Image processing

The goal of our image analysis algorithm is to compute P_0, P_P and P_T for each leaf and each time step with minimal user interaction. The algorithm is implemented in Matlab (MathWorks Inc., Natick, MA, USA) and illustrated in Supplemental Figure 1 online. Each 24h, at ZT3 (time of lowest leaf position), P_0 is manually selected for each plant in the image (e.g. at hourly time steps i=1,25,49,73) and linearly interpolated for intermediate i. At i=1, the approximate position of the tip P_T' for each leaf is manually selected. The algorithm autonomously computes P_T and P_P for each selected leaf (Supplemental Figure 1 online). At

following time steps $i = i + 1$, we set $P_T'(i) = P_T(i-1)$ and compute P_T and P_P. Note that in our experiments *Arabidopsis* leaves were between 1.0 and 2.0 cm long. Between successive time steps, the leaf tip did usually not move more than 2 mm away from the previous positions. Hence the Euclidian distance $|P_T(i)-P_T(i-1)|$ was usually smaller than 2 mm, which facilitated automated leaf tracking over time. Apart from manual selection of P_0 for each plant (each 24h) and P_T' for each leaf at i=1, the algorithm is fully automated. To assess the precision of the semi-automated computation of P_P and P_T, we plotted time-courses of l_{pet} , l_{tip} and Φ_{pet}, Φ_{tip} (spherical coordinates of P_P and P_T) for each analyzed leaf. This yields smooth and continuous curves if the algorithm worked properly. Wrongly computed values for P_P or P_T led to discontinuities (e.g. missing values or sharp peaks) in plotted curves. Leaves showing such discontinuities were not considered in further analyses. The whole analysis pipeline can be run on a regular notebook running Matlab (min. 8 GB RAM) and requires 1-2 minutes of user interaction per plant including post-processing quality assessment (Dornbusch et al., 2012).

Data processing

Leaf elongation rate was computed as the difference in leaf length l_{tip} between successive time steps i for each leaf 1 and 2 (and each plant) in one experiment (Supplemental Figure 2A). Owing to the variance in the data, elongation curves for each individual leaf were smoothed using a moving average over 3h. We then computed mean values for each time point (Supplemental Figure 2A online, blue line) and 95% confidence interval of mean estimate (Supplemental Figure 2A online, opaque blue band around mean line).

Leaf elevation angle Φ_{tip} follows a characteristic diurnal pattern frequently overlaid with short-period ultradian circumnutations (Supplemental Figure 2B online). Leaf movements as rate of change in $^{\circ}h^{-1}$ were computed as difference in Φ_{tip} between successive hourly time-steps (Figure 3C). Diurnal leaf movements were visualized using computed hourly mean values for Φ_{tip} and 95% confidence interval of mean estimate (Supplemental Figure 2B online, blue curve). This compensated for the nutation effects. These circumnutations are visualized in a separate plot as nutations around the diurnal trendline of Φ_{tip} (Supplemental Figure 2C online). This trendline is computed for each individual leaf using piecewise linear regression (regression parameter tau=0.7). Data for Φ_{tip} for each leaf is subtracted from this trend line and plot as opaque line (Supplemental Figure 2C online). Diel elongation rates and leaf movements (absolute changes in leaf elevation angle) were computed summing corresponding hourly values over a period of 24h starting from ZT2.25 (Figure 1B, Figure 5).

Reference

Dornbusch, T., Lorrain, S., Kuznetsov, D., Fortier, A., Liechti, R., Xenarios, I., and Fankhauser, C. (2012). Measuring the diurnal pattern of leaf hyponasty and growth in Arabidopsis - a novel phenotyping approach using laser scanning. Funct Plant Biol. *39*: 860-869.

CHAPTER II

The importance of auxin signaling for local leaf hyponasty in response to neighbor proximity signals

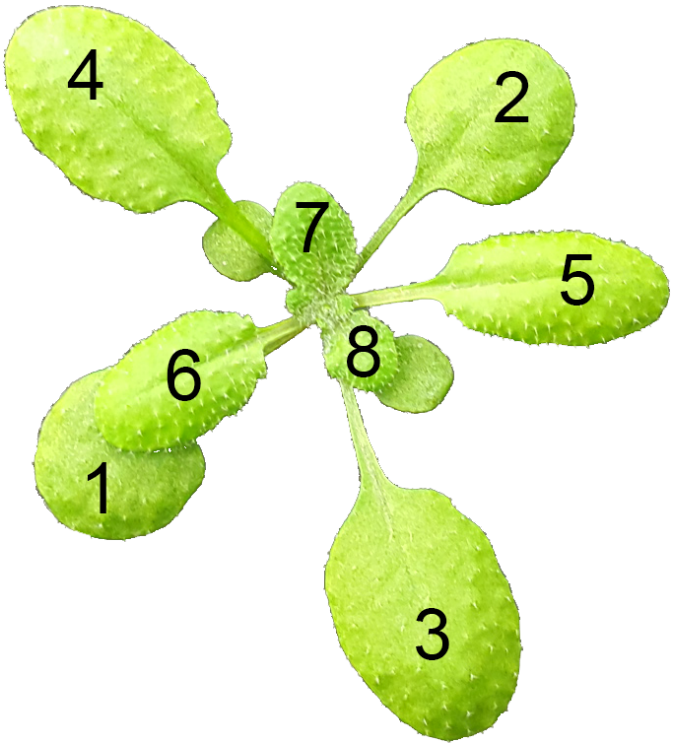

Numbered leaves from youngest to oldest in a 4-week-old Arabidopsis rosette.

2017. O. Michaud

Overview

From the second to the fourth year of my thesis, I conducted a project relative to the importance of auxin during shade-induced nastic responses in Arabidopsis leaves, under the supervision of my thesis directors and in collaboration with a colleague. This project was published in the journal Proceedings of the National Academy of Sciences of the United States of America (PNAS) in 2017 (227). This work was then recommended by the Faculty of 1000 and highlighted in the Annual Reviews of Plant Biology which yearly summarizes important advances in the field (228).

The objective of this project was to explore the mechanisms underlying growth and particularly movement in Arabidopsis leaves when grown in standard (high R:FR) and neighbor detecting (low R:FR) conditions. For this, we used our newly developed phenotyping methodology (225) along with pharmacological and molecular genetic approaches. Our work led to discoveries concerning the essentiality of auxin in the nastic response, the local nature of shade-induced traits as well as the relationship between elongation growth and movement in petiole organs.

I stood as the leading investigator for this project. My involvement consisted first in designing and performing experiments by combining phenotyping, pharmacological and genetic approaches. For the phenotyping experiments based on a photogrammetric approach (Fig. 5B-C, S3B, S4F, S5C and S9), I relied on the help of my colleague Dr. Anne-Sophie Fiorucci who performed those experiments. In a second time, I analyzed and interpreted data with the participation of the authors of the publication. Finally, I wrote the paper in collaboration with my supervisor Prof. Christian Fankhauser.

Local auxin production underlies a spatially restricted neighbor-detection response in *Arabidopsis*

Olivier Michaud[a], Anne-Sophie Fiorucci[a], Ioannis Xenarios[b], and Christian Fankhauser[a,1]

[a]Center for Integrative Genomics, Faculty of Biology and Medicine, University of Lausanne, CH-1015 Lausanne, Switzerland; and [b]Swiss Institute of Bioinformatics, University of Lausanne, CH-1015 Lausanne, Switzerland

Edited by Winslow R. Briggs, Carnegie Institution for Science, Stanford, CA, and approved May 31, 2017 (received for review February 9, 2017)

Competition for light triggers numerous developmental adaptations known as the "shade-avoidance syndrome" (SAS). Important molecular events underlying specific SAS responses have been identified. However, in natural environments light is often heterogeneous, and it is currently unknown how shading affecting part of a plant leads to local responses. To study this question, we analyzed upwards leaf movement (hyponasty), a rapid adaptation to neighbor proximity, in *Arabidopsis*. We show that manipulation of the light environment at the leaf tip triggers a hyponastic response that is restricted to the treated leaf. This response is mediated by auxin synthesized in the blade and transported to the petiole. Our results suggest that a strong auxin response in the vasculature of the treated leaf and auxin signaling in the epidermis mediate leaf elevation. Moreover, the analysis of an auxin-signaling mutant reveals signaling bifurcation in the control of petiole elongation versus hyponasty. Our work identifies a mechanism for a local shade response that may pertain to other plant adaptations to heterogeneous environments.

neighbor detection | organ-specific response | hyponasty | auxin | PIF

The availability of essential resources, including micro- and macronutrients, water, CO_2, and sunlight, is an important regulator of plant phenotypic plasticity (1, 2). A well-known example is the response of plants to foliar shade known as the "shade-avoidance syndrome" (SAS) (3–5). In shade-avoiding plants the SAS comprises a suite of growth and developmental responses including elongation of hypocotyls, stems, and petioles and repositioning of the leaves to higher positions in the canopy (known as "leaf hyponasty") (3). These responses confer an adaptive advantage, with shade-avoiding plants having improved relative fitness in environments with high plant density (6, 7). Interestingly, many of the physiological responses elicited by neighboring plants are triggered before shading, a response known as "neighbor detection" that enables plants to anticipate potentially unfavorable light conditions (3, 8, 9).

A primary signal informing plants about the presence of neighbors is the red (R) to far-red (FR) ratio (3). In sunlight the R/FR is slightly above a value of 1, but, because of the strong absorbance of R and blue by photosynthetic pigments and the substantial reflection of FR by leaves, this ratio drops before actual shading and decreases further in true shade (3, 10, 11). Phytochromes (phy) sense the R/FR ratio, with phyB playing a predominant function in shade and neighbor detection (3). In sunlight a substantial fraction of phyB is active in preventing the SAS, while a reduction of the R/FR ratio gradually enhances elongation of hypocotyls, petioles, and stems (11). These growth responses are controlled by extensive transcriptional reprograming mediated primarily by three members of the phytochrome-interacting factor (PIF) family of basic helix–loop–helix (bHLH) transcription factors acting immediately downstream of phyB (12–14). In sunlight, phyB inhibits these PIFs through complex mechanisms, but in the shade this inhibition is released, resulting in PIF-mediated promotion of elongation (3, 5). Shade cues are sensed mostly in leaf blades (or cotyledons), leading to auxin production in green tissues (15, 16). Auxin then is transported to the elongating parts of the plant (e.g., petioles and hypocotyls) to elicit the growth response (17, 18). A key step in this process is PIF-dependent expression of several members of the YUCCA family of auxin biosynthetic enzymes (12, 13, 19). PIFs also control the expression of additional players contributing to growth regulation, including several hormonal pathways and cell-wall components (20–25).

In natural environments, shading is often heterogeneous, leading to situations in which plants are only partly shaded by competitors. This heterogeneous shading led to the concept of foraging for light that is mediated by local tuning of the SAS specifically in the shaded part of the plant, thus promoting canopy gap filling (26). Examples of such local responses have been identified in several species (27, 28). We decided to investigate the molecular basis of such local shade responses in *Arabidopsis* by studying leaf hyponasty, an early response to increasing plant density that is induced rapidly by lowering the R/FR (29). Our experiments show that auxin production in the leaf blade is necessary and sufficient to trigger a leaf hyponastic response. Interestingly, the response depends on the site of auxin production/application and selectively affects the treated leaf, thereby providing a molecular basis for local shade responses in *Arabidopsis* leaves.

Results

The PIF-YUC Regulon Controls Low R/FR-Induced Leaf Hyponasty. Leaf hyponasty is a complex, dynamic response, and the position of leaves is controlled by both internal (e.g., circadian) and external cues (30). To study this process dynamically, we tracked

Significance

Being photoautotrophic, plant growth is exquisitely sensitive to the light environment. In response to light cues from potential competitors, plants initiate a neighbor-proximity response favoring direct access to sunlight. This response includes elevation of the leaf (hyponasty) that is rapidly triggered following perception of neighbors. Light signals emanating from surrounding vegetation are heterogeneous; however, it is unknown how plants trigger a localized response in such conditions. We show that auxin synthesis in the leaf blade coupled with transport into the petiole induces a hyponastic response restricted to the leaf perceiving the signal. Moreover, we identify a branch of auxin signaling controlling petiole elevation while not affecting elongation. Our work uncovers a mechanism underlying plant responses to a heterogeneous environment.

Author contributions: O.M., A.-S.F., and C.F. designed research; O.M. and A.-S.F. performed research; I.X. contributed new reagents/analytic tools; O.M., A.-S.F., I.X., and C.F. analyzed data; and O.M. and C.F. wrote the paper.

The authors declare no conflict of interest.

This article is a PNAS Direct Submission.

Freely available online through the PNAS open access option.

[1]To whom correspondence should be addressed. Email: christian.fankhauser@unil.ch.

This article contains supporting information online at www.pnas.org/lookup/suppl/doi:10.1073/pnas.1702276114/-/DCSupplemental.

leaf position (tip elevation angle) with high spatial and temporal resolution in plants growing in control (high R/FR) and low R/FR (simulated neighbors) conditions using previously described methodology (31). We typically monitored leaves 1 and 2, which are at the same developmental stage, but similar response patterns were observed in younger leaves (Fig. 1 and Fig. S1 *A* and *B*) (31). A photogrammetric approach showed that tip and petiole elevation angles are highly correlated, justifying the choice of tip position as a proxy for leaf movement (Fig. S1 *C* and *D*). In wild-type (Col-0 accession) plants a reduction in R/FR led to an increase in the leaf elevation angle starting 3–4 h after transfer into simulated shade, and leaves reached maximal elevation in the late afternoon (Fig. 1*A* and Fig. S1*A*). In leaves 1 and 2 the effect of low R/FR was more pronounced during the first day of treatment but was less apparent in younger leaves with more growth potential (Fig. 1*A* and Fig. S1*A*). In addition, shade led to a higher baseline for the diurnal movements, resulting in an approximate 20° increase in the lowest elevation angle in low R/FR as compared with high R/FR (Fig. 1*A* and Fig. S1*A*). *phyB* mutants show a constitutive shade-avoidance phenotype including leaf hyponasty (32), a phenotype that we confirmed in our growth conditions (Fig. S2 *A* and *B*). PIF4, PIF5, and PIF7 act immediately downstream of phyB to promote shade-induced hypocotyl and petiole elongation (14, 33, 34). We therefore analyzed shade-regulated leaf movements in *pif7*, *pif4pif5*, and *pif4pif5pif7* mutants. The amplitude of leaf movement in *pif4pif5* and *pif4pif5pif7* mutants was reduced in control conditions (Fig. 1*A* and Fig. S2 *B*–*D*) (31). Moreover, a reduction of the R/FR led to a strongly reduced leaf hyponastic response in *pif4pif5pif7* and *pif7* mutants, indicating that the low R/FR-controlled leaf position is predominantly regulated by PIF7 (Fig. 1*A* and Fig. S2 *B*–*D*).

PIF-controlled auxin biosynthesis is an essential step in shade-regulated hypocotyl and petiole elongation (11). Moreover, a role for auxin biosynthesis in shade-regulated leaf hyponasty was previously identified by analyzing the *taa1/sav3* mutant (35). The amplitude of leaf movement in *taa1/sav3* plants was reduced in high R/FR (Fig. S3*A*), in contrast with other aspects of the *taa1/sav3* phenotype that are normal in control conditions (17) but correlating with the reduced indole-3 acetic acid (IAA) levels in the mutant (17). In addition, we confirmed the strongly diminished shade-mediated leaf hyponastic response in *taa1/sav3* mutants (Fig. S3*A*). PIFs control auxin production downstream of TAA1, at the level of *YUC* expression, and a *yuc2yuc5yuc8yuc9* mutant lacking four shade-induced *YUC* genes lacks several shade responses (19, 25). Therefore, we analyzed the *yuc2yuc5yuc8yuc9* mutant and found that it maintained normal leaf movements in control conditions but was unresponsive to a reduction of the R/FR (Fig. 1*B*). Consistent with these genetic data, pharmacological inhibition of YUC enzymes also inhibited low R/FR-induced hyponasty (Fig. S3*B*). To control petiole and hypocotyl elongation, auxin needs to be transported from the site of synthesis to the site of action, a process requiring several members of the PIN-FORMED family of auxin efflux carriers (16, 18, 25). Therefore, we examined the *pin3pin4pin7* mutant and found that these plants displayed severely reduced movements in control conditions as well as in response to shade (Fig. S3*C*). In contrast, a mutant lacking *PIN1* retained normal diurnal and shade-induced hyponasties (Fig. S3*D*). Considering these findings together, we conclude that both auxin synthesis and PIN3,4,7-mediated auxin transport are required to trigger low R/FR-induced leaf hyponasty.

Auxin Synthesized in the Blade and Transported to the Petiole Induces Hyponasty. To test whether auxin is sufficient to trigger leaf hyponasty, we applied auxin to the tip of wild-type leaves. We focused on the leaf tip because previous studies identified the leaf margin as the major source of newly synthesized auxin during shade responses (16, 17). Auxin (IAA) application led to

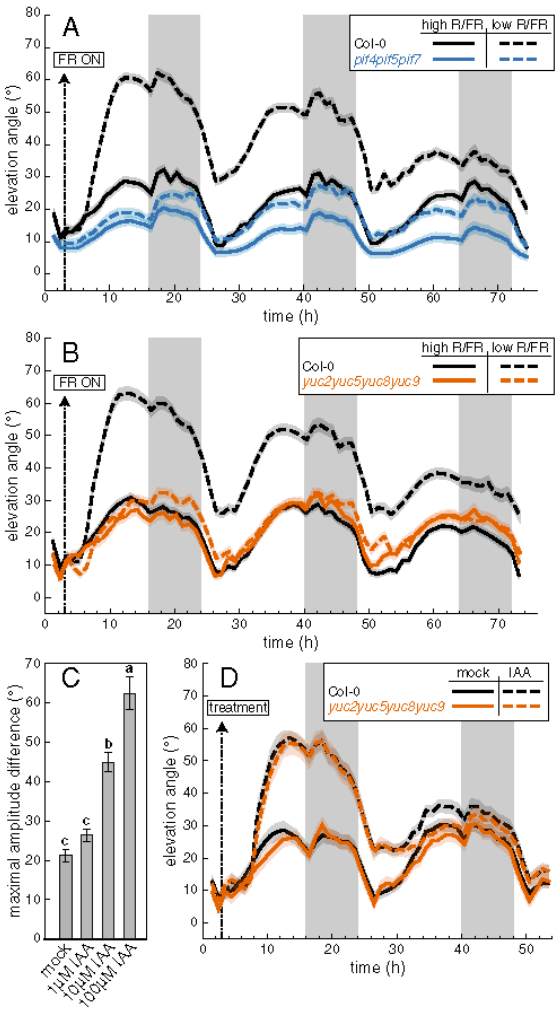

Fig. 1. Low R/FR-induced hyponasty is controlled by PIFs and requires YUC-mediated auxin biosynthesis. (*A*) Leaf elevation angle of leaves 1 and 2 in Col-0 plants (black lines) and *pif4pif5pif7* mutants (blue lines) in high (solid lines) versus low (dashed lines) R/FR conditions. Leaf elevation angles are mean values (n = 55–58). (*B*) Leaf elevation angle of leaves 1 and 2 in Col-0 plants (black lines) and *yuc2yuc5yuc8yuc9* mutants (orange lines) in high (solid lines) versus low (dashed lines) R/FR conditions. Leaf elevation angles are mean values (n = 51–60). In *A* and *B*, shade treatment started on day 15 at ZT3 (t = 3) by adding FR light (FR ON) to decrease the R/FR. (*C*) Bar plot representing the amplitude of leaf movement between maximum and minimum leaf elevation angles over the time period from ZT3 (t = 3) to ZT16 (t = 16) on day 15 and computed for each individual leaf analyzed in Fig. S4*A*. Error bars represent the twofold SE of mean estimates. One-way ANOVAs followed by Tukey's Honestly Significant Difference (HSD) test were performed, and different letters were assigned to significantly different groups ($P < 0.05$). (*D*) Leaf elevation angle of leaves 1 and 2 treated with mock solution (solid lines) or 10 μM IAA (dashed lines) in Col-0 plants (black lines) and *yuc2yuc5yuc8yuc9* mutants (orange lines). Leaf elevation angles are mean values (n = 35–40). Shaded bands around mean lines in *A*, *B*, and *D* represent the 95% CIs of mean estimates. Vertical gray bars represent night periods. In *C* and *D* a 1-μL drop of solution was applied to the leaf tip (adaxial side) at ZT3 on day 15. Plants were grown for 14 d in standard long-day [LD, 16-h light, 8-h dark (16/8)] conditions. Imaging started on day 15 at ZT0 (t = 0), and plants were maintained in LD conditions.

a leaf hyponasty that increased with the concentration of the phytohormone (Fig. 1*C* and Fig. S4*A*). Moreover, the kinetics of the response was comparable to shade treatments (Fig. 1 and Fig. S4*A*). We also noticed that the initial response to auxin application was a decrease in the leaf elevation angle that was followed by a rapid increase (Fig. S4*A*). A similar but less pronounced pattern was also observed in some low R/FR treatments. By comparing the effect of IAA application on the leaf tip with an application on the margin in the middle of the longitudinal blade axis, we found that tip application was most efficient in triggering leaf hyponasty (Fig. S4*B*). However, IAA application on one side of the leaf also led to a lateral repositioning of the leaf (Fig. S4*C*). Given that shade-induced leaf hyponasty depends on YUC-mediated auxin biosynthesis (Fig. 1*B* and Fig. S3*B*), we tested whether induction of *YUC* expression at the leaf tip also triggers an upward movement of leaves. Application of estradiol on the leaf tip of a YUC3-inducible line (iYUC3) resulted in strong leaf hyponasty, confirming that application or production of auxin at the leaf tip was sufficient to elicit the response (Fig. S4*D*). Importantly, auxin application restored leaf hyponasty in the *yuc2yuc5yuc8yuc9* auxin biosynthetic mutant but not in the *pin3pin4pin7* auxin transport mutant, confirming that auxin biosynthesis at the leaf tip followed by PIN-mediated transport is required for the hyponastic response (Fig. 1*D* and Fig. S4*E*). In line with this conclusion, we found that simultaneous application of IAA on the leaf tip and 1-naphthylphthalamic acid (NPA) on the blade–petiole boundary inhibited auxin-induced leaf hyponasty (Fig. S4*F*).

Low R/FR-Induced Leaf Hyponasty Is Restricted to the Treated Leaf. Because shade treatments on parts of a plant result in local effects for some responses but trigger systemic effects for others (16, 27, 36), we aimed at determining whether application of auxin on one leaf selectively affected the movement of the treated leaf or led to systemic effects. We found that only the auxin-treated leaf responded to hormone application (Fig. 2*A* and Fig. S5 *A*–*C*). Next we treated individual leaves with a low R/FR to determine whether a localized shade treatment also leads to a local response. We found that the hyponastic response was restricted to the leaf that was treated with low R/FR on its tip, indicating that a local reduction of the R/FR does not lead to a systemic signal affecting other leaves (Fig. 2 *B* and *C* and Fig. S5 *D* and *E*). Because leaf hyponasty is produced primarily by a change in the petiole angle (31), we tested whether reducing the R/FR on the petiole rather than on the leaf blade also triggered the response. Interestingly, an increase in leaf elevation angle was specifically induced upon reduction of the R/FR on the leaf tip but not on the petiole (Fig. 2 *B*–*D*). Therefore, we also compared leaf movement following auxin production/application at the tip versus the petiole. As observed following a reduction of the R/FR, applying auxin or inducing *YUC3* expression at the petiole did not trigger leaf hyponasty (Fig. S6). In contrast, we noticed that such treatments instead led to a reduction of the leaf angle (Fig. S6). We observed similar results when those treatments were performed at the petiole–blade junction (Fig. S6). Collectively these experiments indicate that auxin production in the leaf blade, but not in the petiole, induces a local leaf hyponastic response.

To study the auxin response triggered by shade or auxin application, we used the *DR5:GUS* auxin response marker line. As reported previously, a reduction of the R/FR led to an increase in GUS signal at the leaf margins (Fig. 3 *A* and *B*) (17). In addition, in the petiole we observed that the GUS signal was concentrated in the vasculature (Fig. 3 *A* and *B*, *Insets*). When auxin was applied to the leaf tip, we observed broad staining in the blade, whereas in the petiole the signal again was strongest in the vasculature (Fig. 3*C*, *Right Inset*). Moreover, the restriction of auxin-induced *DR5:GUS* expression to the blade and petiole

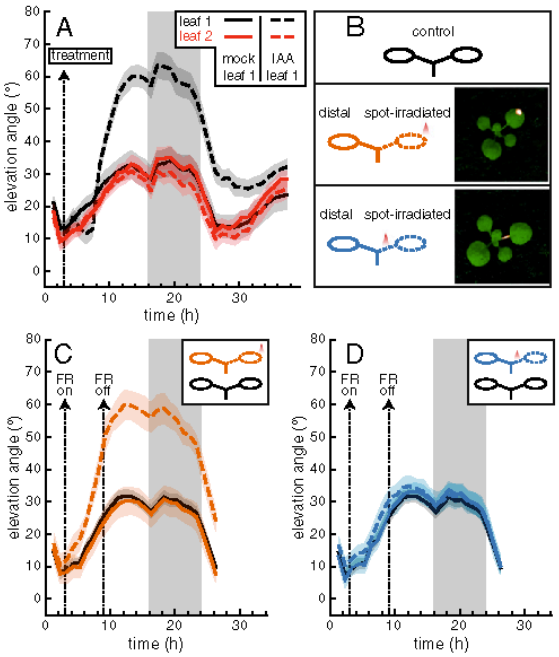

Fig. 2. Shade-induced hyponasty is restricted to the treated leaf and requires sensing at the tip rather than at the petiole. (*A*) Leaf elevation angle of Col-0 leaf 1 (black lines) and leaf 2 (red lines) with mock solution (solid lines) or 10 μM IAA (dashed lines) applied to the tip of leaf 1. Plants were grown as in Fig. 1 except that imaging started at ZT0 on day 16 ($t = 0$), and at ZT3 a 1-μL drop of solution was applied to the tip of leaf 1 (adaxial side). Data are mean of $n = 14$–15. (*B*) Illustration of the different treatments applied in *C* and *D*. (*Upper*) Leaves 1 and 2 growing in standard high R/FR conditions (control solid black outlines). (*Middle*) One single leaf (leaf 1 or 2) was spot-irradiated with FR on the tip (indicated by an orange triangle; the irradiated leaf is drawn with a dashed orange outline), while the opposite leaf was growing in high R/FR conditions (distal leaf drawn with a solid orange outline). Note the illumination on the representative plant shown on the right. (*Lower*) One single leaf (leaf 1 or 2) was spot-irradiated with FR on the petiole (indicated by an orange triangle; the leaf is drawn with a dashed blue outline) while the opposite leaf was growing in high R/FR conditions (distal leaf drawn with a solid blue outline). Note the illumination on the representative plant on the right. (*C*) Leaf elevation angles of Col-0 leaves grown in control conditions (solid black line, $n = 48$) or with FR spot illumination on the leaf tip (dashed orange line, $n = 12$), and of the distal untreated leaves of the same plants (solid orange line, $n = 12$). (*D*) Leaf elevation angle of Col-0 leaves grown in control conditions (solid black line, $n = 48$) or with FR spot illumination on the petiole (dashed blue line, $n = 12$) and of the distal untreated leaves of the same plants (solid blue line, $n = 12$). Plants in *C* and *D* were grown as in Fig. 1 except that FR illumination started on day 15 at ZT3 ($t = 3$) and stopped at ZT9 ($t = 9$). Leaf elevation angles are mean values. Opaque bands around mean lines in *A*, *C*, and *D* represent the 95% CIs of mean estimates. Vertical gray bars represent night periods.

of the treated leaf further confirmed the local nature of the auxin response (Fig. 3*C*) (37). The GUS signal in the vasculature of the petiole was prevented by the simultaneous application of IAA on the tip and NPA on the blade–petiole boundary, a treatment that also inhibited leaf hyponasty (Fig. 3*D* and Fig. S4*F*). When IAA was applied on one side at the margin in the middle of the longitudinal blade axis, we observed that the GUS signal was restricted to half of the leaf blade, with the midvein acting as a boundary (Fig. S7*A*). Following such a treatment, staining in the petiole vasculature was also prominent, but in addition we

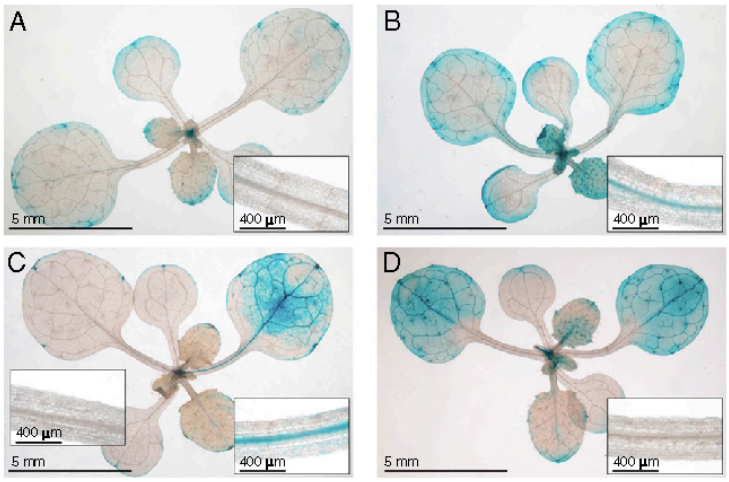

Fig. 3. Shade and auxin application both lead to an increased auxin response within the vasculature of the petiole. The auxin response was visualized in leaves of *DR5:GUS* reporter plants after 7 h in high R/FR (*A*), in low R/FR (*B*), after exogenous auxin application on the tip of leaf 1 in high R/FR (*C*, leaf on the right), or after simultaneous exogenous auxin and NPA applications on the tip and petiole–blade junction, respectively, of leaves 1 and 2 in high R/FR (*D*). Plants were grown as in Fig. 1. (*B*) Shade treatment started on day 15 at ZT3. (*C*) At ZT3 on day 15, a 1-μL drop of 10 μM IAA was applied to the tip of leaf 1 (adaxial side). The petioles of both the treated (*Right Inset*) and untreated (*Left Inset*) leaves are shown. (*D*) At ZT3 on day 15, 1-μL drops of 10 μM IAA and 20 μM NPA were administered simultaneously to the tip and the petiole–blade junction, respectively, of leaves 1 and 2 (adaxial side). Plants were harvested on day 15 at ZT10. *Insets* in all panels show close-ups of petioles.

observed a lateral GUS gradient across the petiole (Fig. S7*A*). We also applied auxin to the petiole–blade junction and to the petiole of *DR5:GUS* plants. Such IAA applications resulted in a broader GUS signal in the petiole (Fig. S7 *B* and *C*). When IAA was applied to the petiole–blade junction, the signal was very broad close to the application site but was concentrated inside the vasculature at the petiole base (Fig. S7*B*), suggesting that polar auxin transport, which is required for shade-induced hyponasty (Figs. S3 and S4), leads to a focused auxin response in the vasculature.

Auxin Signaling in the Vasculature and the Epidermis Controls Low R/FR-Induced Hyponasty. To determine whether a similar trend was also observed for other auxin-regulated genes, we analyzed an *IAA19:GUS* reporter line, because *IAA19* expression is induced by shade and auxin. Low R/FR enhanced the GUS signal, particularly in the petiole vasculature of expanding leaves (Fig. S8 *A* and *B*) (38). To determine the functional importance of IAA19 in this process, we used the *massugu2* (*msg2*) allele expressing a stabilized IAA19 auxin-signaling inhibitor (39). Interestingly, this mutant displayed a diurnal leaf hyponastic pattern similar to that of the wild type in control conditions but a reduced low R/FR-induced response (Fig. 4*A* and Fig. S8 *C* and *D*). This observation is noteworthy, because the *msg2* mutant exhibited normal shade-induced petiole elongation (Fig. 4*B*) (40), thereby demonstrating that IAA19 function is restricted to specific shade-induced responses. Taken together, our data show that a neighbor-proximity signal leads to an auxin response that is particularly strong in the petiole vasculature and suggests that this response is important for the leaf hyponastic response (Figs. 3 and 4 and Fig. S8).

It was previously proposed that elevation of the petiole angle is caused by differential growth between the adaxial and abaxial sides of the petiole (41, 42). Moreover, auxin signaling in the epidermis is important to control low R/FR-induced hypocotyl elongation (43), suggesting that auxin signaling in the epidermis is important to mediate shade-induced leaf hyponasty. To test this notion we used epidermal-specific expression of *axr3-1* (*CER6:axr3-1*), coding for a stable version of the IAA17 auxin-signaling inhibitor (43). In this mutant leaf movements were altered in control conditions, and low R/FR-induced leaf hyponasty was largely suppressed (Fig. 5 *A* and *B* and Fig. S9 *A*–*C*). Moreover, we found that application of auxin on the tip of *CER6:axr3-1* leaves did not trigger leaf hyponasty (Fig. 5*C* and Fig. S9*D*). Because epidermal expression of *axr3-1* leads to obvious morphological alterations (Fig. S9*A*) (43), rendering leaf tip tracking more difficult, we validated our observation by photogrammetric experiments (Fig. S9). This method allowed us to show that neither the leaf nor the petiole angle increased when *CER6:axr3-1* leaves were treated with low R/FR or auxin (Fig. S9). Collectively our data suggest that shade-induced leaf hyponasty requires auxin signaling in both the vasculature and the epidermis.

Discussion

Neighbor proximity triggers a reduction in the R/FR elicited by FR light reflected from surrounding plants (3, 8). In *Arabidopsis*, this light cue is perceived primarily by phyB, which controls a suite of low R/FR- or shade-induced responses (3). Key players controlling hypocotyl and petiole elongation have been identified.

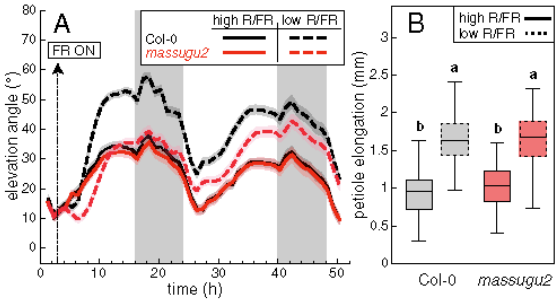

Fig. 4. A gain-of-function mutation in *IAA19* confers reduced shade-induced leaf hyponasty while maintaining a wild-type elongation response. (*A*) Leaf elevation angle of leaves 1 and 2 in Col-0 plants (black lines) and *massugu2* mutants (red lines) in high (solid lines) versus low (dashed lines) R/FR conditions. Plants were grown as in Fig. 1. Leaf elevation angles are mean values ($n = 57$–59). Opaque bands around mean lines represent the 95% CIs of mean estimates. Vertical gray bars represent night periods. (*B*) Boxplots representing petiole elongation over the time period from ZT2 on day 15 ($t = 2$) to ZT2 on day 16 ($t = 26$) computed for each individual leaf analyzed in *A*. Solid and dashed outlines represent data from high R/FR and low R/FR conditions, respectively. Two-way ANOVAs followed by Tukey's HSD test were performed, and different letters were assigned to significantly different groups ($P < 0.05$).

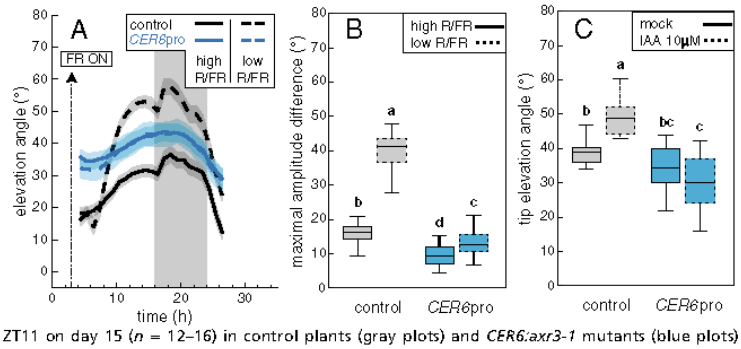

Fig. 5. Auxin signaling in the epidermis is required for shade- and auxin-induced leaf hyponastic responses. (*A*) Leaf elevation angle of leaves 1 and 2 in control plants (black lines) and *CER6:axr3-1* mutants (blue lines) in high (solid lines) versus low (dashed lines) R/FR conditions. Plants were grown as in Fig. 1. Leaf elevation angles are mean values (n = 24–30). Opaque bands around mean lines represent the 95% CIs of mean estimates. Vertical gray bars represent night periods. (*B*) Boxplots representing the amplitude of leaf movement between maximum and minimum leaf elevation angles over the time period from ZT3 (t = 3) to ZT16 (t = 16) on day 15 and computed for each individual leaf analyzed in *A*. Plots with solid and dashed outlines represent data from high and low R/FR conditions, respectively. (*C*) Boxplots representing tip elevation angle for leaf 1 at ZT11 on day 15 (n = 12–16) in control plants (gray plots) and *CER6:axr3-1* mutants (blue plots) treated with mock solution (solid outlines) or 10 µM IAA (dashed outlines). Plants were grown as in Fig. 1, with the exception of the application of solution to the tip of leaf 1 (adaxial side). For *B* and *C*, two-way ANOVAs followed by Tukey's HSD test were performed, and different letters were assigned to significantly different groups ($P < 0.05$). Groups with multiple assigned letters are not significantly different from groups sharing one of these letters, at least.

They include PIFs orchestrating transcriptional reprograming induced by shade cues (12, 13, 21, 24). Among the numerous PIF targets, several *YUC* genes were directly linked to auxin production and elongation responses (12, 19, 25). In this study we show that the PIF-YUC regulon is also essential for low R/FR-induced leaf hyponasty (Fig. 1 and Fig. S2). Moreover, PIN3, 4, and 7 are required for both shade-regulated growth responses and leaf hyponasty (Fig. S3) (18, 24, 25). Despite the involvement of common elements controlling petiole growth and position, our study reveals a bifurcation in the signaling pathways underlying these responses. Indeed, in low R/FR the *msg2* mutant elongates its petiole normally, but leaf hyponasty is impaired (Fig. 4 and Fig. S8) (40).

We establish the importance of auxin for low R/FR-induced hyponasty based on both gain- and loss-of-function studies (Fig. 1 and Figs. S3 and S4). The phenotype of the *yuc* quadruple mutant lacking the *YUC* genes that are rapidly induced upon shade treatment is particularly noteworthy (12, 19, 25). This mutant displays a normal diel-regulated leaf position in high R/FR, but it is essentially unresponsive to the reduction in the R/FR (Fig. 1). Given that the application of auxin or induction of *YUC* expression at the leaf tip triggers a hyponastic response with kinetics comparable to a low R/FR treatment (Fig. 1 and Fig. S4), we conclude that localized shade-induced auxin synthesis is both necessary and sufficient to trigger leaf hyponasty.

The site of auxin production strongly influences the hyponastic response. This conclusion is based on localized reduction of the R/FR (Fig. 2), *YUC* expression (Fig. S6), or auxin application (Fig. 1 and Figs. S4 and S6). In all cases, treatment of the petiole did not lead to leaf hyponasty, whereas the same treatment on the leaf margin was effective. IAA application to the leaf tip led to stronger hyponasty than application on the middle of the margin (Fig. 1 and Fig. S4). However, the latter also resulted in lateral displacement of the leaf (Fig. S4*C*), suggesting that local modulation of IAA levels triggers highly plastic leaf repositioning, as previously observed in densely grown *Arabidopsis* plants (28). Local auxin application to *DR5:GUS* plants gave a strong GUS response irrespective of the application site, indicating that auxin is perceived throughout the leaf (Fig. 3 and Fig. S7). Moreover, it was previously shown that low R/FR is sensed either at the petiole or the blade to trigger petiole elongation (15). Finally, low R/FR induces *YUC* expression in both the blade and the petiole (40). Therefore, we conclude that the absence of hyponastic response following treatments on the petiole is not caused by its inability to produce or sense auxin. In contrast, this situation is analogous to shade-induced elongation, in which low R/FR sensing and auxin production occur in the cotyledon/leaf blade, but the response is observed distally in the hypocotyl/petiole (Fig. 2 and Figs. S4 and S6) (15, 16, 25). An interesting question is why *Arabidopsis* uses information from the blade rather than from the petiole to control leaf hyponasty. Our data based on local shade/auxin application suggest that this mechanism allows highly plastic repositioning of the leaf (Fig. S4 *B* and *C*). Moreover, the advantage of using the leaf tip to perceive the presence of competitors was predicted using a modeling approach in the accompanying paper by Pantazopoulou et al. (44) in this issue of *PNAS*.

That the regulation of auxin levels directly in the petiole does not induce a hyponastic response suggests that auxin needs to be distributed properly within the petiole to trigger the response. Indeed, polar auxin transport and PIN proteins have been implicated in the control of leaf hyponasty (Fig. S3) (45). We show that low R/FR-induced hyponasty requires the activities of PIN3, 4, and 7 but not PIN1 (Fig. S3). To identify sites with a strong auxin response correlating with the hyponastic response, we used *DR5:GUS* lines, which suggest the importance of the petiole vasculature (Fig. 3 and Fig. S7) (46). In addition, the petiole vasculature also corresponds to a site of strong shade-induced *IAA19/MSG2* expression (Fig. S8 *A* and *B*) (38). Finally, the *msg2* mutant expressing a stable form of the IAA19 protein has a reduced hyponastic response in low R/FR (Fig. 4, S8). We therefore propose that auxin signaling in the vasculature is important for shade-mediated leaf elevation. In addition, we show that auxin signaling is also required in the epidermis (Fig. 5 and Fig. S9), as previously observed for shade-induced hypocotyl elongation (43). We thus propose that auxin, which is synthesized in the blade, must be canalized toward the midvein, from which point it forms a gradient in the petiole leading to directional leaf movement through asymmetric auxin-controlled epidermal cell expansion (Fig. 3 and Figs. S4 and S7) (41, 42, 44). Of note, communication between events modulating auxin content in the blade with an effect on the petiole was observed more than 60 years ago (47).

When considering the entire plant, leaf elevation represents a good example of a localized response (Fig. 2 and Fig. S5). In this respect, leaf hyponasty differs from systemic shade responses such as the control of stomatal density (36) or hypocotyl elongation (16). Shade control of stomatal density occurs through developmental regulation of newly emerging leaves that have not experienced the shade treatment (36). In this case a shade signal influences young leaf primordia, a response that may involve distal shade signals leading to reprograming of gene expression at the shoot apex (48). Local shade responses, which have been observed in several species (9, 26, 28), are

considered to be particularly important in the heterogeneous light conditions that are typical in natural environments (26, 27). However, the molecular mechanism underlying local shade responses was unknown. Our study provides a mechanism underlying one such response which combines localized low R/FR-controlled IAA production coupled with PIN3, 4, 7-mediated transport. Auxin produced in the shaded leaf is transported toward the lower parts of the plant where it influences the growth of hypocotyls, stems, or roots as well as branching (3). However, in agreement with models explaining the major routes of auxin transport (49), production of auxin in one leaf does not appear to trigger an auxin response in other rosette leaves (Fig. 3).

Materials and Methods

Detailed experimental procedures are provided in *SI Materials and Methods*.

ACKNOWLEDGMENTS. We thank Christian Hardtke (University of Lausanne), Yunde Zhao (University of California, San Diego), Julin Maloof (University of California, Davis), Carl Procko, and Joanne Chory (Salk Institute) for sharing seeds; Dmitry Kuznetsov, Hon Wai Wan, and Robin Liechti for help in maintaining the phenotyping resource; Ronald Pierik for sharing information prior to publication; and Edward E. Farmer, Mieke de Wit, and Vinicius Costa Galvao for helpful comments on the manuscript. This work was funded by the University of Lausanne and Swiss National Science Foundation Grant FNS 31003A_160326, Sinergia Grant CRSII3_154438, and SystemsX Grant PlantMechanix 51RT-0_145716 (to C.F.). The computations were performed at the Vital-IT Center (www.vital-it.ch).

1. Satbhai SB, Ristova D, Busch W (2015) Underground tuning: Quantitative regulation of root growth. *J Exp Bot* 66:1099–1112.
2. Abley K, Locke JCW, Leyser HMO (2016) Developmental mechanisms underlying variable, invariant and plastic phenotypes. *Ann Bot (Lond)* 117:733–748.
3. Casal JJ (2013) Photoreceptor signaling networks in plant responses to shade. *Annu Rev Plant Biol* 64:403–427.
4. de Wit M, Galvão VC, Fankhauser C (2016) Light-mediated hormonal regulation of plant growth and development. *Annu Rev Plant Biol* 67:513–537.
5. Fraser DP, Hayes S, Franklin KA (2016) Photoreceptor crosstalk in shade avoidance. *Curr Opin Plant Biol* 33:1–7.
6. Schmitt J, Dudley SA, Pigliucci M (1999) Manipulative approaches to testing adaptive plasticity: Phytochrome-mediated shade-avoidance responses in plants. *Am Nat* 154:543–554.
7. Chitwood DH, et al. (2012) Native environment modulates leaf size and response to simulated foliar shade across wild tomato species. *PLoS One* 7:e29570.
8. Ballare CL, Sanchez RA, Scopel AL, Casal JJ, Ghersa CM (1987) Early detection of neighbor plants by phytochrome perception of spectral changes in reflected sunlight. *Plant Cell Environ* 10:551–557.
9. de Wit M, et al. (2012) Plant neighbor detection through touching leaf tips precedes phytochrome signals. *Proc Natl Acad Sci USA* 109:14705–14710.
10. Ballaré CL, Scopel AL, Sánchez RA (1990) Far-red radiation reflected from adjacent leaves: An early signal of competition in plant canopies. *Science* 247:329–332.
11. Legris M, Nieto C, Sellaro R, Prat S, Casal JJ (2017) Perception and signalling of light and temperature cues in plants. *Plant J* 90:683–697.
12. Li L, et al. (2012) Linking photoreceptor excitation to changes in plant architecture. *Genes Dev* 26:785–790.
13. Hornitschek P, et al. (2012) Phytochrome interacting factors 4 and 5 control seedling growth in changing light conditions by directly controlling auxin signaling. *Plant J* 71:699–711.
14. de Wit M, et al. (2016) Integration of phytochrome and cryptochrome signals determines plant growth during competition for light. *Curr Biol* 26:3320–3326.
15. Kozuka T, et al. (2010) Involvement of auxin and brassinosteroid in the regulation of petiole elongation under the shade. *Plant Physiol* 153:1608–1618.
16. Procko C, Crenshaw CM, Ljung K, Noel JP, Chory J (2014) Cotyledon-generated auxin is required for shade-induced hypocotyl growth in Brassica rapa. *Plant Physiol* 165:1285–1301.
17. Tao Y, et al. (2008) Rapid synthesis of auxin via a new tryptophan-dependent pathway is required for shade avoidance in plants. *Cell* 133:164–176.
18. Keuskamp DH, Pollmann S, Voesenek LACJ, Peeters AJM, Pierik R (2010) Auxin transport through PIN-FORMED 3 (PIN3) controls shade avoidance and fitness during competition. *Proc Natl Acad Sci USA* 107:22740–22744.
19. Nozue K, et al. (2015) Shade avoidance components and pathways in adult plants revealed by phenotypic profiling. *PLoS Genet* 11:e1004953.
20. Keuskamp DH, et al. (2011) Blue-light-mediated shade avoidance requires combined auxin and brassinosteroid action in Arabidopsis seedlings. *Plant J* 67:208–217.
21. Leivar P, et al. (2012) Dynamic antagonism between phytochromes and PIF family basic helix-loop-helix factors induces selective reciprocal responses to light and shade in a rapidly responsive transcriptional network in Arabidopsis. *Plant Cell* 24:1398–1419.
22. Bou-Torrent J, et al. (2014) Plant proximity perception dynamically modulates hormone levels and sensitivity in Arabidopsis. *J Exp Bot* 65:2937–2947.
23. Hersch M, et al. (2014) Light intensity modulates the regulatory network of the shade avoidance response in Arabidopsis. *Proc Natl Acad Sci USA* 111:6515–6520.
24. Pedmale UV, et al. (2016) Cryptochromes interact directly with PIFs to control plant growth in limiting blue light. *Cell* 164:233–245.
25. Kohnen MV, et al. (2016) neighbor detection induces organ-specific transcriptomes, revealing patterns underlying hypocotyl-specific growth. *Plant Cell* 28:2889–2904.
26. Ballaré CL (2009) Illuminated behaviour: Phytochrome as a key regulator of light foraging and plant anti-herbivore defence. *Plant Cell Environ* 32:713–725.
27. Izaguirre MM, Mazza CA, Astigueta MS, Ciarla AM, Ballaré CL (2013) No time for candy: Passionfruit (Passiflora edulis) plants down-regulate damage-induced extra floral nectar production in response to light signals of competition. *Oecologia* 173:213–221.
28. Crepy MA, Casal JJ (2015) Photoreceptor-mediated kin recognition in plants. *New Phytol* 205:329–338.
29. van Zanten M, Pons TL, Janssen JAM, Voesenek LACJ, Peeters AJM (2010) On the relevance and control of leaf angle. *CRC Crit Rev Plant Sci* 29:300–316.
30. Sasidharan R, et al. (2010) Light quality-mediated petiole elongation in Arabidopsis during shade avoidance involves cell wall modification by xyloglucan endotransglucosylase/hydrolases. *Plant Physiol* 154:978–990.
31. Dornbusch T, Michaud O, Xenarios I, Fankhauser C (2014) Differentially phased leaf growth and movements in Arabidopsis depend on coordinated circadian and light regulation. *Plant Cell* 26:3911–3921.
32. Ballare CL, Scopel AL (1997) Phytochrome signalling in plant canopies: Testing its population-level implications with photoreceptor mutants of Arabidopsis. *Funct Ecol* 11:441–450.
33. Lorrain S, Allen T, Duek PD, Whitelam GC, Fankhauser C (2008) Phytochrome-mediated inhibition of shade avoidance involves degradation of growth-promoting bHLH transcription factors. *Plant J* 53:312–323.
34. Keller MM, et al. (2011) Cryptochrome 1 and phytochrome B control shade-avoidance responses in Arabidopsis via partially independent hormonal cascades. *Plant J* 67:195–207.
35. Moreno JE, Tao Y, Chory J, Ballaré CL (2009) Ecological modulation of plant defense via phytochrome control of jasmonate sensitivity. *Proc Natl Acad Sci USA* 106:4935–4940.
36. Casson SA, Hetherington AM (2014) phytochrome B is required for light-mediated systemic control of stomatal development. *Curr Biol* 24:1216–1221.
37. Lilley JL, Gee CW, Sairanen I, Ljung K, Nemhauser JL (2012) An endogenous carbon-sensing pathway triggers increased auxin flux and hypocotyl elongation. *Plant Physiol* 160:2261–2270.
38. Pierik R, Djakovic-Petrovic T, Keuskamp DH, de Wit M, Voesenek LACJ (2009) Auxin and ethylene regulate elongation responses to neighbor proximity signals independent of gibberellin and DELLA proteins in Arabidopsis. *Plant Physiol* 149:1701–1712.
39. Tatematsu K, et al. (2004) MASSUGU2 encodes Aux/IAA19, an auxin-regulated protein that functions together with the transcriptional activator NPH4/ARF7 to regulate differential growth responses of hypocotyl and formation of lateral roots in Arabidopsis thaliana. *Plant Cell* 16:379–393.
40. de Wit M, Ljung K, Fankhauser C (2015) Contrasting growth responses in lamina and petiole during neighbor detection depend on differential auxin responsiveness rather than different auxin levels. *New Phytol* 208:198–209.
41. Polko JK, et al. (2012) Ethylene-induced differential petiole growth in Arabidopsis thaliana involves local microtubule reorientation and cell expansion. *New Phytol* 193:339–348.
42. Rauf M, et al. (2013) NAC transcription factor speedy hyponastic growth regulates flooding-induced leaf movement in Arabidopsis. *Plant Cell* 25:4941–4955.
43. Procko C, et al. (2016) The epidermis coordinates auxin-induced stem growth in response to shade. *Genes Dev* 30:1529–1541.
44. Pantazopoulou CK, et al. (2017) Neighbor detection at the leaf tip adaptively regulates upward leaf movement through spatial auxin dynamics. *Proc Natl Acad Sci USA* 114:7450–7455.
45. van Zanten M, Voesenek LA, Peeters AJ, Millenaar FF (2009) Hormone- and light-mediated regulation of heat-induced differential petiole growth in Arabidopsis. *Plant Physiol* 151:1446–1458.
46. Müller-Moulé P, et al. (2016) YUCCA auxin biosynthetic genes are required for Arabidopsis shade avoidance. *PeerJ* 4:e2574.
47. Sequeira L, Steeves TA (1954) Auxin inactivation and its relation to leaf drop caused by the fungus Omphalia Flavida. *Plant Physiol* 29:11–16.
48. Nito K, et al. (2015) Spatial Regulation of the gene expression response to shade in Arabidopsis seedlings. *Plant Cell Physiol* 56:1306–1319.
49. Leyser O (2011) Auxin, self-organisation, and the colonial nature of plants. *Curr Biol* 21:R331–R337.
50. Willige BC, et al. (2013) D6PK AGCVIII kinases are required for auxin transport and phototropic hypocotyl bending in Arabidopsis. *Plant Cell* 25:1674–1688.
51. Bennett T, et al. (2006) The Arabidopsis MAX pathway controls shoot branching by regulating auxin transport. *Curr Biol* 16:553–563.
52. Chen Q, et al. (2014) Auxin overproduction in shoots cannot rescue auxin deficiencies in Arabidopsis roots. *Plant Cell Physiol* 55:1072–1079.
53. Dornbusch T, et al. (2012) Measuring the diurnal pattern of leaf hyponasty and growth in Arabidopsis - a novel phenotyping approach using laser scanning. *Funct Plant Biol* 39:860–869.
54. Kakei Y, et al. (2015) Small-molecule auxin inhibitors that target YUCCA are powerful tools for studying auxin function. *Plant J* 84:827–837.
55. Kami C, et al. (2014) Reduced phototropism in pks mutants may be due to altered auxin-regulated gene expression or reduced lateral auxin transport. *Plant J* 77:393–403.

Supporting Information

Michaud et al. 10.1073/pnas.1702276114

SI Materials and Methods

Plant Material and Growth Conditions. We used the following *Arabidopsis thaliana* genotypes (cv Columbia-0): *phyB-9*, *pif4pif5*, *pif7*, *pif4pif5pif7* (40), *yuc2yuc5yuc8yuc9* (19), *pin3pin4pin7* (50), *pin1* (Salk_047613) (51), *taa1/sav3-2* (17), iYUC3 [FRO6:XVE: YUC3 (52)], and *massugu2-1* (39). The progeny from a heterozygous *pin1* mutant was analyzed for the experiment shown in Fig. S3*D*. Plants were genotyped after completion of the experiment. For lines expressing *axr3-1::mCit* in specific tissues (43), we used F1 hemizygous seeds from at least three independent crosses of *UAS::axr3-1*::mCit with either a Col-0 plant (control) or *CER6::GAL4::VP16* (*CER6:axr3-1*). Seeds were stratified at 4 °C for 3 d in darkness and then were sown on soil saturated with deionized water in a Percival CU-36L4 incubator (Percival Scientific) at 21 °C, 85% relative humidity, and light =175 μmol·m ^{2}·s ^{1} for 13 d (or 12 d for the experiments shown in Figs. S3*B* and S4*F*) under LD conditions. Plants were transferred to the Scanalyzer HTS (LemnaTec) for acclimation (with day–night cycles and light conditions as in the incubator) 24 h before scanning. For shade treatments, the R/FR was decreased from 4.21 to 0.20 using FR-emitting diodes positioned on the ceiling of the Scanalyzer HTS. Further experimental details, spectral composition of light, computation of the R/FR ratio, and technical specifications of the phenotyping device are described in detail in ref. 53.

Pharmacological Treatments. IAA (1–100 μM) (Sigma-Aldrich), NPA (20 μM) (Sigma-Aldrich) and PPBo (100 μM) (Sigma-Aldrich) (54) solutions were freshly prepared from concentrated DMSO stocks before each application. Estradiol (10 μM) (Sigma-Aldrich) solutions were freshly prepared from concentrated EtOH stocks before each application. Mock solutions were similarly prepared to contain 0.15% Tween-20, 0.1% DMSO, and 0.1% EtOH, respectively.

Spotted FR Irradiation. Specific leaf parts were irradiated with FR-emitting diodes (λ = 740 nm) (M740F2; Thorlabs, Inc.) sufficiently distant (~10 cm) from the plant to avoid growth interference. The localization of the irradiated spot was readjusted to account for the movement of the leaf.

GUS Histochemical Staining. *DR5:GUS* rosettes at day 15 were harvested at ZT10, 7 h after shade treatment or exogenous auxin application, and were incubated in 90% acetone overnight at −20 °C. Plants were washed twice in 50 mM sodium phosphate buffer (pH 7.2) and then were vacuum infiltrated for 20 min in 5-bromo-4-chloro-3-indolyl-β-glucuronide (X-gluc) buffer [50 mM $NaPO_4$ (pH 7.2), 0.1% Triton X-100, and 2 mM X-gluc] and subsequently were incubated at 37 °C for 16 h. Rosettes were cleared overnight in 70% ethanol at 4 °C before being photographed under a light stereomicroscope (SMZ1500; Nikon) with a Nikon D7000 camera. The same protocol was applied to the *IAA19:GUS* line (55), except that plants were incubated in buffer consisting of 50 mM sodium phosphate (pH 7.2), 0.1% Triton X-100, 4 mM $K_3[Fe(CN)_6]$, and 2 mM X-gluc at 37 °C for 30 min after vacuum infiltration.

Analysis of Leaf and Petiole Elevation Angles, Leaf Azimuth Angle, and Petiole Length. For time-lapse experiments, plants were scanned at 60-min intervals with the ScanAayzer HTS (LemnaTec). As output, we obtained time-lapse images in which the distances of points measured on the plant surface from a reference plane were color-coded. These images were then transformed into 3D point clouds that yield a precise representation of plant surfaces over time, as previously described (53). Leaf elevation and leaf azimuth angles (also named "tip elevation" and "tip azimuth angles") were delineated by the vector taking as origin the position of the basal end of the petiole organ and as extremity the position of the tip of the blade organ. Petiole length was delineated by the vector taking as origin the position of the basal end of the petiole organ and as extremity the position of the junction between the petiole and the blade organs. A detailed description of the geometric definitions of leaf elevation angle (ϕ_{tip}), leaf azimuth angle (θ_{tip}), and petiole length (l_{pet}), as well as details of image and data processing, are available in refs. 31 and 53. For Fig. S4*C*, the leaf azimuth angle at time t is calculated relative to the leaf azimuth position at time $t = 1$ (ZT1 on day 15, the reference position). Positive and negative azimuth angle values indicate a lateral leaf displacement to the right and to the left, respectively, relative to the leaf azimuth position at $t = 1$.

For photogrammetric experiments, silhouette images were taken with a Canon EOS 550D camera. Elevation angles were measured using Image J (NIH). Tip elevation angle was considered similarly as in time-lapse experiments (ϕ_{tip}) (31). Petiole elevation angle was delineated by the vector taking as origin the position of the basal end of the petiole organ and as extremity the position of the junction between the petiole and the blade organs. A detailed description of the geometric definition of petiole elevation angle (ϕ_{pet}) is presented in ref. 31.

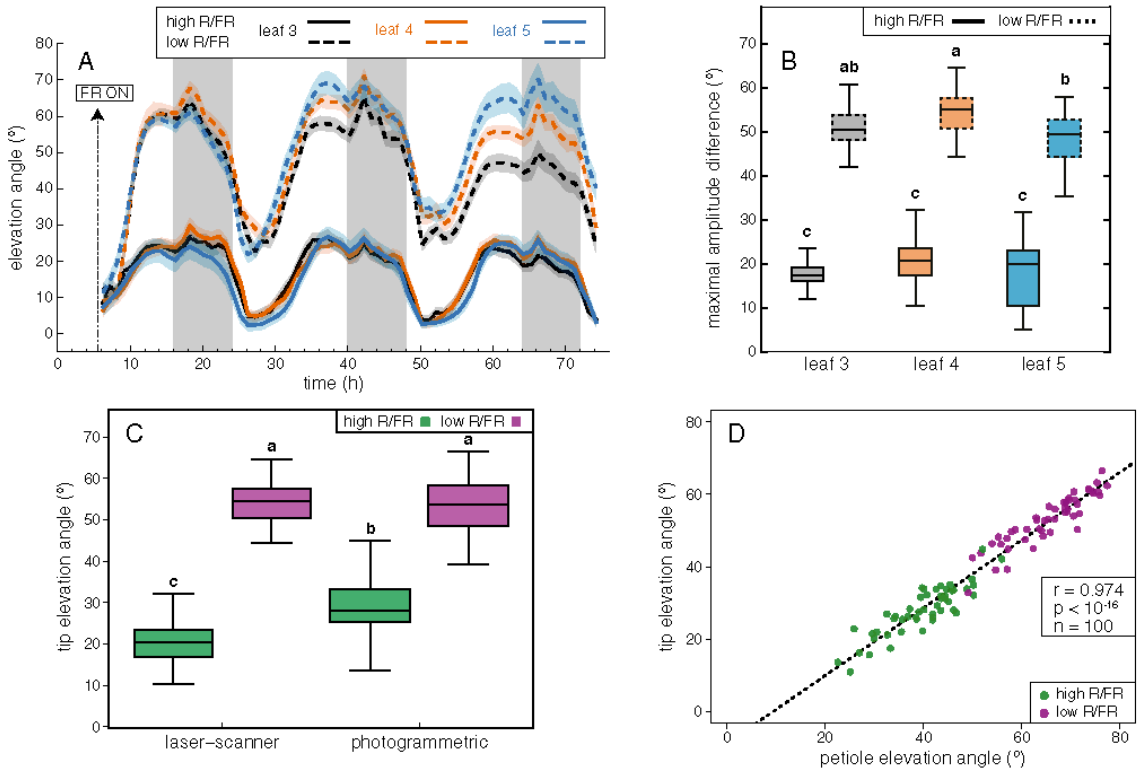

Fig. S1. Low R/FR conditions induce comparable hyponastic responses in different leaves. (*A*) Leaf elevation angle of leaf 3 (black lines), leaf 4 (orange lines), and leaf 5 (blue lines) in Col-0 plants in high (solid lines) versus low (dashed lines) R/FR conditions. Plants were grown as in Fig. 1 except that imaging started at ZT0 on day 18 ($t = 0$), and shade treatment started at ZT5.5 on day 18 ($t = 5.5$). Leaf elevation angles are mean values ($n = 33–41$). Opaque bands around mean lines represent the 95% CIs of mean estimates. Vertical gray bars represent night periods. (*B*) Boxplots representing the amplitude of leaf movement between maximum and minimum leaf elevation angles over the time period from ZT3 ($t = 3$) to ZT16 ($t = 16$) on day 18 and computed for each individual leaf analyzed in *A*. Plots with solid and dashed outlines represent data from high R/FR and low R/FR conditions, respectively. Color coding is as in *A*. (*C*) Boxplots representing tip elevation angle of leaf 4 at ZT11 on day 18 measured in laser scanning ($n = 39–43$) and photogrammetric ($n = 50$) experiments with plants in high (green boxes) and low (purple boxes) R/FR conditions. For *B* and *C*, two-way ANOVAs followed by Tukey's HSD test were performed, and different letters were assigned to significantly different groups ($P < 0.05$). Groups with multiple assigned letters are not significantly different from groups sharing one of these letters, at least. (*D*) Petiole elevation angle (*x* axis) plotted against tip elevation angle (*y* axis) for leaf 4 at ZT11 on day 18. Angles were measured from silhouette images of the plants in the photogrammetric experiment in *C*. Each dot corresponds to one leaf from a single plant. The dashed black line is the regression line.

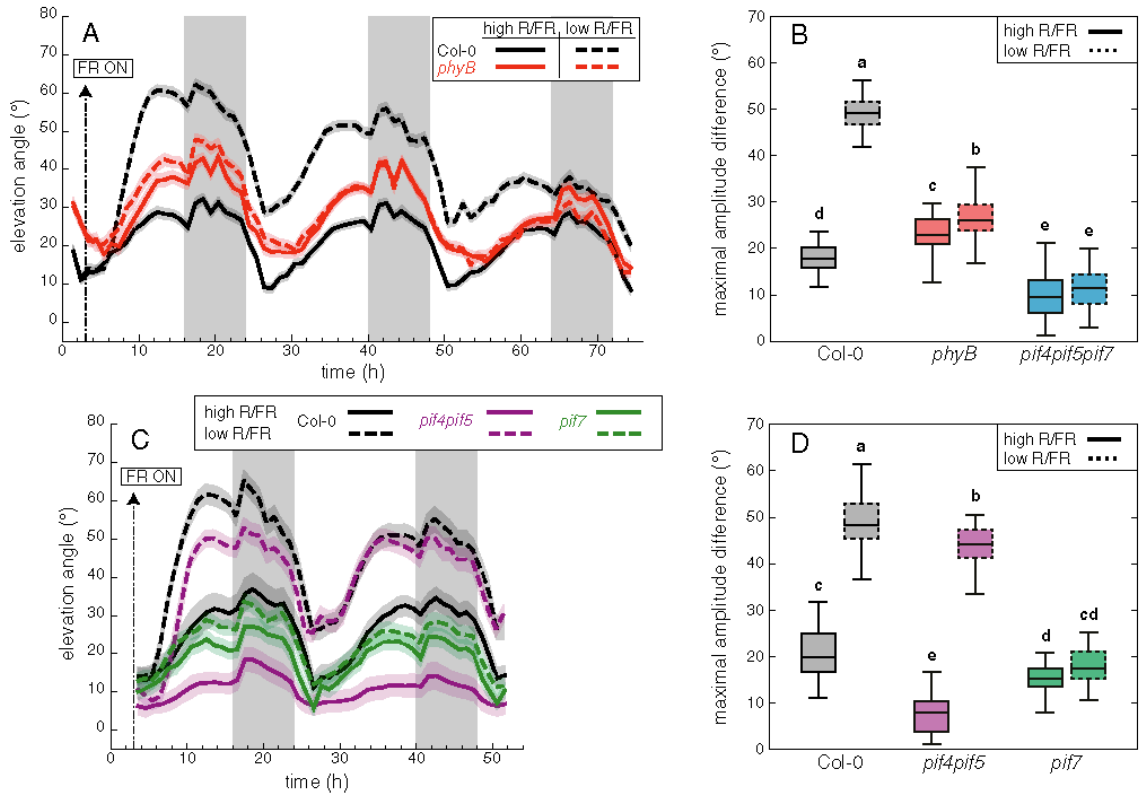

Fig. S2. Leaf hyponasty is controlled by low R/FR sensing and PIFs. Plants were grown as described in Fig. 1. (*A*) Leaf elevation angle of leaves 1 and 2 in Col-0 plants (black lines) and *phyB* mutants (red lines) in high (solid lines) versus low (dashed lines) R/FR conditions. Data are mean of $n = 56–60$. (*B*) Boxplots representing the amplitude of leaf movement between maximum and minimum leaf elevation angles over the time period from ZT3 ($t = 3$) to ZT16 ($t = 16$) on day 15 and computed for each individual leaf analyzed in *A* and Fig. 1*A*. (*C*) Leaf elevation angle of leaves 1 and 2 in Col-0 plants (black lines), *pif4pif5* mutants (purple lines), and *pif7* mutants (green lines) in high (solid lines) versus low (dashed lines) R/FR conditions. Data are the mean of $n = 19–29$. Opaque bands around mean lines in *A* and *C* represent the 95% CIs of mean estimates. Vertical gray bars represent night periods. (*D*) Boxplots representing the amplitude of leaf movement between maximum and minimum leaf elevation angles over the time period from ZT3 ($t = 3$) to ZT16 ($t = 16$) on day 15 and computed for each individual leaf analyzed in *C*. In *B* and *D*, plots with solid and dashed outlines represent data from high and low R/FR conditions, respectively. Two-way ANOVAs followed by Tukey's HSD test were performed, and different letters were assigned to significantly different groups (P value < 0.05). Groups with multiple assigned letters are not significantly different from groups sharing one of these letters, at least.

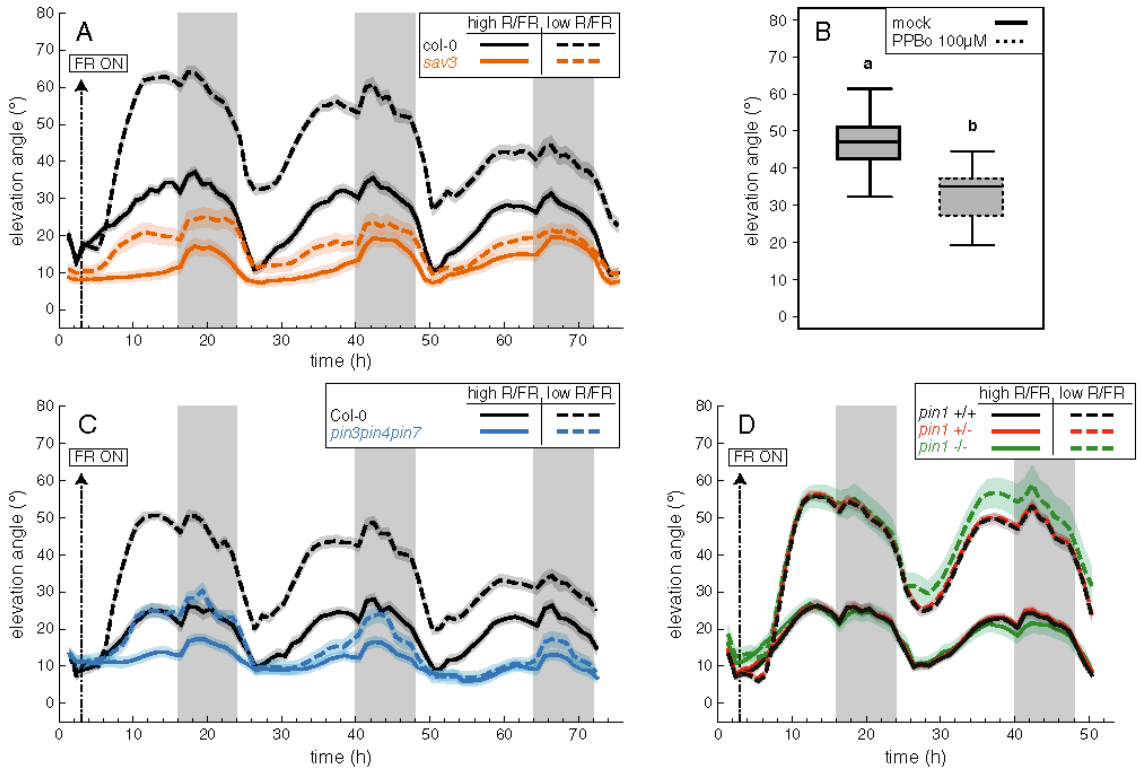

Fig. S3. Auxin synthesis and transport are required for the shade-induced leaf hyponastic response. (*A*) Leaf elevation angle of leaves 1 and 2 in Col-0 plants (black lines) and *taa1/sav3* mutants (orange lines) in high (solid lines) versus low (dashed lines) R/FR conditions. Data are the mean of $n = 50–59$. (*B*) Boxplots representing the tip elevation angle in low R/FR for leaves 1 and 2 at ZT11 on day 14 ($n = 32$). Plants were grown for 13 d in standard LD conditions. On day 14, at ZT3, a 1-µL drop of 100 µM PPBo (dashed outlines) or mock solution (solid outlines) was applied to the tip of leaves 1 and 2 (adaxial side), and plants were moved into low R/FR. One-way ANOVAs followed by Tukey's HSD test were performed, and different letters were assigned to significantly different groups ($P < 0.05$). (*C*) Leaf elevation angle of leaves 1 and 2 in Col-0 plants (black lines) and *pin3pin4pin7* mutants (blue lines) in high (solid lines) versus low (dashed lines) R/FR conditions. Data are the mean of $n = 53–60$. (*D*) Leaf elevation angle of leaves 1 and 2 in wild-type plants (black lines, *pin1* $^{+/+}$), *pin1* heterozygous mutants (red lines, *pin1* $^{+/-}$), and *pin1* homozygous mutants (green lines, *pin1* $^{-/-}$) in high (solid lines) versus low (dashed lines) R/FR conditions. Data are the mean of $n = 36–189$. Plants In *A*, *C*, and *D* were grown as in Fig. 1. Opaque bands around mean lines represent the 95% CIs of mean estimates. Vertical gray bars represent night periods.

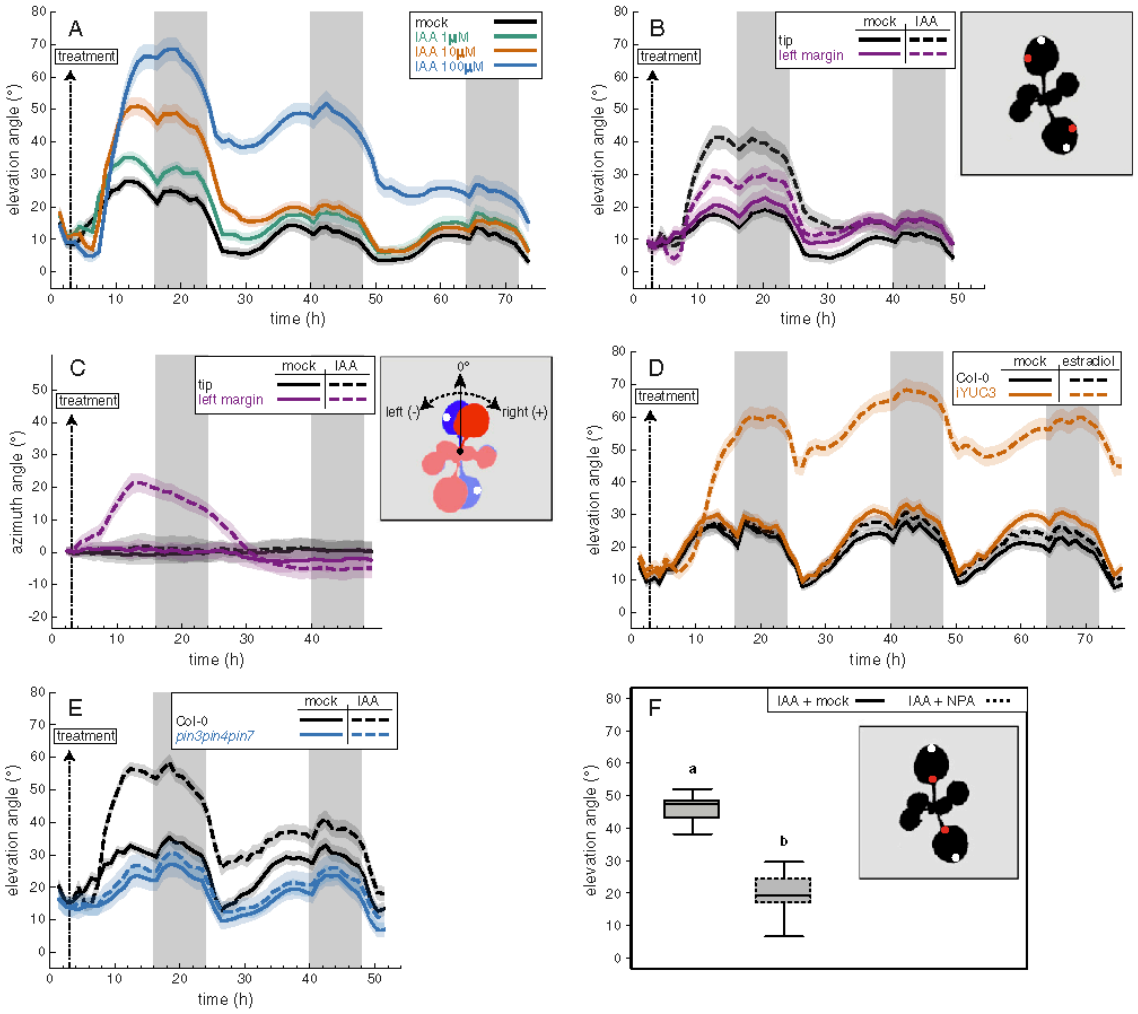

Fig. S4. Auxin application is sufficient to trigger a leaf hyponastic response. (*A*) Leaf elevation angle of Col-0 leaves 1 and 2 treated with mock solution (black line), 1 µM IAA (green line), 10 µM IAA (orange line), or 100 µM IAA (blue line) applied to the leaf tip. Data are the mean of $n = 37–40$. (*B*) Leaf elevation angle of Col-0 leaves 1 and 2 treated with mock solution (solid lines) or 10 µM IAA (dashed lines) applied to the tip (black line; see white dots in *Inset*) or to the left blade margin (purple line; see red dots in *Inset*). Data are the mean of $n = 24–30$. (*C*) Leaf azimuth angle of Col-0 leaves 1 and 2 treated with mock solution (solid lines) or 10 µM IAA (dashed lines) applied to the tip (black lines) or to the left blade margin (purple lines). Data are the mean of $n = 24–30$. (*Inset*) Illustration of the measurement of the leaf azimuth angle. Blue and red silhouettes represent top-down views on day 15 at ZT1 ($t = 1$) and ZT13 ($t = 13$), respectively, of the same individual plant treated (white dots) with 10 µM IAA on the left blade margin of leaves 1 and 2 at ZT1. (*D*) Leaf elevation angle of leaves 1 and 2 treated with mock solution (solid lines) or 10 µM estradiol (dashed lines) applied to the leaf tip in Col-0 plants (black lines) and iYUC3 plants (orange lines). Data are the mean of $n = 38–40$. (*E*) Leaf elevation angle of leaves 1 and 2 treated with mock solution (solid lines) or 10 µM IAA (dashed lines) applied to the leaf tip in Col-0 plants (black lines) and *pin3pin4pin7* mutants (blue lines). Data are the mean of $n = 30–40$. Plants in *A*–*E* were grown as in Fig. 1 except that at ZT3, on day 15, a 1-µL drop of solution was applied to the indicated site on leaves 1 and 2 (adaxial side). Opaque bands around mean lines represent the 95% CIs of mean estimates, and vertical gray bars represent night periods. (*F*) Boxplots representing tip elevation angle for leaves 1 and 2 at ZT11 on day 14 ($n = 20$). Plants were grown for 13 d in standard LD conditions. On day 14, at ZT3, a 1-µL drop of 10 µM IAA solution was applied to the tip of leaves 1 and 2 (adaxial side, white dots in *Inset*), and a 1-µL drop of 20 µM NPA (box with dashed outline) or mock solution (box with solid outline) was simultaneously applied to the petiole–blade junction of leaves 1 and 2 (adaxial side, red dots in *Inset*). One-way ANOVAs followed by Tukey's HSD test were performed; different letters were assigned to significantly different groups ($P < 0.05$).

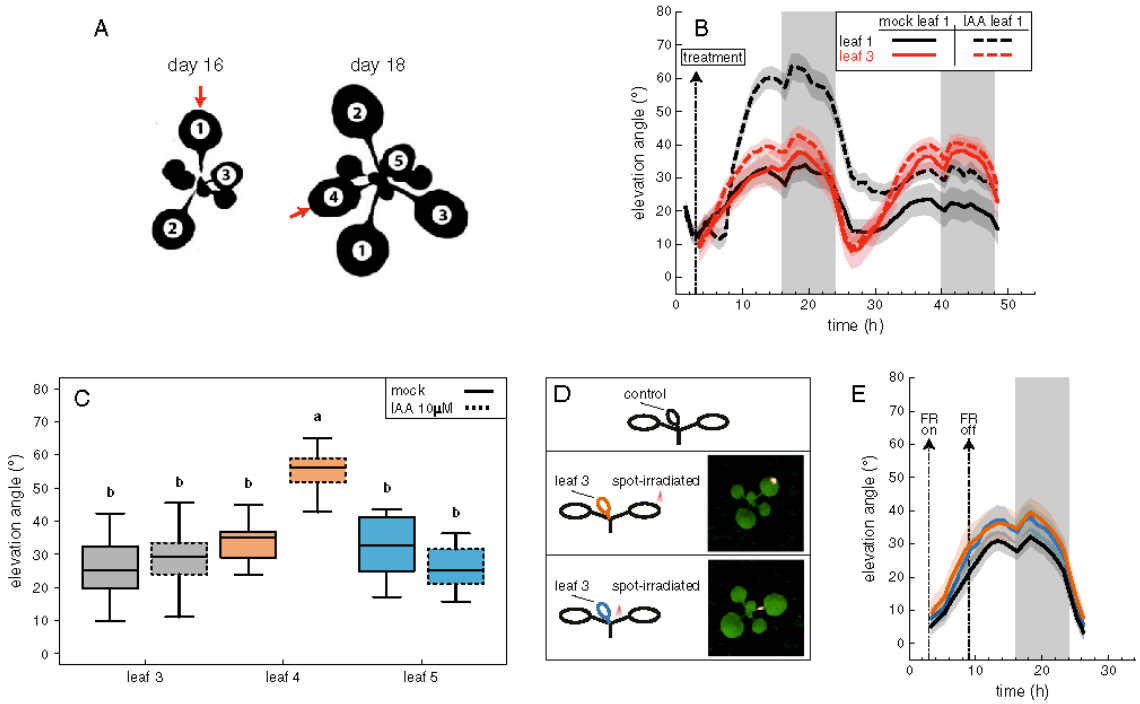

Fig. S5. Shade- and auxin-induced hyponastic responses are restricted to the treated leaf. (*A*) Top-down views of representative *Arabidopsis* rosettes on day 16 (*Left*) and 18 (*Right*). Numbers are attributed to true rosette leaves starting from the oldest (leaves 1 and 2) to the youngest (leaf 5). Red arrows indicate treated leaves for data shown in Fig. 2*A* and Fig. S5*B* (16-d-old plants) and in Fig. S5*C* (18-d-old plants). (*B*) Leaf elevation angle of leaf 1 (black lines) and leaf 3 (red lines) with mock solution (solid lines) or 10 µM IAA (dashed lines) applied to the tip of leaf 1 in Col-0 plants. Leaf elevation angles are mean values (n = 10–15). Plants were grown as in Fig. 1 except that imaging started at ZT0 on day 16 (t = 0), and at ZT3 a 1-µL drop of solution was applied to the tip of leaf 1 (adaxial side). (*C*) Boxplots representing leaf elevation angles at ZT11 on day 18 (n = 20). Plants were grown as in Fig. 1 except that on day 18, at ZT3, a 1-µL drop of 10 µM IAA (dashed outline) or mock solution (solid outline) was applied to the tip of leaf 4 (adaxial side). Two-way ANOVAs followed by Tukey's HSD test were performed, and different letters were assigned to significantly different groups (P < 0.05). (*D*) Illustration of the different treatments applied in *E*. (*Upper*) Leaf 3 growing in standard high R/FR conditions (control; solid black outline). (*Middle*) One single leaf (leaf 1 or 2) is spot irradiated with FR on the tip (indicated by an orange triangle), whereas leaf 3 is growing in high R/FR conditions (distal, solid orange outline). Note the illumination on the representative plant shown on the right. (*Lower*) One single leaf (leaf 1 or 2) is spot irradiated with FR on the petiole (indicated by an orange triangle), whereas leaf 3 is growing in high R/FR conditions (distal, solid blue outline). Note the illumination on the representative plant shown on the right. (*E*) Leaf elevation angle of Col-0 leaf 3 grown in control conditions (solid black line, n = 22), of the distal untreated leaf 3 of plants spot-irradiated with FR on the tip of leaf 1 or 2 (solid orange line, n = 11), and of the distal untreated leaf 3 of plants spot-irradiated with FR on the petiole of leaf 1 or 2 (solid blue line, n = 10). Plants were grown as in Fig. 1 except that FR illumination started on day 15 at ZT3 (t = 3) and stopped at ZT9 (t = 9). Leaf elevation angles are mean values. In *B* and *E* opaque bands around mean lines represent the 95% CIs of mean estimates. Vertical gray bars represent night periods.

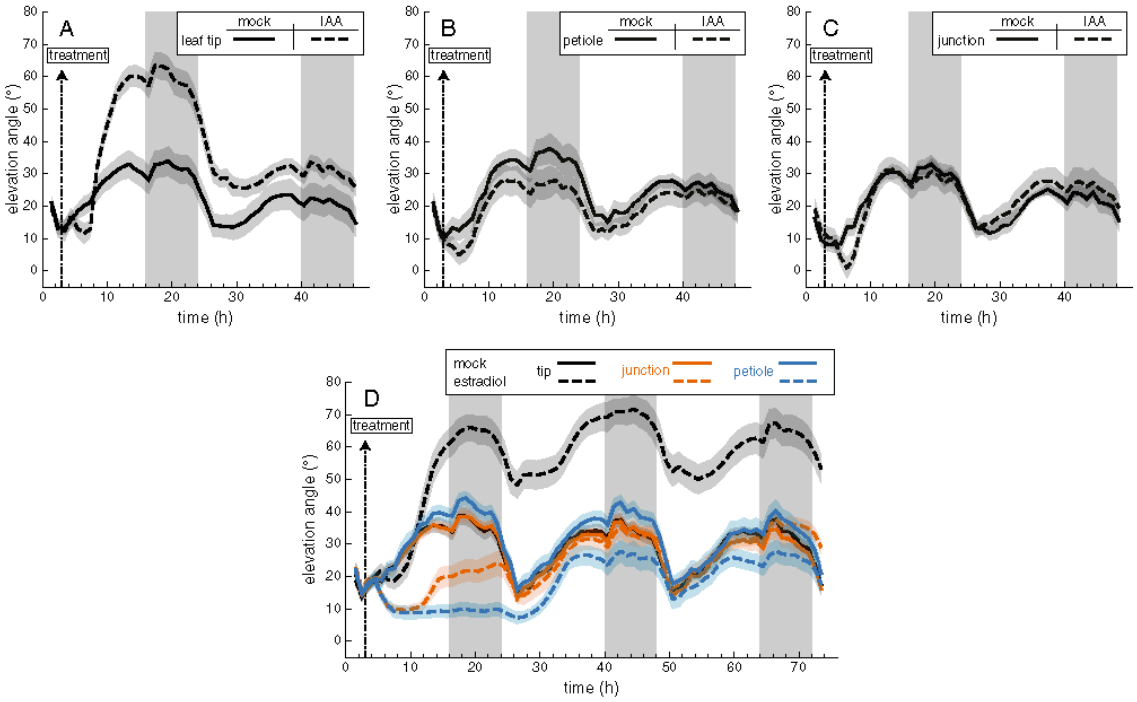

Fig. S6. Production or application of auxin at the leaf tip but not at the petiole leads to leaf hyponasty. (*A*–*C*) Leaf elevation angle of Col-0 leaf 1 with mock solution (solid lines) or 10 μM IAA (dashed lines) applied to the tip (*A*), the petiole (*B*), or the petiole–blade junction (*C*) of leaf 1. Plants were grown as in Fig. 1 except that imaging started at ZT0 on day 16 ($t = 0$), and at ZT3, a 1-μL drop of solution was applied to the specified site on leaf 1 (adaxial side). Leaf elevation angles are mean values ($n = 11$–15). (*D*) Leaf elevation angle of iYUC3 leaves 1 or 2 with mock solution (solid lines) or 10 μM estradiol (dashed line) applied on the tip (black lines), the petiole–blade junction (orange lines), or the petiole (blue lines) of leaves 1 or 2. Plants were grown as in Fig. 1 except that on day 15, at ZT3, a 1-μL drop of solution was applied to the specified leaf site (adaxial side). Leaf elevation angles are mean values ($n = 21$–30). Opaque bands around mean lines represent the 95% CIs of mean estimates, and vertical gray bars represent night periods.

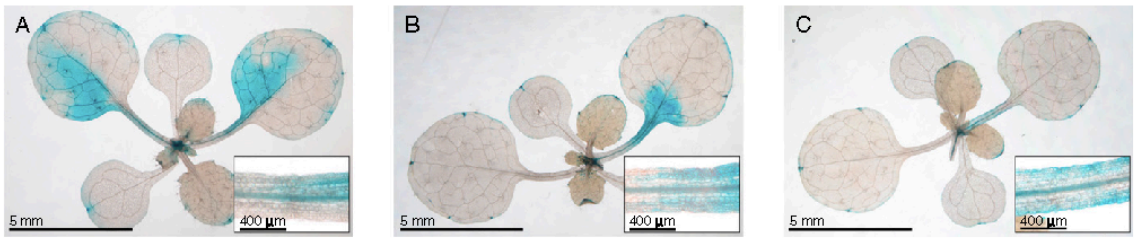

Fig. S7. *DR5:GUS* auxin response following the application of IAA to different parts of the leaf. The auxin response was visualized in leaves of *DR5:GUS* reporter plants 7 h after the application of exogenous auxin (10 μM) to the left blade margin of leaves 1 and 2 (*A*), to the petiole–blade junction of leaf 1 (*B*, leaf on the right), or to the petiole of leaf 1 (*C*, leaf on the right). Plants were grown as in Fig. 1 except that on day 15, at ZT3, a 1-μL drop of solution was applied to the indicated adaxial site on leaf 1 (*B* and *C*) or on leaves 1 and 2 (*A*). Plants were harvested on day 15 at ZT10. *Insets* show close-ups of petioles of right leaves in each panel.

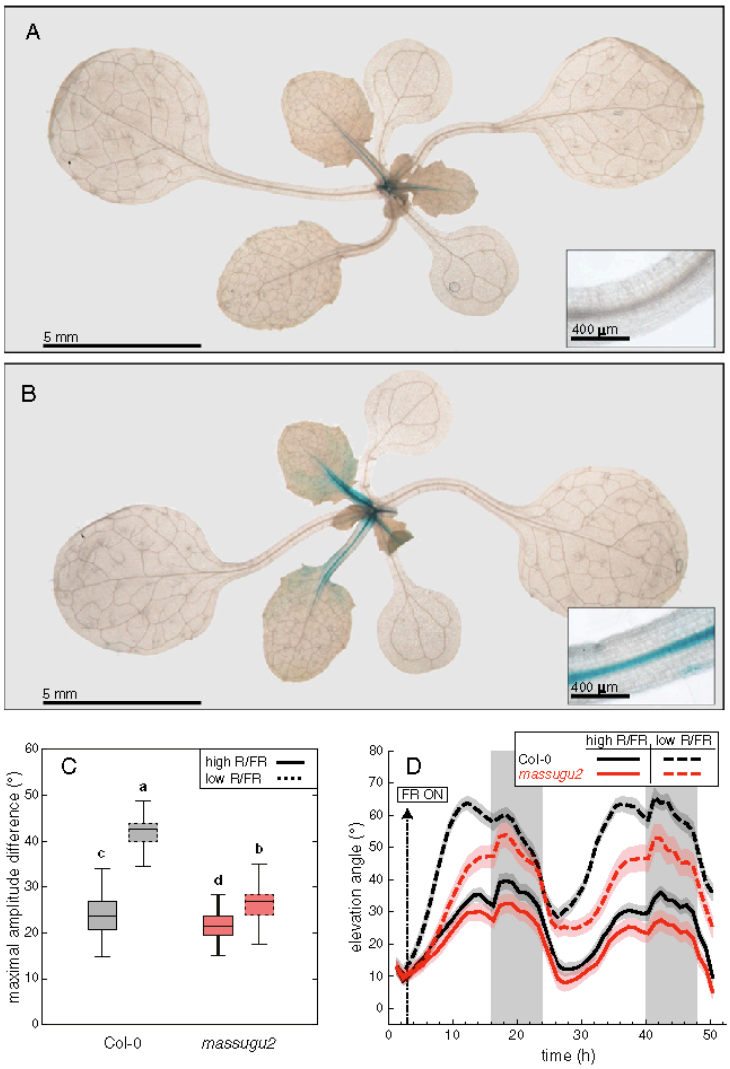

Fig. S8. Shade response of the *msg2-1* mutant. (*A* and *B*) Auxin response visualized in leaves of *IAA19:GUS* reporter plants after 7 h in high (*A*) or low (*B*) R/FR conditions. Shade treatment started on day 15 at ZT3, and plants were harvested at ZT10 on the same day. *Insets* in *A* and *B* show close-up views of the petioles of leaf 3 (downward-pointing leaves). (*C*) Boxplots representing the amplitude of leaf movement between maximum and minimum leaf elevation angles over the time period from ZT3 ($t = 3$) to ZT16 ($t = 16$) on day 15 and computed for each individual leaf analyzed in Fig. 4*A*. Plots with solid and dashed outlines represent data from high and low R/FR conditions, respectively. Two-way ANOVAs followed by Tukey's HSD test were performed, and different letters were assigned to significantly different groups ($P < 0.05$). (*D*) Elevation angle of leaf 3 in Col-0 plants (black lines) and *massugu2* mutants (red lines) in high (solid lines) versus low (dashed lines) R/FR conditions. For low R/FR conditions, shade treatment started on day 15 at ZT3. Leaf elevation angles are mean values (n = 24–30). Opaque bands around mean lines represent the 95% CIs of mean estimates. Vertical gray bars represent night periods. Plants were grown as in Fig. 1.

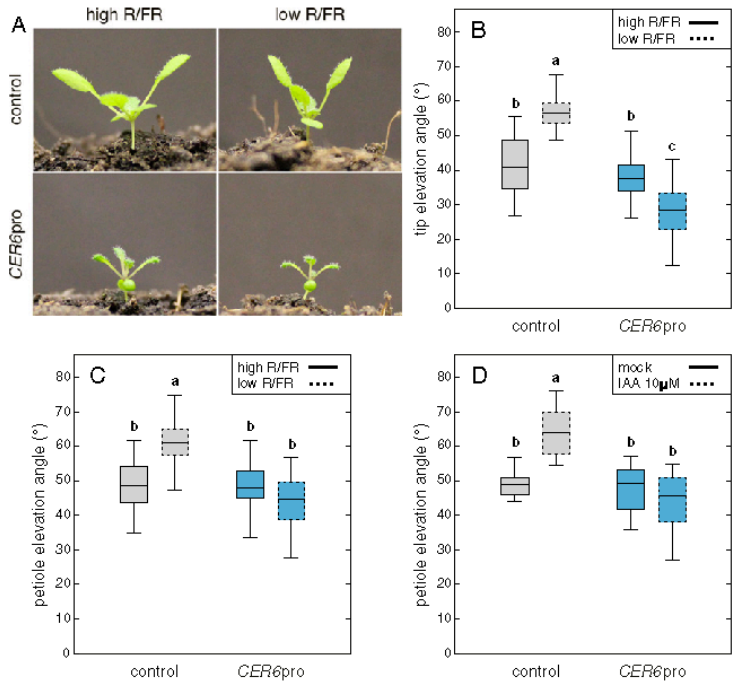

Fig. S9. Epidermal expression of *axr3-1* prevents shade- and auxin-induced leaf hyponasties. (*A*) Silhouettes of representative individual control plants (*Upper*) and *CER6:axr3-1* mutants (*Lower*) grown in high (*Left*) or low (*Right*) R/FR conditions. Plants were grown as in Fig. 1. The low R/FR treatment started at ZT3 on day 15, and plants were imaged at ZT11 on the same day. (*B*) Boxplots representing tip elevation angle for leaves 1 and 2 at ZT11 on day 15 ($n = 30$) in control plants (gray boxes) and *CER6:axr3-1* mutants (blue boxes) grown in high (solid outlines) or low (dashed outlines) R/FR conditions. (*C*) Boxplots representing petiole elevation angle for leaves 1 and 2 at ZT11 on day 15 ($n = 30$) in control plants (gray boxes) and *CER6:axr3-1* mutants (blue boxes) grown in high (solid outlines) or low (dashed outlines) R/FR conditions. Plants in *B* and *C* were grown as in Fig. 1. Low R/FR treatment started at ZT3 on day 15, and plants were imaged 8 h later (ZT11). Data for both types of angle were obtained from the same plants. (*D*) Boxplots representing the petiole elevation angle for leaf 1 at ZT11 on day 15 ($n = 12–16$) in control plants (gray boxes) and *CER6:axr3-1* mutants (blue boxes) treated with mock solution (solid outlines) or 10 μM IAA (dashed outlines). Plants were grown as in Fig. 1 except that on day 15, at ZT3, a 1-μL drop of solution was applied to the tip of leaf 1 (adaxial side). Data were obtained from the plants in Fig. 5*C*. For data in *B–D*, two-way ANOVAs followed by Tukey's HSD test were performed, and different letters were assigned to significantly different groups ($P < 0.05$).

Complementary results

Additional experiments were conducted in relation with the work published in Michaud *et al.* (2017). These experiments are about the involvement of polar auxin transport in the low R/FR-induced leaf hyponasty. We aimed at investigating further the mechanisms underlying the transport of auxin from its site of production towards the site where it can trigger downstream signaling responsible for leaf movement.

First, we monitored leaf movement in high versus low R/FR conditions in the quadruple *aux1lax1lax2lax3* mutant (Fig. 1). This mutant is defective for the four genes composing the *AUX/LAX* family of auxin influx carriers which mediate the transport of auxin from the outside to the inside of the cells (61). Quadruple *aux1lax1lax2lax3* mutants although displaying a wild type movement in standard high R/FR conditions were strongly impaired in their response to low R/FR treatment (Fig. 1). These results show that AUX/LAX auxin influx carriers are required for shade-induced hyponasty and point towards the importance of auxin cellular uptake from the site of increased auxin production to the site of auxin action during shade response.

Then, we compared the kinetics of hyponastic responses in leaves treated at the tip either with the natural auxin IAA or with synthetic auxin analogs including 2,4-Dichlorophenoxyacetic acid (2,4-D) and 1-Naphthaleneacetic acid (1-NAA) (Fig. 2). Although generally mimicking the effects of IAA on plant physiology, 2,4-D and 1-NAA have different effectiveness concerning their ability to be transported into or out of the cells. While 1-NAA has a strongly reduced capacity for cellular influx relatively to IAA, 2,4-D seems to be rather affected in its ability for cellular efflux (229). When applied at the tip, IAA triggered a similar hyponastic response to what is observed in shade conditions, this response being restricted to the treated leaf (Fig. 2B). On the contrary, 2,4-D and 1-NAA failed to trigger such hyponastic response in the treated leaf (Fig. 2C-D). However, 1-NAA application still led to a slow and gradual upward movement in the treated leaf especially observable the following day. Effects of 2,4-D on leaf movement were opposite to effects of IAA as 2,4-D rather induced an downward movement in the treated leaf.

In addition, we studied the response induced by auxin and synthetic auxin analogs when applied at the leaf tip of *DR5:GUS* auxin reporter plants (Fig. 3). In line with the previous results on leaf movement, the two synthetic auxin analogs were unable

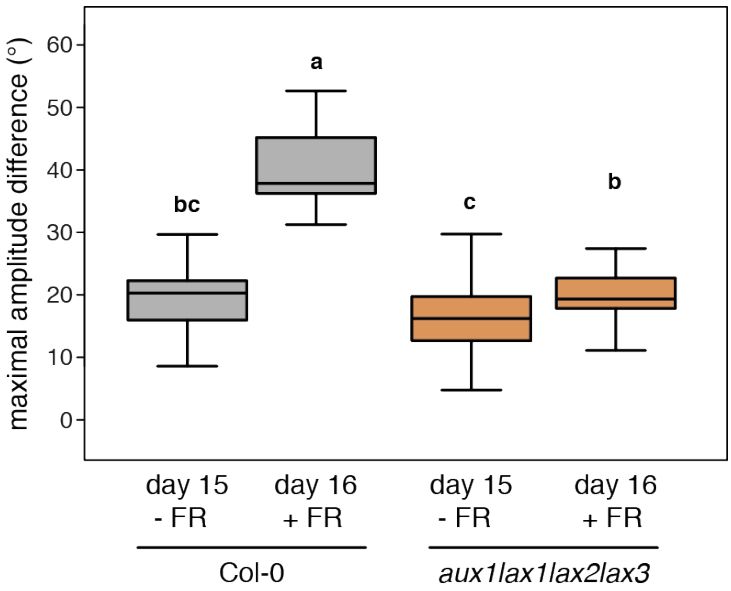

Figure 1. Low R/FR-induced hyponasty is strongly affected in quadruple *aux1lax1lax2lax3* mutants.

Boxplots representing the amplitude of leaf movement in Col-0 (black) versus quadruple *aux1lax1lax2lax3* mutant (orange) plants between maximum and minimum leaf elevation angles over day 15 (high R/FR, time period from t = 3 to t = 16) and day 16 (low R/FR, time period from t = 27 to t = 40). Each boxplot represents 26-27 individual leaves. Plants were grown for 14 d in standard long-day [LD, 16-h light, 8-h dark (16/8)] conditions. Imaging started on day 15 at ZT0 (t = 0) and plants were maintained in LD conditions. Shade treatment started on day 16 at ZT6.5 (t = 30.5) by adding FR light to decrease the R/FR ratio. Two-way ANOVA followed by Tukey's Honestly Significant Difference (HSD) test were performed and different letters were assigned to significantly different groups (p-value < 0.05).

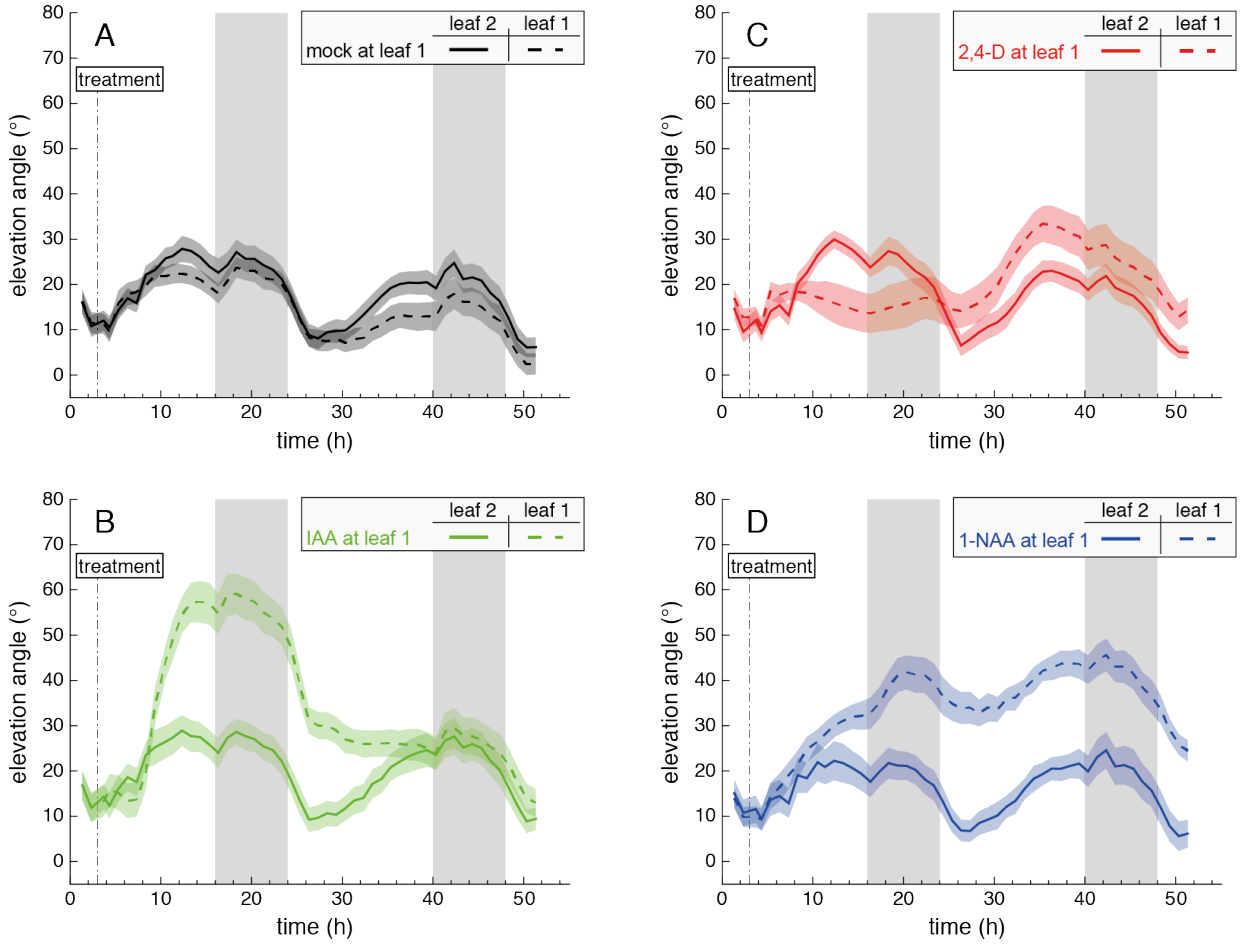

Figure 2. Synthetic auxin analogs are unable to mimic the effects of natural IAA on leaf hyponasty.

Leaf elevation angle of Col-0 leaf 1 (dashed lines) and leaf 2 (full lines) with mock solution (A, black), 10μM IAA (B, green), 10μM 2,4-D (C, red) or 10μM 1-NAA (D, blue) applied to the tip of leaf 1 (adaxial side). Plants were grown for 14 d in standard long-day [LD, 16-h light, 8-h dark (16/8)] conditions. Imaging started on day 15 at ZT0 (t = 0) and plants were maintained in LD conditions. At ZT3 (t = 3) on day 15 a 1-μL drop of solution was applied to the tip of leaf 1 (adaxial side). Data are mean of n = 15.

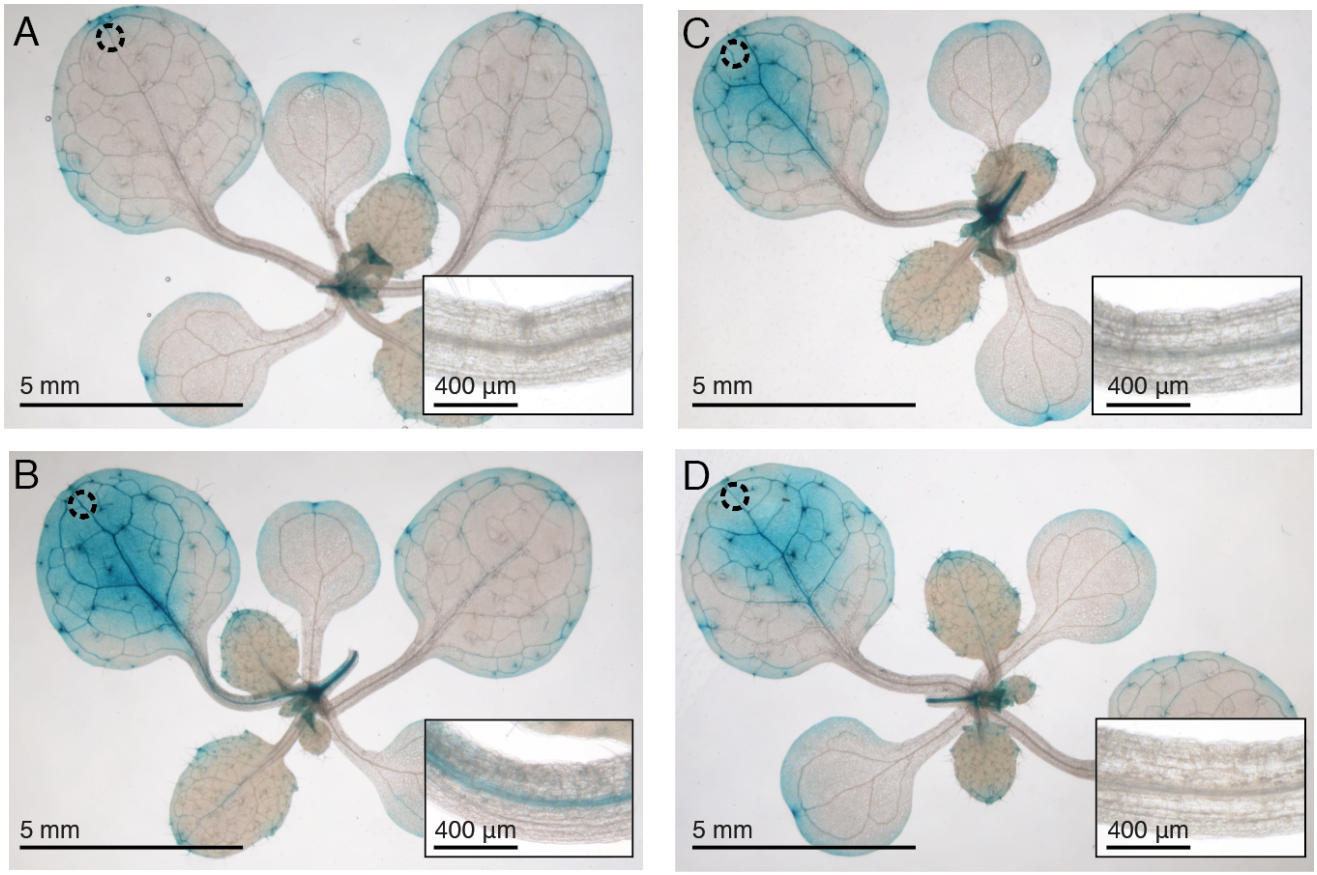

Figure 3. Synthetic auxin analogs are unable to trigger a distal auxin response in the vasculature of the petiole.

The auxin response was visualized in leaves of *DR5:GUS* reporter plants after exogenous application of mock solution (A), 10µM IAA (B), 10µM 2,4-D (C) or 10µM 1-NAA (D) on the tip of leaf 1 (adaxial side) in high R/FR. Plants were grown for 14 d in standard long-day [LD, 16-h light, 8-h dark (16/8)] conditions. At ZT3 (t = 3) on day 15 a 1-µL drop of solution was applied to the tip of leaf 1 (adaxial side). Plants were harvested on day 15 at ZT10. Sites of application are represented by dashed circles. Insets in all panels show close-ups of leaf 1 petiole.

to trigger an auxin response in the distal petiole organ. Indeed, although a strong auxin response was observed near the site of application in the blade organ after IAA, 2,4-D and 1-NAA applications, only IAA was able to induce a response in the vasculature of the petiole.

Overall, the combination of these genetic and pharmacological approaches have proved to be very informative concerning the molecular mechanisms of auxin action in leaf hyponastic responses. Our data support the hypothesis that in shade auxin needs to be efficiently transported from the site of production at the margins towards the petiole organ where it can trigger downstream events involved in leaf movement. Also, these results are in line with our previously published observations of *pin3pin4pin7* mutants and of plants treated with 1-N-naphthylphthalamic acid (NPA), an inhibitor of PAT (227).

CHAPTER III

A key role for abscisic acid downstream of auxin signaling in shade-induced leaf hyponastic response

Sequence shot illustrating a local leaf hyponastic response in Arabidopsis.
2017. O. Michaud

Overview

During the fifth year of my thesis, I conducted a project relative to the importance of ABA during shade-induced nastic responses in Arabidopsis leaves, under the supervision of my thesis directors.

The objective of this project was to investigate the putative role of ABA during leaf hyponasty in response to neighbor detection. To tackle this question, we used our newly developed phenotyping methodology (225) along with phytohormone quantification and molecular genetic approaches. Our work led to discoveries concerning (1) the process of ABA biosynthesis in leaf organs growing in low R:FR conditions as well as (2) the essentiality of ABA biosynthesis and ABA signaling in low R:FR-induced leaf hyponasty.

I stood as the leading investigator for this project. My involvement consisted in designing and performing experiments by combining phenotyping, hormone quantification and genetic approaches. Concerning the quantification of ABA (Fig. 4 and Fig. 7), I relied on the expertise of Dr. Gaétan Glauser who performed this task. Throughout my project, I analyzed and interpreted data with the participation of my supervisor Prof. Christian Fankhauser.

Introduction

Neighbor-detecting conditions (low R:FR) trigger a suite of adaptive responses in plants including increased shoot elongation and upward leaf movement (hyponasty) thereby allowing plants to consolidate their access to sunlight (41). Among the several phytohormones involved in SAS (38), only auxin has been shown to be implicated in low R:FR-induced hyponasty so far (48, 49, 227, 230). Besides the major role of auxin, plant hydraulics also represent a crucial aspect in light-modulated leaf movements (113, 114, 161, 224). Plant hydraulics are largely mediated by another phytohormone named abscisic acid (ABA) (159, 202). Although there is increasing evidence for ABA being involved in plant adaptation to stressful light conditions (203, 209) as well as in organ movement (100, 161), no clear implication of ABA in shade-induced hyponasty has been highlighted so far.

At the cellular level, first steps in ABA production take place in plastids where successive reactions lead to the transformation of isopentenyl diphosphate into carotenoids (Fig. 1) (231). Among carotenoids derived from isopentenyl diphosphate, only β-carotene is subsequently metabolized into zeaxanthin through β-CAROTENOID HYDROXYLASES 1 and 2 (BCH1 and BCH2). Zeaxanthin is then converted to violaxanthin by ZEAXANTHIN EPOXIDASE (ZEP) also named ABA-DEFICIENT 1 (ABA1) (232). Members of the NCED family in turn catalyze the rate-limiting step in ABA biosynthesis which is the transformation of zeaxanthin to xanthoxin (90). A close relationship is observed between *NCED* expression and ABA levels (207, 233, 234). So far, five genes (*NCED2,3,5,6,9*) were shown to code for NCED in Arabidopsis (234). Next, two successive cytosolic steps allow the conversion of xanthoxin to ABA. The first step is mediated by SHORT-CHAIN DEHYDROGENASE REDUCTASE (SDR) called ABA2 while the second step is catalyzed by a complex formed by one of the three ABSCISIC ALDEHYDE OXIDASES (AAO1,3,4) with the molybdenum cofactor (MoCo) whose production depends on ABA-DEFICIENT 3 (ABA3). The amount of ABA in a cell not only depends on biosynthesis but also on conjugation and oxidation processes. On the one hand, ABA can be transformed into phaseic acid and this reaction is catalyzed by the members of the CYTOCHROME P450 707 A (CYP707A) family (235). On the other hand, ABA can be inactivated by conjugation to other molecules such as

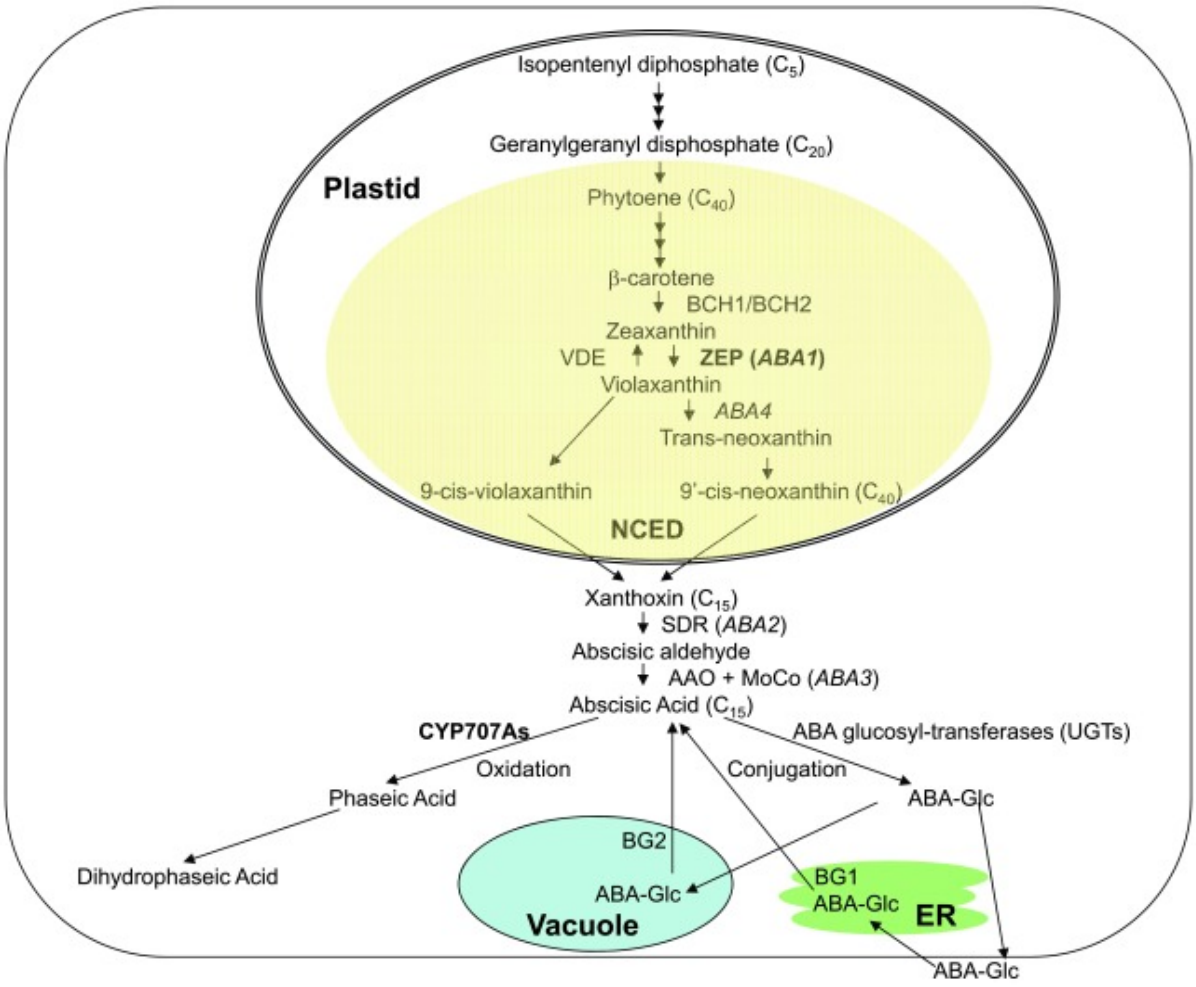

Figure 1. Current view of ABA metabolic pathways.

(from Finkelstein, 2013, Arabidopsis Book)

Scheme representing the biochemical reactions involved in ABA metabolism. Early steps in ABA biosynthesis happen in the cell plastid during which isopentenyl diphosphate is transformed into β-carotene. β-carotene is then converted to zeaxanthin, violaxanthin and xanthoxin through BCHs, ABA1 and NCEDs, respectively. In the cytosol, xanthoxin is further metabolized into ABA through two successive steps involving ABA2 and an AAO-MoCo complex. ABA amounts in the cytoplasm depend on their biosynthesis but also on their degradation by the CYP707As as well as on their inactivation through conjugation to other molecules.

glucosyl ester (ABA-GE) but, contrary to phaseic acid transformation, this inactivation is not definitive and can be reversed by the β-GLUCOSIDASES 1 and 2 (BG1,2) (165).

At the plant level, ABA is generally produced in the vascular system (231). Regarding the shoots especially, although stomata are also capable of autonomous ABA production (207, 208, 236) it is assumed that the hormone is mainly synthesized in leaf vasculature (207, 212, 236, 237, 238). In many species, ABA levels are under the control of the circadian clock (239). In Arabidopsis leaves, ABA levels peak at the end of the day and reach minimal values at dawn (165). This daily hormonal fluctuation is apparently regulated at the biosynthetic level (165, 240). In case of water stress, ABA production is enhanced in leaves with NCED3 playing a prominent role among NCEDs in the process (241). However, based on the stronger phenotype of *nced3nced5* double mutants compared to *nced3* single mutants, NCED5 also contributes to ABA responses in leaves (241). In addition to water stress, low R:FR signals can also modulate ABA production in Arabidopsis (86, 242). Moreover, induction of *NCED* expression was recently observed in Arabidopsis plants grown under low R:FR (45, 58) and also when plants were treated with exogenous auxin (55, 243). From the site where it is produced in the plant, ABA can be transported to targeted tissues in both rootward or shootward directions through the xylem and phloem tissues (212, 236, 237, 238). The way ABA transport is achieved is not fully understood (231). However recent research led to the discovery of several ABA transporters thereby indicating a certain complexity in the process (244, 245, 246).

In order to activate downstream ABA responses, functional ABA perception is required in targeted tissues (Fig. 2) (231). Perception of ABA in plant cells mainly relies on the receptors of the PYRABACTIN RESISTANCE 1 (PYR1)/PYR1-LIKE (PYL)/REGULATORY COMPONENTS OF ABA RECEPTORS (RCAR) family which constitute the core ABA signaling pathway in Arabidopsis (247). The PYR1/PYL/RCAR family is composed of thirteen members (PYR1 and PYL1-12) which are present in the cytoplasm and the nucleus. In leaves, expression of *PYR1/PYL/RCARs* is mostly associated to leaf veins and stomata, and plants with combined mutations in these genes are significantly affected in leaf growth and transpiration (248). Direct interaction between ABA and PYR1/PYL/RCARs leads to the formation of a ternary complex with one member of the PROTEIN

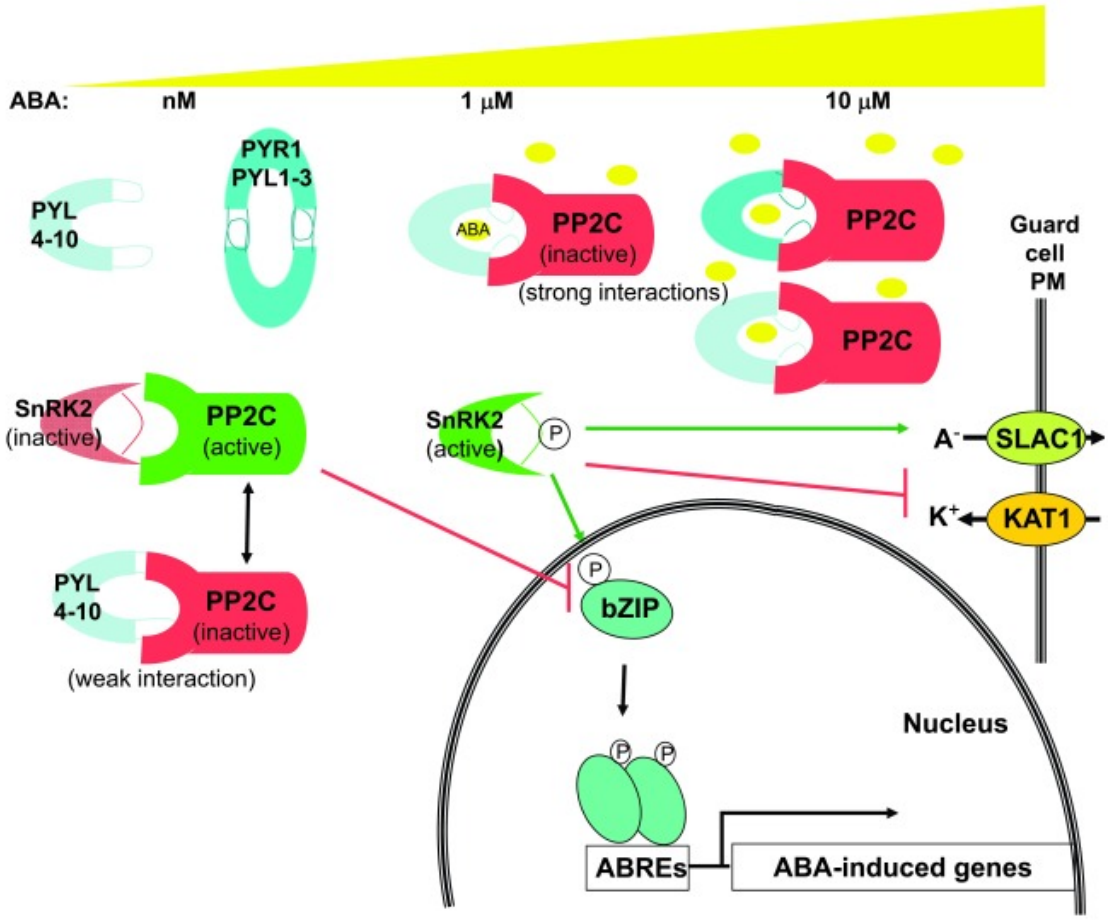

Figure 2. Core network for ABA perception and signaling.

(from Finkelstein, 2013, Arabidopsis Book)

Scheme representing the interactions between the components of the main ABA signaling pathway at different ABA concentrations. PYR1/PYL/RCARs ABA receptors have no or low affinity for the negative regulators PP2Cs in absence of ABA. In this situation, PP2Cs can therefore interact with SnRK2s and inhibit their activity. In the presence of the hormone, a ternary complex is formed between ABA, PYR1/PYL/RCARs and PP2Cs thereby leading to the derepression of SnRK2s which can then activate transcriptional regulators involved in ABA responses. In addition, SnRK2s also play a role in the ABA-mediated regulation of ion channels such as the K+ ARABIDOPSIS THALIANA 1 (KAT1) and the SLOWLY ACTIVATING ANION CHANNEL 1 (SLAC1). ABREs: ABA-responsive elements. PM: plasma membrane. bZIP: a class of transcription factors.

PHOSPHATASES 2C (PP2C) family. PP2Cs generally act negatively on ABA signaling by directly inhibiting the activity of SNF1-RELATED PROTEIN KINASES 2 (SnRK2s) which are positive regulators of the response. Stabilization of the ABA-PYR1/PYL/RCAR-PP2C complex releases the activity of SnRK2s that can further interact with numerous targets involved in ABA responses like transcriptional regulators or ion channels. This is important to note that besides the importance of phosphatase inhibition and kinase activation in ABA signaling (Fig. 2), a study reported similar amounts of phosphorylation and dephosphorylation events during rapid ABA-induced responses thereby indicating the existence of other signaling pathways (215). Interestingly, among the proteins being rapidly dephosphorylated in response to ABA are some aquaporins of the PIP family such as PIP2;1.

Mutants impaired in ABA biosynthesis and signaling show defects in general leaf positioning and root hydrotropic bending thereby pointing towards a potential involvement for ABA in shade-induced organ movement responses (100, 129, 140, 161). However, no role has been established for ABA biosynthesis and signaling in leaf movement in response to neighbor detection so far. In the present study, we investigated the role of ABA in the response to neighbor proximity in Arabidopsis. To this purpose, we focused on the analysis of leaf hyponasty which consists in an enhancement in leaf elevation angle triggered by a lowering in the R:FR ratio (227, 230). Our experiments demonstrate that proximity signals lead to a rapid increase in ABA levels in leaves, increase which is mediated by the PIF-YUC regulon as well as two members of the NCED family. In addition, plants with defective ABA biosynthesis or signaling display a significant impairment in both shade- and auxin-induced hyponasties while maintaining wild type movements in standard light conditions. Overall, our results highlight a new role for ABA, potentially acting downstream of auxin signaling, in shade-induced leaf movement responses.

Materials and methods

Plant material and growth conditions

We used the following *Arabidopsis thaliana* genotypes (cv Columbia-0): *nced3nced5* (241), *aba2* (249), *pyr1pyl1pyl2pyl4* (250), *pyr1pyl1pyl2pyl4pyl5pyl8* (248), *pyr1pyl1pyl2pyl4pyl8pyl9*, *pyr1pyl1pyl2pyl4pyl5pyl8pyl9* (gift from Pedro Rodriguez), *pif4pif5pif7* (51), *yuc2yuc5yuc8yuc9* (251). Seeds were stratified at 4°C for 3 d in darkness and then sown on soil saturated with deionized water in a Percival CU-36L4 incubator (Percival Scientific) at 21 °C, 85% relative humidity, and PAR =175 $\mu mol \cdot m^{-2} \cdot s^{-1}$ under LD (16:8) conditions. After 13 d, plants were transferred to the ScanAlyzer HTS (LemnaTec) for acclimation (with day–night cycles and light conditions as in the incubator) 24 h before scanning. For shade treatments, the R/FR was decreased from 4.2 to 0.2 using FR-emitting diodes positioned on the ceiling of the ScanAlyzer HTS. Further experimental details, spectral composition of light, computation of the R/FR ratio, and technical specifications of the phenotyping device are described in detail in ref. (110). For gene expression experiment in Fig. 1, Col-0 plants were grown as described in ref. (51). In brief, seeds were directly sown on soil and stratified at 4°C for 3 d in darkness. Plants were then grown for 14 d at 20 °C, 70% relative humidity, and PAR =220 $\mu mol \cdot m^{-2} \cdot s^{-1}$ under LD (16:8) conditions. Afterwards, plants were divided over two Percival I-66L incubators (Percival Scientific) at PAR =130 $\mu mol \cdot m^{-2} \cdot s^{-1}$ 24 h before the start of the experiment. Experiment was performed the following day (day 16). At ZT3 on day 16, R/FR was decreased in one of the incubators from 1.4 to 0.2 using FR-emitting diodes positioned on the ceiling.

Hormone quantification

ABA measurements were performed as previously described in ref. (252). In brief, fresh frozen samples were ground to a fine powder using mortars and pestles under liquid nitrogen and about 40 mg of powder was weighed in 2.0 mL Eppendorf tubes. To the tubes were added 5-6 glass beads (2mm diameter), 990 µL of extraction solvent (ethylacetate/formic acid, 99.5 : 0.5, v/v) and 10 µL of internal standard solution containing D_6-ABA at 100 ng/ml. The tubes were shaken for 4 min at 30 Hz

in a tissue lyser, centrifuged for 3 min, the supernatant was recovered and the pellet re-extracted with 500 µL of extraction solvent. Both solutions were then combined, evaporated and reconstituted in 100 µL of methanol 70%. The final extracts were analyzed by UHPLC-MS/MS using an Ultimate 3000 RSLC (Thermo Scientific Dionex) coupled to a 4000 QTRAP (AB Sciex). To quantify ABA in plant samples, a calibration curve based on calibration points at 0.2, 2, 10, 50 and 200 ng/mL, all containing D_6-ABA at a fixed concentration of 10 ng/mL, and weighted by 1/x was used (x refers to the concentration of the corresponding calibration point).

RNA extraction and real-time reverse transcription (RT)-PCR

For gene expression experiments, RNA extraction, cDNA reverse transcription and RT-qPCR were performed as described in ref. (51). In brief, petioles and lamina of leaves 3 (Fig. 3, samples from de Wit *et al.* , 2015) (51) were separately pooled into three biological replicates and frozen in liquid nitrogen. After consecutive RNA extraction and reverse transcription, RT-qPCR was performed in three technical replicates for each sample using ABI prism 7900HT sequence detection system (Applied Biosystems) and FastStart Universal SYBR green Master mix (Roche). Data were normalized against two reference genes (*YLS8*, *UBC*) using the Biogazelle qbase software. Sequences of qPCR primer pairs used in this study are the following ones:
NCED3: TCCCTAAGCAATCATCAAACTC / ATTCTTTGGCTTTGGGCTTAAC.
NCED5: GCTCTCATGGCTTGTTCTTAC / GTGAAACTAACGGAGGATGAC.

Analysis of leaf elevation angles

For time-lapse experiments, plants were scanned at 60-min intervals with the ScanAnalyzer HTS (LemnaTec). As output, we obtained time-lapse images in which the distances of points measured on the plant surface from a reference plane were color-coded. These images were then transformed into 3D point clouds that yield a precise representation of plant surfaces over time, as previously described in ref. (53). Leaf elevation angles (also named “tip elevation angles”) were de- lineated by the vector taking as origin the position of the basal end of the petiole organ and as extremity the position of the tip of the blade organ. A detailed description of the

geometric definition of leaf elevation angle (ϕ_{tip}) as well as details of image and data processing are available in refs. (110) and (225).

Results

Low R/FR triggers an increase in ABA production through regulation of *NCED* expression

As the *NCED* gene family stands as the rate-limiting step of ABA biosynthesis and was previously shown to be involved in light-mediated physiological responses in Arabidopsis (86, 203), we started by investigating how it was regulated by low R/FR in young Arabidopsis leaves. We focused our analysis on *NCED3* and *NCED5* because they are the two most abundant *NCED* isoforms in leaves and their expression was recently shown to be upregulated in shaded seedlings (45, 234). Interestingly, we observed a strong induction of these two genes by low R/FR signals in Arabidopsis leaves (Fig. 3). While *NCED3* was induced in both petiole and blade organs in similar relative amounts, *NCED5* induction was restricted to the petiole organ. Interestingly, specific *NCED5* expression in petiole was also observed previously using *NCED5:GUS* reporter lines (241). Shade-induced expression peaked two hours after the start of treatment for both *NCED3* and *NCED5* independently of the organ considered.

Increased ABA levels due to a lowering in R/FR was previously highlighted in leaves of tomato and sunflower as well as in axillary buds of Arabidopsis (87, 88, 89). To test if neighbor-detecting conditions also lead to such an increase in ABA production in Arabidopsis leaves, we quantified the concentration of ABA in leaves 1 and 2 of two-week-old Arabidopsis rosettes grown in high versus low R/FR conditions (Fig. 4A). As for *NCED* gene expression, we observed a significant increase in ABA levels already two hours after the start of the treatment (ZT5). Although the strongest relative induction happened at ZT5 (155-184% compared to high R/FR), ABA levels were still significantly higher in low R/FR conditions at the end of the photoperiod (130% compared to high R/FR) (Fig. 4B). It is important to note that ABA levels were diurnally regulated in our conditions with maxima at the end of day which was in accordance with previous observations (165).

We further aimed at investigating the role of NCED3 and NCED5 in the low R/FR-induced ABA production by analyzing ABA concentration in *nced3nced5* double mutants. However, as *nced3nced5* double mutants are impaired in growth and display smaller rosettes relatively to wild type plants, we decided to harvest whole

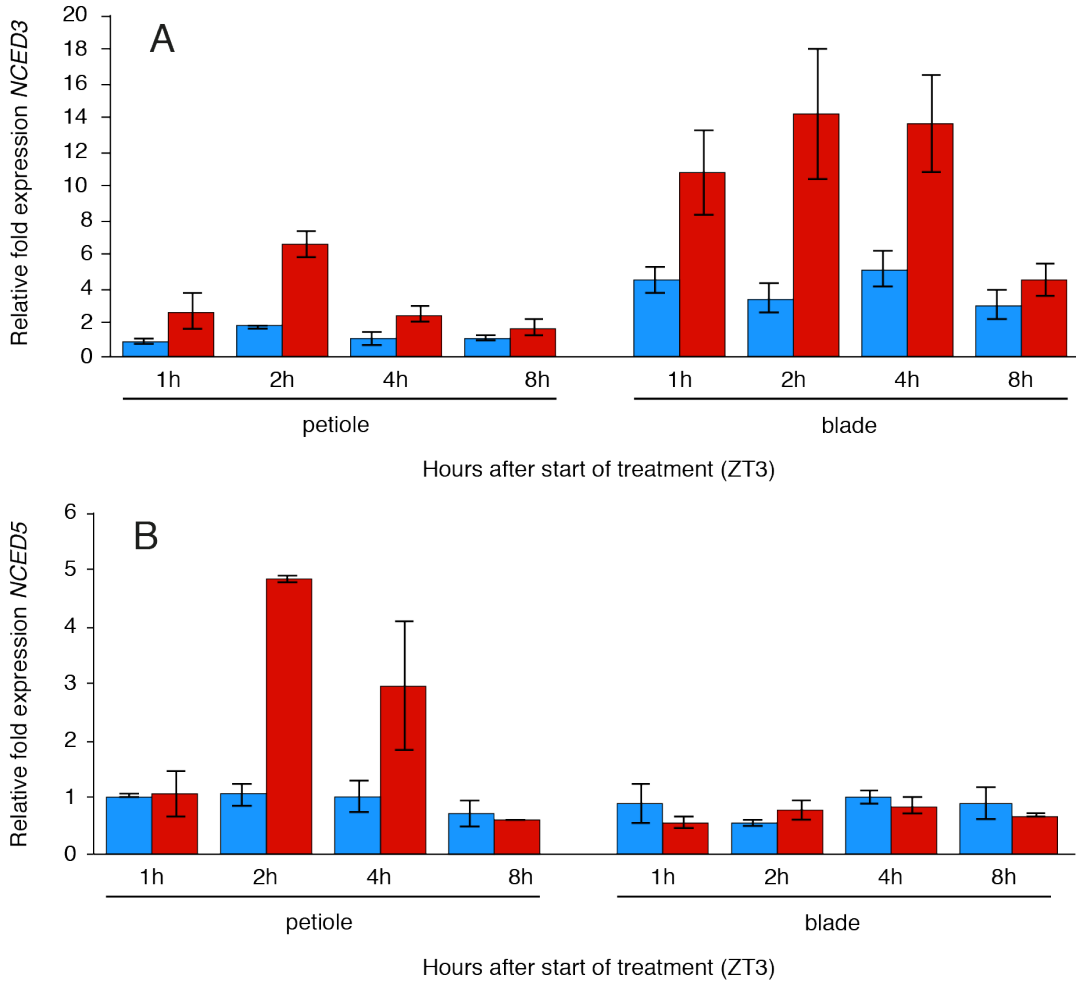

Figure 3. Low R/FR induces expression of *NCED3* and *NCED5* in leaves.

Relative fold gene expression of *NCED3* (A) and *NCED5* (B) from leaf 3 of Col-0 plants in high R/FR (blue) versus low R/FR (red) conditions over time. Gene expression values were calculated as fold induction relative to a petiole sample at time=1h (ZT4) in high R/FR conditions. Plants were grown for 15 d in standard long-day [LD, 16-h light, 8-h dark (16/8)] conditions. ZT0 corresponds to the beginning of the light period on day 16. Shade treatment started on day 16 at ZT3 by adding FR light to decrease the R/FR ratio. Error bars represent the twofold SE of mean estimates from biological replicates.

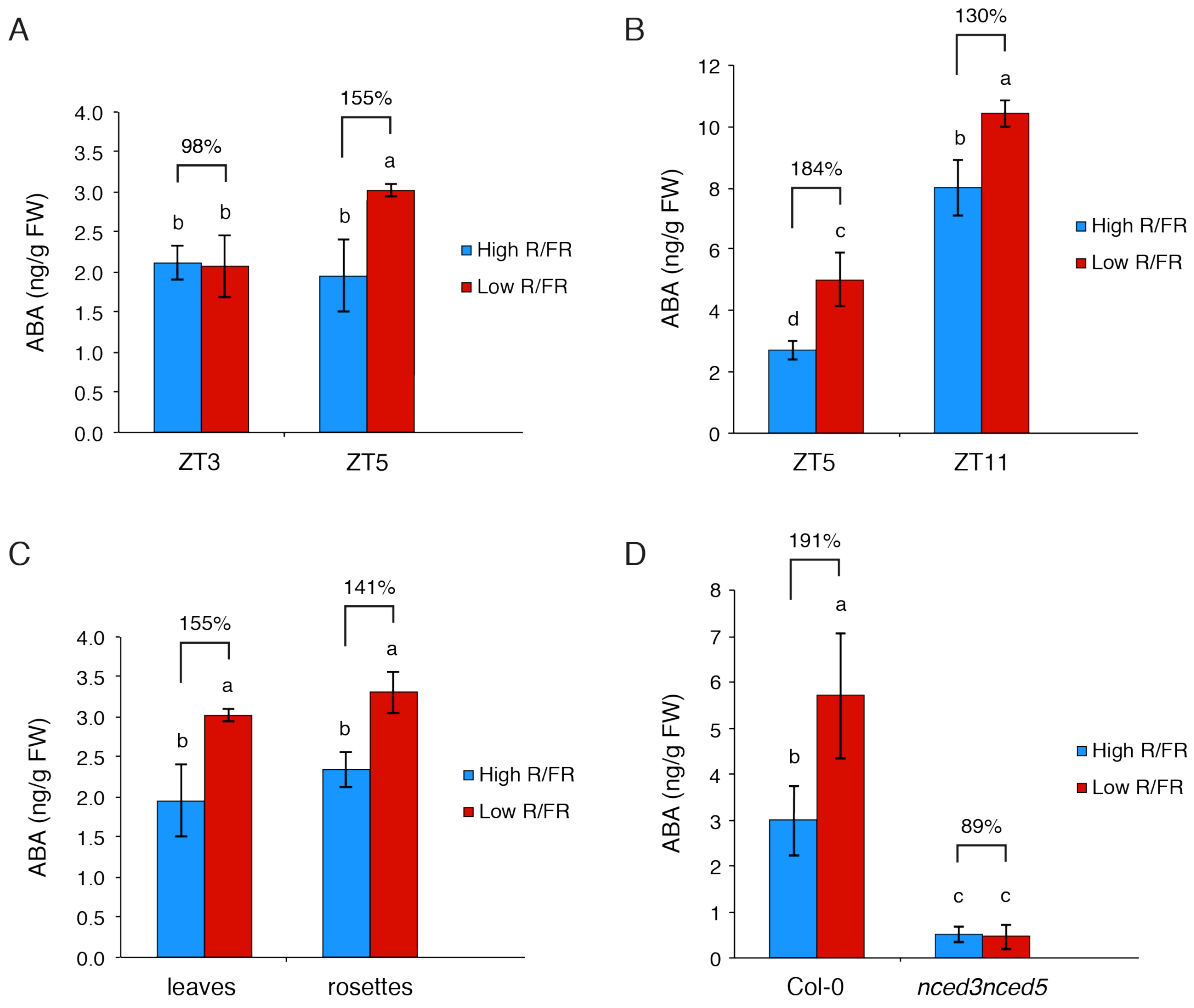

Figure 4. Shade-induced ABA biosynthesis in leaves is mediated by *NCED3* and *NCED5*.

(A-B) ABA concentration in entire Col-0 leaves 1 and 2 in high R/FR (blue) versus low R/FR (red) conditions either at 0 hour (ZT3) and 2 hours (ZT5) (A) or at 2 hours (ZT5) and 8 hours (ZT11) (B) after the start of the treatment. **(C)** ABA concentration in entire leaves versus entire rosettes of Col-0 plants in high R/FR (blue) versus low R/FR (red) conditions at 2 hours (ZT5) after the start of the treatment. Data for leaves are same as in (A, right). **(D)** ABA concentration in entire rosettes of Col-0 versus *nced3nced5* double mutant plants in high R/FR (blue) versus low R/FR (red) conditions at 2 hours (ZT5) after the start of the treatment.

(A-D) Plants were grown for 14 d in standard long-day [LD, 16-h light, 8-h dark (16/8)] conditions. ZT0 corresponds to the beginning of the light period on day 15. Shade treatment started on day 15 at ZT3 by adding FR light to decrease the R/FR ratio. Each bar plot represents data from 4 (A, C, D) or 3 (B) biological replicates. Per replicate, 40 leaves (A, C left), 10 rosettes (C right), 30 leaves (B), 15 rosettes (D left) or 20 rosettes (D right) were harvested and frozen in liquid nitrogen. Error bars represent the twofold SE of mean estimates. Two-way ANOVAs followed by Tukey's HSD test were performed, and different letters were assigned to significantly different groups.

rosettes to avoid technical difficulties in case of insufficient biological material (241). Indeed, we showed that harvesting individual leaves 1 and 2 or entire rosettes led to similar results (Fig. 4C). No increase in ABA concentration was observed in the *nced3nced5* double mutants in low R/FR conditions thereby indicating that these two genes mediate the increase in ABA production in shaded leaves (Fig. 4D). In addition, the very low ABA levels in *nced3nced5* double mutants in standard conditions confirmed the generally reduced capacity for ABA biosynthesis in those mutants (Fig. 4D) (241).

Low R/FR-induced hyponasty requires functional ABA biosynthesis and signaling

The role of ABA in shade-induced hyponasty has remained elusive so far. This lack of knowledge is reinforced by the fact that mutant analysis led to diverging results concerning the role of ABA biosynthesis in low light-induced hyponasty (155). To test the importance of this hormone in shade-induced leaf movement, we monitored leaf elevation angle (tip angle) in mutants defective in ABA biosynthesis. For this, we focused on *nced3nced5* double and *aba2* single mutants as they were reported to have similar reductions in ABA and rosette sizes in standard growing conditions (241). Strikingly, both mutants were strongly affected in their capacity for upward leaf movement in response to low R/FR signals (Fig. 5). The fact that the amplitude of diurnal movements in standard conditions remained unaffected in these mutants points towards a specific role for ABA during the shade response. Moreover, our analysis confirmed the role for ABA in general leaf positioning as the mutants displayed more erect leaves (10-15° higher angle at ZT3 relative to wild type plants) in standard light conditions (Fig. 5A-B) (129, 140).

Next, we aimed at investigating if not only ABA biosynthesis but also ABA signaling was required for maintaining a functional shade-induced hyponastic response. We therefore analyzed leaf elevation angle in plants with combined mutations in genes of the *PYR/PYL/RCAR* family (Fig. 6). Indeed, the PYR/PYL/RCAR family is widely considered as the major class of ABA receptors in ABA-mediated plant responses (247). First, we analyzed leaf hyponasty in standard versus shade conditions using the quadruple *pyr1pyl1pyl2pyl4* mutant which is strongly impaired in ABA sensitivity in seedlings (Fig. 6A,E) (250). This mutant did not show any defect in leaf

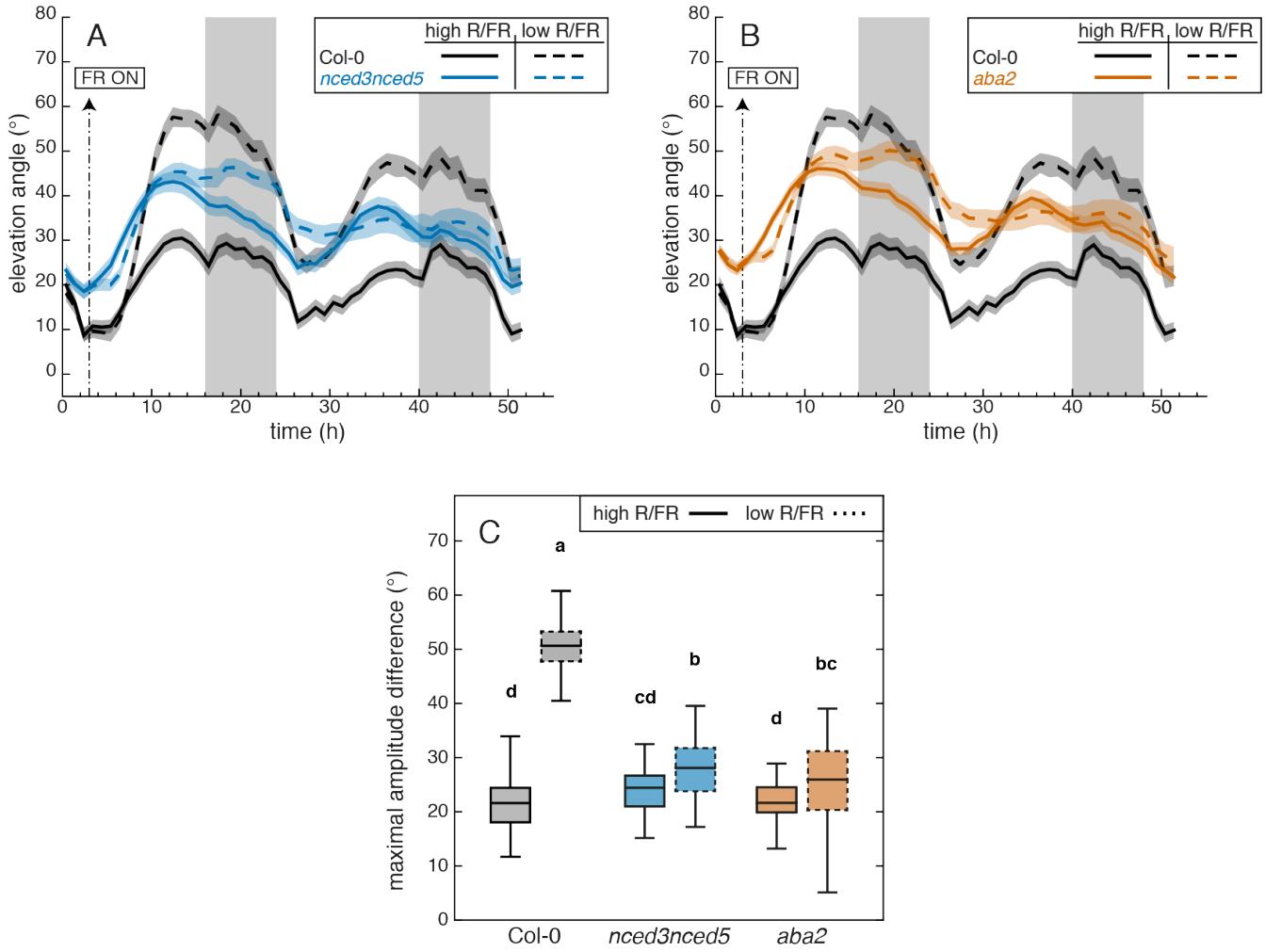

Figure 5. Low R/FR-induced hyponasty is strongly impaired in ABA biosynthetic mutants.

(A-B) Leaf elevation angle of leaves 1 and 2 in Col-0 (black), *nced3nced5* mutant (blue) and *aba2* mutant (orange) plants in high R/FR (solid) versus low R/FR (dashed) conditions. Data are mean of n=44-60. Plants were grown for 14 days in standard long-day (LD, 16/8) conditions. Imaging started on day 15 at ZT0 (t=0), plants were maintained in LD. Shade treatment started at t=3 by adding FR light to decrease the R/FR ratio. Opaque bands around mean lines represent the 95% confidence interval of mean estimates. Vertical gray bars represent night periods. Data for Col-0 in (A) and (B) are same.

(C) Boxplots representing the amplitude of leaf movement between maximum and minimum leaf elevation angles over the time period from t = 3 to t = 16 and computed for each individual leaf analyzed in (A-B). Solid and dashed plots represent data from high R/FR and low R/FR conditions, respectively. Two-way ANOVA followed by Tukey's HSD test were performed and different letters were assigned to significantly different groups (p-value < 0.05).

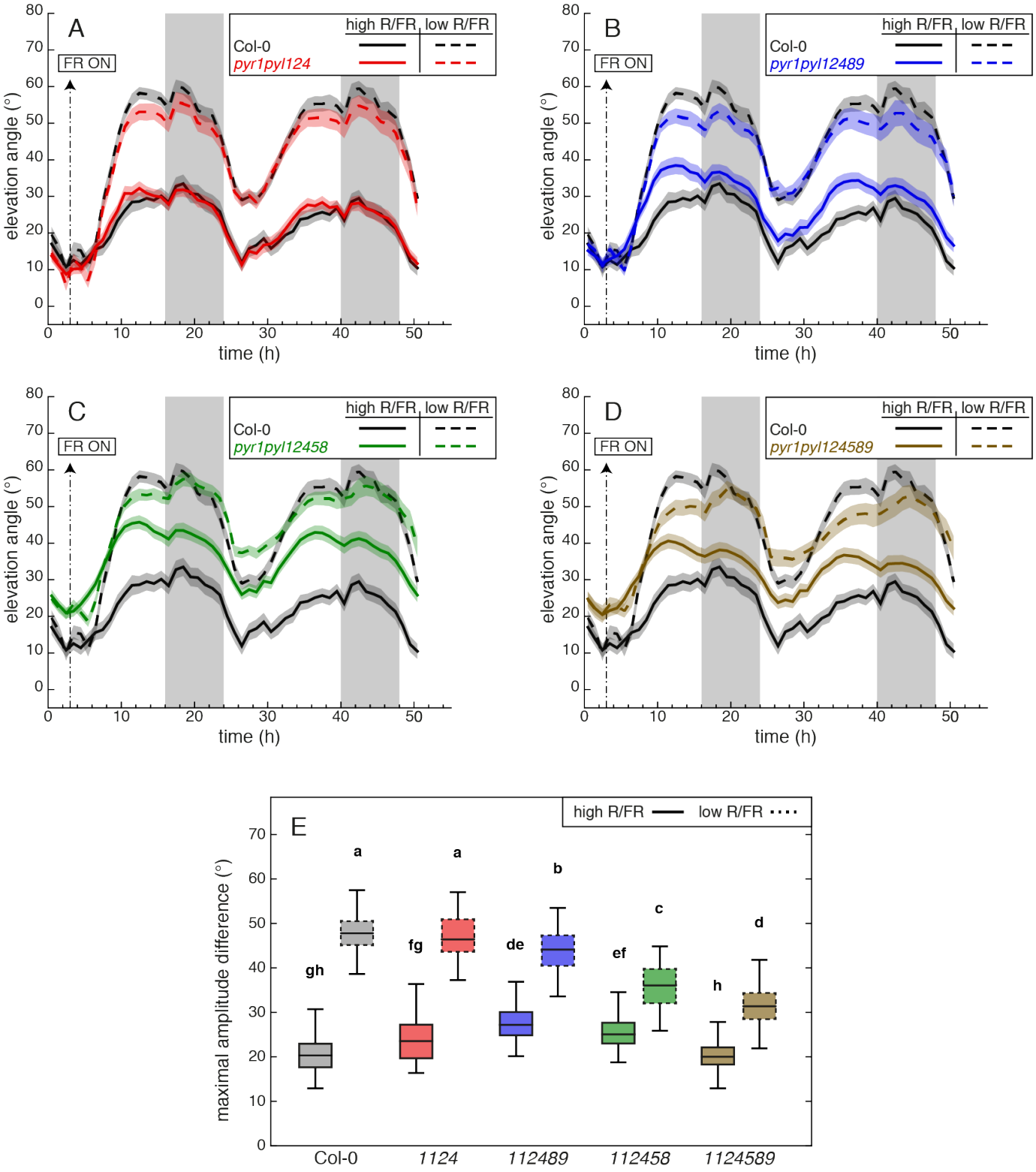
A
FR ON
high R/FR
low R/FR
Col-0
pyr1pyl124
elevation angle (°)
time (h)
B
Col-0
pyr1pyl12489
C
Col-0
pyr1pyl12458
D
Col-0
pyr1pyl124589
E
high R/FR
low R/FR
maximal amplitude difference (°)
a
a
b
c
d
gh
fg
de
ef
h
Col-0
1124
112489
112458
1124589

Figure 6. Low R/FR-induced hyponasty requires a functional ABA signaling.

(A-D) Leaf elevation angle of leaves 1 and 2 in Col-0 (black), quadruple *pyr1pyl124* mutant (red), sextuple *pyr1pyl12489* mutant (blue), sextuple *pyr1pyl12458* mutant (green) and septuple *pyr1pyl124589* mutant (brown) plants in high R/FR (solid) versus low R/FR (dashed) conditions. Data are mean of n=34-40. Plants were grown for 14 days in standard long-day (LD, 16/8) conditions. Imaging started on day 15 at ZT0 (t=0), plants were maintained in LD. Shade treatment started at t=3 by adding FR light to decrease the R/FR ratio. Opaque bands around mean lines represent the 95% confidence interval of mean estimates. Vertical gray bars represent night periods. Data for Col-0 in (A), (B), (C) and (D) are same.
(E) Boxplots representing the amplitude of leaf movement between maximum and minimum leaf elevation angles over the time period from t = 3 to t = 16 and computed for each individual leaf analyzed in (A-D). Solid and dashed plots represent data from high R/FR and low R/FR conditions, respectively. Two-way ANOVA followed by Tukey's HSD test were performed and different letters were assigned to significantly different groups (p-value < 0.05).

movement in any of the two light conditions. Knowing that this mutant does not fully lack ABA responses and that additional members of the *PYR1/PYL/RCAR* family can be involved in the response, we further tested *pyr1pyl1pyl2pyl4pyl8pyl9* and *pyr1pyl1pyl2pyl4pyl5pyl8* sextuple mutants as well as the *pyr1pyl1pyl2pyl4pyl5pyl8pyl9* septuple mutant (Fig. 6B-D). Interestingly, while the amplitude of the movement in standard conditions was higher in sextuple mutants compared to wild type, the former displayed a decreased response to shade (Fig. 6E). This points towards opposite roles for ABA in diurnally-controlled versus low R:FR-induced hyponastic responses. The septuple mutant displayed the greatest defects in shade-induced hyponasty compared to the other mutants while it retained a wild type amplitude response in standard conditions. It is important to note that, similarly to ABA biosynthesis, a lack in ABA sensitivity may also lead to constitutively more erect leaves (Fig. 6C-D). Overall, the results obtained from ABA biosynthetic and signaling mutants clearly demonstrate the existence of a positive role for ABA during shade-induced leaf hyponasty.

A potential role for ABA downstream of auxin signaling in shade avoidance

Considering the importance of auxin in shade-induced leaf hyponasty (227, 230), we asked whether the increase in ABA levels observed in shade may potentially occur upstream or downstream of auxin signaling by quantifying ABA in key SAS mutants (43, 51, 54). Interestingly, the increase in ABA concentration observed in shaded wild type plants was totally or partially suppressed in triple *pif4pif5pif7* and quadruple *yuc2yuc5yuc8yuc9* mutants, respectively (Fig. 7). Based on these results, we can conclude that PIFs are crucial regulators of shade-induced biosynthesis of two major hormones, auxin and abscisic acid. In addition, these data suggest that shade-induced ABA production may happen downstream of auxin signaling. This hypothesis would be in line with a previous observation in cleaver (*Galium aparine*) where exogenous auxin was shown to induce *NCED* expression and trigger consecutive increase in ABA levels (253). To challenge this hypothesis further, we tested if the positive effects of exogenous auxin on leaf hyponastic response observed in wild type plants were still present in *aba2* mutants (Fig. 8). Interestingly, we observed that *aba2* mutants were not only impaired in hyponasty induced by shade (Fig. 5) but also when triggered by exogenous auxin at the tip (Fig. 8).

Although these results are in agreement with our hypothesis according to which auxin signaling may lie upstream of ABA in the regulation of shade-induced leaf hyponasty, additional experiments will be required in the future in order to verify such a supposition.

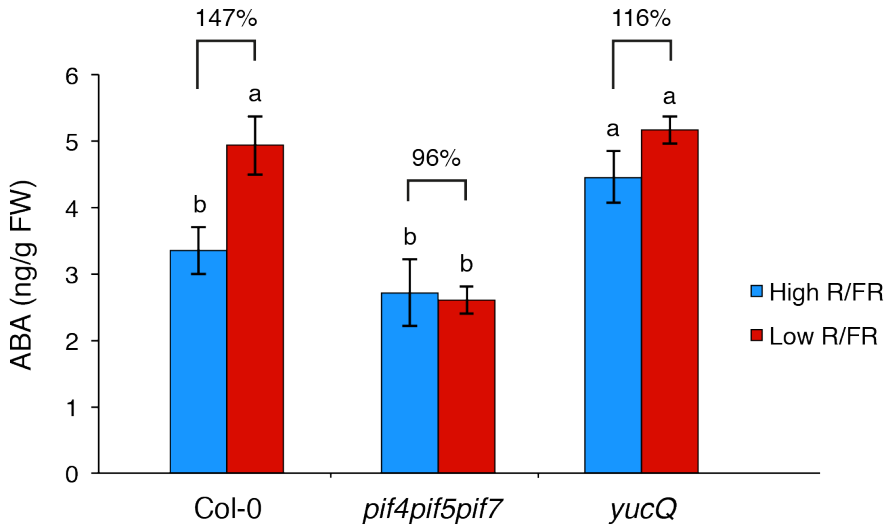

Figure 7. Shade-induced ABA biosynthesis is controlled by the PIF-YUC regulon.

ABA concentration in rosettes of Col-0, *pif4pif5pif7* triple and *yuc2yuc5yuc8yuc9* quadruple mutant plants in high R/FR (blue) versus low R/FR (red) conditions at 2 hours (ZT5) after the start of the shade treatment. Plants were grown for 14 d in standard long-day [LD, 16-h light, 8-h dark (16/8)] conditions. ZT0 corresponds to the beginning of the light period on day 15. Shade treatment started on day 15 at ZT3 by adding FR light to decrease the R/FR ratio. Each bar plot represents data from 4 biological replicates. Per replicate, 15 entire rosettes were harvested and frozen in liquid nitrogen. Error bars represent the twofold SE of mean estimates. Two-way ANOVAs followed by Tukey's HSD test were performed and different letters were assigned to significantly different groups.

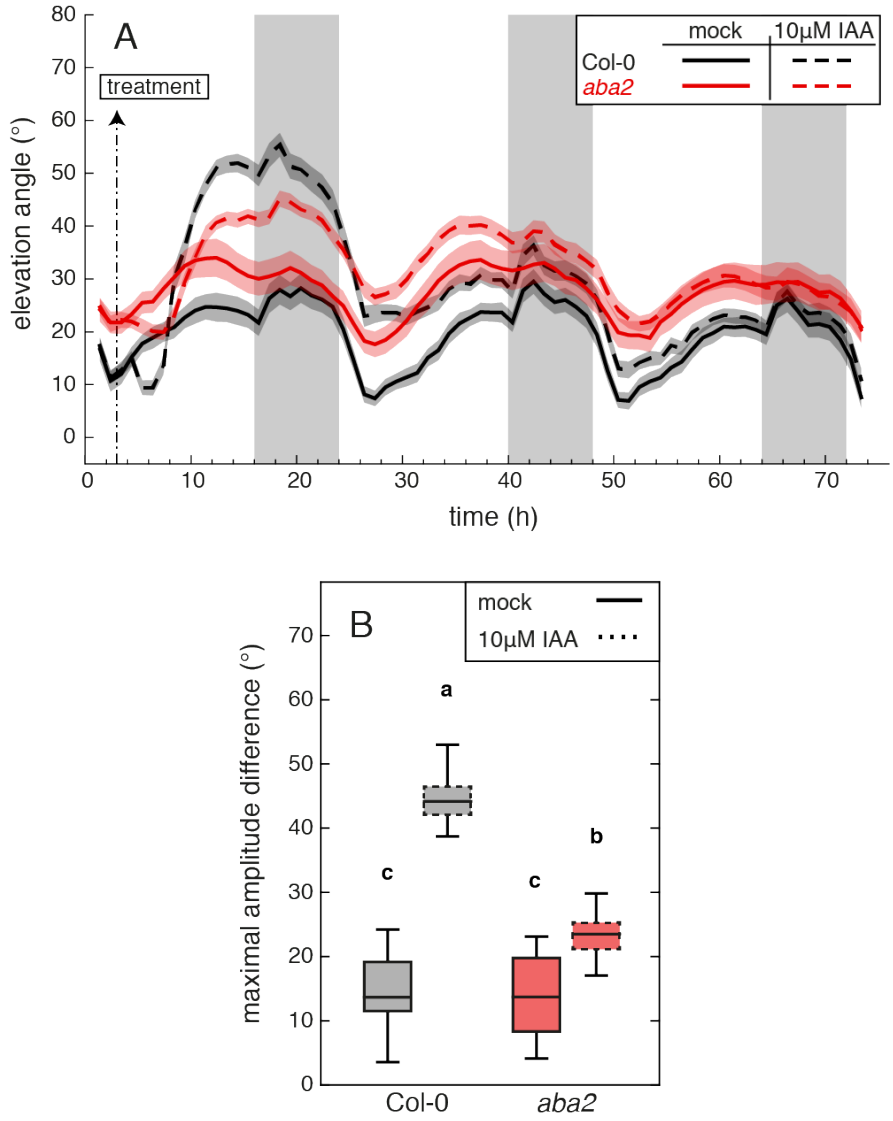

Figure 8. Effects of exogenous auxin on hyponasty are strongly reduced in *aba2* mutant.

(A) Leaf elevation angle of leaves 1 and 2 in Col-0 (black) and *aba2* mutant (red) plants with mock solution (solid lines) or 10µM IAA (dashed lines) applied to the tip of leaves 1 and 2. Plants were grown for 14 d in standard long-day [LD, 16-h light, 8-h dark (16/8)] conditions. Imaging started on day 15 at ZT0 (t = 0) and plants were maintained in LD conditions. At ZT3 (t = 3) on day 15 a 1-µL drop of solution was applied to the tip of leaves 1 and 2 (adaxial sides). Data are mean of n = 26-30. Opaque bands around mean lines represent the 95% confidence interval of mean estimates. Vertical gray bars represent night periods.

(B) Boxplots representing the amplitude of leaf movement between maximum and minimum leaf elevation angles over the time period from t = 3 to t = 16 and computed for each individual leaf analyzed in (A). Solid and dashed plots represent data from mock and IAA treatments, respectively. Two-way ANOVA followed by Tukey's HSD test were performed and different letters were assigned to significantly different groups (p-value < 0.05).

Discussion

The reduction in the environmental R:FR ratio constitutes an important signal informing the plant about the presence of competitors (254). In neighbor-detecting conditions, plants trigger an upward leaf movement which allows enhancing plant access to sunlight (112). Phytohormones are key actors in shade avoidance (38) and auxin was shown to be particularly important in the case of leaf hyponasty (48, 49, 227, 230). Indeed, knocking out the four shade-induced genes of the *YUCCA* family, which are responsible for the rate-limiting step in auxin biosynthesis, totally suppresses low R:FR-induced hyponasty (227). So far, ABA had no clearly defined role in general leaf adaptation to shade including the response in leaf movement. In our study, we show for the first time that neighbor proximity signals induce a significant increase in expression of both *NCED3* and *NCED5* in Arabidopsis leaves, two genes playing an important role in growth and response to water stress in these organs (241) (Fig. 3). Interestingly, although *NCED3* is widely induced in the leaf *NCED5* induced expression is restricted to the petiole organ. This fits with the pattern in *NCED5:GUS* expression observed by Frey *et al.* (2012) (241).

We also show a significant increase in leaf ABA levels in low R:FR conditions which is mediated by NCED3 and NCED5 (Fig. 4). Such positive effects of low R:FR on ABA levels were previously reported in axillary stem buds in Arabidopsis (86, 242). In addition, we report that this enhancement in ABA levels in the shaded leaves is under the regulation of the PIF-YUC regulon (Fig. 7). How PIFs and YUCs are regulating such increase remains an open question although we suspect that PIF- and YUC-mediated auxin production might be responsible for downstream activation of *NCED* expression in turn leading to increased ABA levels. Indeed, several studies previously noticed significant induction of *NCED* genes by exogenous auxin in different species including Arabidopsis (55, 243, 253). Interestingly, low R:FR signals were shown to induce an auxin response specifically in leaf vasculature which is the main site for NCED-induced ABA production in stressful conditions (227, 234). We can therefore hypothesize that detection of competitors at leaf margins, which are presumably the most adapted leaf sites for such a function, leads to PIF-mediated increase in auxin levels at these same sites (43, 227, 230). Auxin is then loaded in the vascular tissues and transported downwards to the petiole (227). On its way

down, auxin in turn triggers increased *NCED* expression and consecutive ABA production in leaf organs.

Finally, our study sheds light on a direct link between ABA and a physiological response, leaf hyponasty, during leaf adaptation to shade. Indeed, we report here that functional ABA biosynthesis (Figs. 5 and 8) and ABA signaling (Fig. 6) are required for proper low R:FR- and auxin-induced hyponastic responses. Interestingly, *PYR1/PYL/RCARs* are mostly expressed in leaf vasculature and stomata (248), similarly to several ABA biosynthetic enzyme coding genes (207, 234, 236, 238). This suggests that leaf vasculature might not only be a crucial site for ABA biosynthesis but also for ABA perception during shade-induced hyponasty. Considering that ABA plays a key role in leaf hydraulics partly, at least, through its regulation of the "xylem-mesophyll barrier" formed by the bundle sheath tissues (159), we hypothesize a mechanism where shade-induced ABA would influence turgor properties of the leaf rachis and mesophyll tissues in such a way that it would finally lead to more erect leaf organs.

Acknowledgments

We deeply thank Pedro Rodriguez at the Technical University of Valencia in Spain for sharing seeds of the *pyr1pyl1pyl2pyl4pyl8pyl9* sextuple *and pyr1pyl1pyl2pyl4pyl5pyl8pyl9* septuple mutants; Alessandra Boccaccini, Martina Legris and Anne-Sophie Fiorucci for practical help during experiments; Gaétan Glauser for performing phytohormone quantification. This work was funded by the University of Lausanne and Swiss National Science Foundation Grant FNS 31003A_160326, Sinergia Grant CRSII3_154438, and SystemsX Grant PlantMechanix 51RT-0_145716 (to Christian Fankhauser). The computations were performed at the Vital-IT Center (www.vital-it.ch).

General discussion

Link between growth and movement in Arabidopsis

Most studies related to how light regulates growth and movement in Arabidopsis focused on these traits separately (38, 65). Analyzing these traits simultaneously and in organs such as leaves requires sophisticated and costly methods but allows to investigate the way these two traits relate to each other. In recent years, efforts have also been made to develop imaging systems which are able to monitor growth in Arabidopsis leaves in a non-invasive manner (255, 256, 257). Among these systems, some offer the ability for simultaneous tracking of growth and movement in Arabidopsis leaves but further development is needed to increase the power and precision of such approaches (110, 258, 259). Based on the work of Dornbusch *et al.* (2012) (110), we developed a strategy allowing non-invasive monitoring of growth and movement with high temporal and geometrical precision in individual Arabidopsis leaves (225). Thanks to this technique, we described accurately the kinetics of growth and movement in both petiole and blade organs (225). Moreover, at the leaf level we observed a decoupling under certain light conditions between these two traits thereby suggesting a more complex relationship than previously thought (225). This is further supported by observations made by Cerrudo *et al.* (2017) and Keller *et al.* (2011) who reported a dissociation between elongation and movement in petiole organs (21, 260). Indeed, petioles of *phyB* mutants treated with methyl jasmonate and shaded petioles of plants impaired in auxin transport displayed significant defects in elongation while maintaining full hyponastic responses compared to the wild type. In line with these reports, our analysis of the *massugu2* mutants shows that inhibiting auxin signaling strongly affects shade-induced hyponasty without disrupting the elongation response in the petiole (227). In addition, ABA biosynthetic mutants are severely impaired in leaf growth (241) but nevertheless display movements with similar amplitude to wild type plants in standard light conditions (Ch. III, Fig. 5). Interestingly, Goyal *et al.* (2016) also reported a decoupling between growth and bending of the hypocotyl during phototropic response (29). Overall, these studies highlight a separation between growth and movement processes in different plant organs under specific

circumstances and are of particular interest considering the long-standing debate about how these processes are linked.

It is generally assumed that leaf movement in pulvinus-lacking plants like Arabidopsis relies on differential growth. This hypothesis is further supported by a few studies which reported differential cell elongation between ab- and adaxial sides of petioles in Arabidopsis and Rumex plants grown in conditions of submergence (118, 119, 120). However, regarding the actual debate one should be cautious about the terminology and favor the usage of “differential elongation” instead of “differential growth”. Indeed, it is not clear yet if leaf movement in pulvinus-lacking species relies on reversible elongation rather than growth, as it is the case for pulvinus-possessing plants (114). To solve such a technically difficult question, future research should be designed in such a way that they combine non-invasive and long-term analysis of movement and elongation at both organ and cellular levels.

Auxin signaling during shade-induced hyponasty: from site-specific shade perception to local leaf response

Recently, our work and the work of Pantazopoulou *et al.* (2017) shed light on the particular importance of auxin during hyponasty not only when induced by shade but also when happening in standard high R:FR conditions (227, 230). Far more is known about the regulation of stress-induced hyponasties than about the diurnally-regulated hyponastic patterns in Arabidopsis leaves (112). Considering that diurnal hyponasty is maintained in constant light and that mutants with deregulated circadian clock are defective in such movement clearly shows the internal clock is crucial for maintaining the movement in high R:FR conditions (225). In addition, the central PIF4 and PIF5 regulators are essential for the amplitude of the movement in high R:FR (225) but also in low light conditions (21) while PIF7 would rather be involved in the response to neighbor detection (227, 230). In addition to the *PIFs*, the genes encoding for auxin biosynthetic steps are crucial in the establishment of leaf hyponastic responses under certain conditions. Hyponasty in *sav3* mutants is absent in high R:FR, reduced in low R:FR and fully present under low light conditions (21, 49, 110, 227). Concerning the *yuc2yuc5yuc8yuc9* mutant, it maintains a wild type hyponasty in high R:FR while its response to low R:FR is abolished (227). All this suggests that SAV3-dependent auxin production is essential for the hyponastic

response in both high and low R:FR conditions and that YUCCA2,5,8,9-dependent auxin production is specifically stimulated in low R:FR thereby promoting increased leaf elevation in those conditions (45, 54). At late stages of a developing canopy, the role for auxin biosynthesis in hyponasty probably decreases while the role for auxin sensitivity gets more important (20, 56).

Blade margins represent a major site for auxin biosynthesis in leaves (49, 50, 51). Interestingly *YUC8* and *YUC9* are mostly expressed at this place in leaves (54) and *YUC8* and *YUC9* seem to be of greater importance than *YUC2* and *YUC5* for the shade-induced hyponastic phenotype (230). Also, FR irradiation and exogenous auxin trigger a strong hyponastic response specifically when spotted at the leaf tip while similar treatments on the petiole do not lead to any upward movement (227, 230). Overall, this suggests that the margins and the leaf tip in particular are crucial sites regarding shade sensing and the consecutive burst in auxin production. Pantazopoulou *et al.* (2017) further proposed, based on computational modeling approaches, that the tip represents the most adaptive site in leaves for sensing R/FR cues (230). This hypothesis makes sense as the modulation of R/FR ratios at this site relies mainly on the presence of neighbors rather than on the proximity with distal leaves, contrary to what would happen in the petiole. Interestingly when exogenous auxin is applied at side margins instead of tip the amplitude of the upward move is partly reduced and leaves reorient sideways in the opposite direction from the application site (227). In the future, performing such an experiment while replacing auxin treatment by FR irradiation may complement our actual findings. To summarize, we suggest that not only the tip but the margins in general are important for leaf reorientation in neighbor detecting environments. In line with this, SAV3-dependent sideways leaf reorientation was shown to be important to avoid self-shading between kin plant individuals (33). We also propose that sensing shade from side might allow leaves of the same rosette to reorient themselves accordingly to minimize self-shading.

Assuming that margins are mostly responsible for the YUC-mediated auxin production in shade, a signal still has to be transported towards lower parts of the leaf in order to trigger hyponasty. Based on genetic and pharmacological data from auxin signaling and transport experiments (227, 230), we conclude that a strong auxin response happens in leaf vascular tissues in shade conditions and that such a response is required for a proper movement. Recent data obtained from quadruple

aux1lax1lax2lax3 mutants and synthetic auxins further confirmed the need for auxin transport from leaf blade down to the petiole (Ch. II, Figs. 1-3). While most auxin is transported basipetally through the vasculature of the petiole, a certain amount of auxin may be redistributed in lateral tissues through the PIN3,4,7-dependent shoot connective transport where it would then trigger downstream signaling events involved in the hyponastic response (62, 227, 230). Inhibiting auxin signaling specifically in the epidermis impairs both diurnal- and shade-induced leaf hyponastic responses (227). This suggests that auxin is required in the epidermis for movement but does not necessarily imply a specific role for the epidermis in the shade-induced response. To gain more knowledge about the potential involvement of individual leaf tissues in leaf hyponasty, additional experiments using tissue-specific approaches will be required.

Finally, one of the key features of our work and the work of Pantazopoulou *et al.* (2017) concerns the local nature of the low R:FR-induced hyponastic response (227, 230). Light conditions for plants in natural environments are often heterogeneous, especially for plants growing under a canopy where sunflecks and canopy gaps may offer only transient illumination (30). Therefore, plants may encounter situations where they are partly shaded. To adapt to such stressful situations, species like Arabidopsis and passionfruit (*Passiflora edulis*) have developed the ability to trigger local adaptive responses restricted to the shaded parts (33, 36). In both studies, we observed that in response to local shade or local auxin signals consecutive auxin dynamics and hyponastic responses are restricted to the treated leaf (227, 230). Our results constitute a first step in the understanding of local plant adaptation to shade and further research is required to shed light on the signaling events happening downstream of auxin. We therefore propose these spatially-restricted auxin dynamics as being part of a mechanism explaining local leaf hyponasty.

Deciphering the role for abscisic acid during leaf adaptation to shade

While the need for auxin in numerous aspects of plant development and adaptation to shade leaves no room for doubt, our knowledge about the role of ABA in those processes is still scarce. The enduring debate concerning the effects of ABA on plant growth illustrates well this lack of understanding (101, 213). After several days in low

R:FR conditions, an increase in leaf ABA levels was detected in sunflower and tomato seedlings (87, 88). In Arabidopsis, a rapid (6 hours) reduction in ABA levels was observed in axillary stem buds of mature plants upon transfer from low to high R:FR (86, 242). No data has been published relative to the effects of FR signals on ABA levels in Arabidopsis leaves. However, five-week-old plants of the constitutive shade-avoidance *phyB* mutant display higher ABA contents in leaves relatively to wild type plants (261) but these results are in contradiction with recent data showing a reduction in ABA levels in two-week-old *phyB* mutants (209). This being said, the fact that the analyses were performed on plants at different stages of development might be a source of divergence. In our study, we report that neighbor proximity signals induce a rapid (2 hours) increase in ABA concentration in rosette leaves (Ch. III, Fig. 4). Considering endogenous ABA levels which cycle over 24 hours (165), the relative increase in ABA levels is particularly important the first hours after the start of the FR treatment in the morning (Ch. III, Fig. 4).

The NCED family is considered as the rate-limiting step in ABA biosynthesis and has been especially studied during adaptive responses to water deprivation (90). Expression of *NCED3*, which plays a primary role in drought-induced leaf ABA biosynthesis (241), is induced by FR signals in axillary buds, hypocotyl and petioles in Arabidopsis (45, 58, 86). Our results show that, while *NCED3* expression is induced by FR signals in both petiole and blade, *NCED5* induction is restricted to the petiole (Ch. III, Fig. 3). Interestingly, knocking out these two genes suppresses both the enhancement of ABA levels and the hyponastic response observed in shaded leaves (Ch. III, Figs. 3-4). This stresses the particular importance of *NCED3* and *NCED5* in ABA-mediated leaf development (241) but also in ABA-mediated leaf adaptation to shade. More generally, this also confirms the critical role for *NCED3* in the production of ABA in leaves under stressful light conditions (86, 203).

An important question is how shade proximity signals lead to the enhancement of *NCED* expression and consecutive ABA production in leaves. The lack of shade-induced ABA production in triple *pif4pif5pif7* mutants strongly suggests that shade-regulated *NCED* expression relies on these PIFs (Ch. III, Fig. 7). This hypothesis is supported by the fact that *NCED3* expression is deregulated in *pif4pif5* double mutants relatively to wild type plants (44). Moreover, PIF4 binds to the promoter regions of *NCED3* and *NCED5* and this could point towards a direct regulation of *NCED* expression by the PIFs (262). Analysis of *NCED* expression in *pif* mutants as

well as ChIP-qPCR approaches with individual PIFs would allow to understand if and how PIFs regulate *NCED* expression in low R:FR conditions. Intriguingly, the increase in ABA levels in shade is also affected in the quadruple *yuc2yuc5yuc8yuc9* mutant (Ch. III, Fig. 7). This indicates that such enhancement might depend not only on PIFs but also on increased auxin biosynthesis. A few studies support this hypothesis by showing that *NCED* expression, and in some cases ABA production, can be triggered by exogenous auxin treatments (55, 243, 253). To answer this question, one could for instance analyze *NCED* expression and ABA levels in leaves treated with exogenous auxin. In addition to auxin, hydraulic signals induced by an alteration in plant hydraulic properties are also capable of modulating ABA levels (263). In several plant species indeed, an increase in ABA levels is observed within minutes following a reduction in leaf turgor (204). Interestingly, such a rapid increase in ABA levels was accompanied by an increase in *NCED3* expression in Arabidopsis leaves (206). One may further hypothesize that a change in light conditions may rapidly modulate turgor of specific leaf tissues in turn triggering *de novo* ABA biosynthesis.

Another striking feature of our work concerns the discovery of a new functional relationship between shade avoidance and ABA physiology. Formerly, Reddy *et al.* (2013) first highlighted a role for ABA in plant adaptation to proximity signals by showing that ABA is necessary for the suppression of bud outgrowth in low R:FR conditions (86). Here, we attribute a new function to ABA in such light conditions. Clearly, we demonstrate that low R:FR-induced leaf hyponasty requires intact ABA biosynthesis and signaling (Ch. III, Figs. 5 & 6). Curiously, while ABA is required for general leaf positioning (129, 140, 161), ABA mutants still display wild type movements in standard light conditions and seem to be exclusively impaired in their ability to respond to competitive signals (Ch. III, Figs. 5 & 6). Furthermore, the fact that ABA mutants are strongly impaired in leaf elongation (241) under normal conditions while they maintain wild type movements is an additional argument pointing towards a decoupling between these two processes. All this indicates that the presence of ABA remains essential to normal plant development and growth but that ABA levels are specifically modulated in stressful light conditions in order to reorient leaves accordingly.

It was previously reported that exogenous ABA treatments have negative effects on leaf hyponasty in plants grown in high R:FR conditions (140). This may be surprising

when considering the positive effects of this hormone on shade-induced leaf hyponasty (Ch. III). However, one must be cautious in the interpretation of data from experiments using exogenous ABA treatments as literature reports diverging effects for this hormone on growth (101). Moreover, contrary to auxin whose production happens mainly at leaf margins (50, 51), ABA mostly derives from leaf vascular tissues (207, 236, 238). It is therefore complicated to mimic the stress-induced ABA production simply by applying this hormone exogenously. This also points towards the importance of localized approaches and analyzing lines with tissue-specific ABA responsiveness would be an excellent approach to tackle such a challenging issue. Tissue-specific approaches allowed, for instance, to understand ABA-mediated tissue-specific mechanisms underlying root hydrotropism (100). Last but not least, investigating the role of ABA in shade-induced hyponasty by manipulating hydraulic properties in specific plant tissues would be very useful. Indeed, ABA is the major hormone regulating plant hydraulics and this is likely that it affects leaf movement through modulation of plant hydraulic processes. A few studies previously stressed the existence of links between defects in plant hydraulics and defective leaf movements in pulvinus-lacking plants like Arabidopsis (161, 208), not to mention the numerous associations between water transport and leaf movement observed in plants possessing a pulvinus (113, 114).

Conclusion

In the present study, I first develop a new approach based on laser-scanning technology which allows tracking of growth and movement in individual Arabidopsis leaves (225). Using such an approach, I report precise patterns of growth and movement at the whole leaf level but also in petiole and blade organs separately. I show that growth and diurnally-controlled hyponasty, both being regulated by the internal clock and the PIFs, initiate at dawn in the blade and then continue in the petiole. Interestingly, at the whole leaf level growth and movement can decouple in certain light conditions.

Next, I describe a mechanism that allows plants to regulate hyponasty in their leaves in response to neighbor proximity signals (Fig. 1) (227). FR light signals reflected by neighbours are perceived specifically at the tip of the blade where they trigger an increase in auxin production at this location (Fig. 1A). Such increase in auxin production is mediated by PIFs (PIF4, PIF5, PIF7), with PIF7 playing a predominant role, as well as by four shade-induced *YUCCAs* (*YUC2, YUC5, YUC8, YUC9*). Based on these observations, I then discover that the hyponastic movement observed in shade can be mimicked by applying auxin exogenously at the tip of the leaf. In addition, when put at side margins instead of tip auxin triggers a reorientation of the leaf sideways.

Furthermore, I stress the necessity for auxin transport from the tip down to the petiole mainly happening through the vasculature of the leaf and in an AUX1/LAX1,2,3- and PIN3,4,7-dependent manner (Fig. 1B). On its way down, auxin may in turn induce the expression of *NCED3* and *NCED5* thereby leading to increased ABA levels. Indeed, an increase in the production of ABA is observed in shaded leaves, this increase requiring the presence of the PIF-YUC regulon as well as the two NCEDs. However, it cannot be excluded that the induction of *NCEDs* rely on PIF-mediated mechanisms other than shade-induced auxin biosynthesis (45, 56). For instance, one can imagine a direct regulation of *NCEDs* by the PIFs, especially knowing that both *NCED3* and *NCED5* promoters are potentially targeted by PIF4 (262). In order to achieve a proper hyponastic response, auxin signaling is required not only in the vasculature but also in outer tissues of the petiole. Interestingly, blocking auxin signaling in the vasculature decouples growth from movement at the petiole level.

Finally, my study presents new evidence for the involvement of abscisic acid in the shade-induced nastic response (Fig. 1C). Mutants lacking a functional ABA biosynthesis and signaling are affected in both shade- and auxin-induced nastic responses. How and where auxin and ABA signaling pathways are coordinated and ultimately lead to the hyponastic response in shade conditions is still unclear. One hypothesis could be that ABA plays a role in auxin sensitivity in a PIF-dependent manner (44, 45, 56, 264), potentially by enhancing the effects of auxin on hyponasty through inhibition of the negative Aux/IAAs regulators (91). The present study also determines the local nature of leaf hyponasty in response to neighbor detection. Indeed, simulating shade conditions at the tip of a specific leaf triggers a movement that is restricted to this same leaf. Similarly, I observed that the auxin response is limited to the treated leaf and I therefore propose that such restricted auxin dynamics are part of a mechanism underlying the shade-induced leaf hyponastic response.

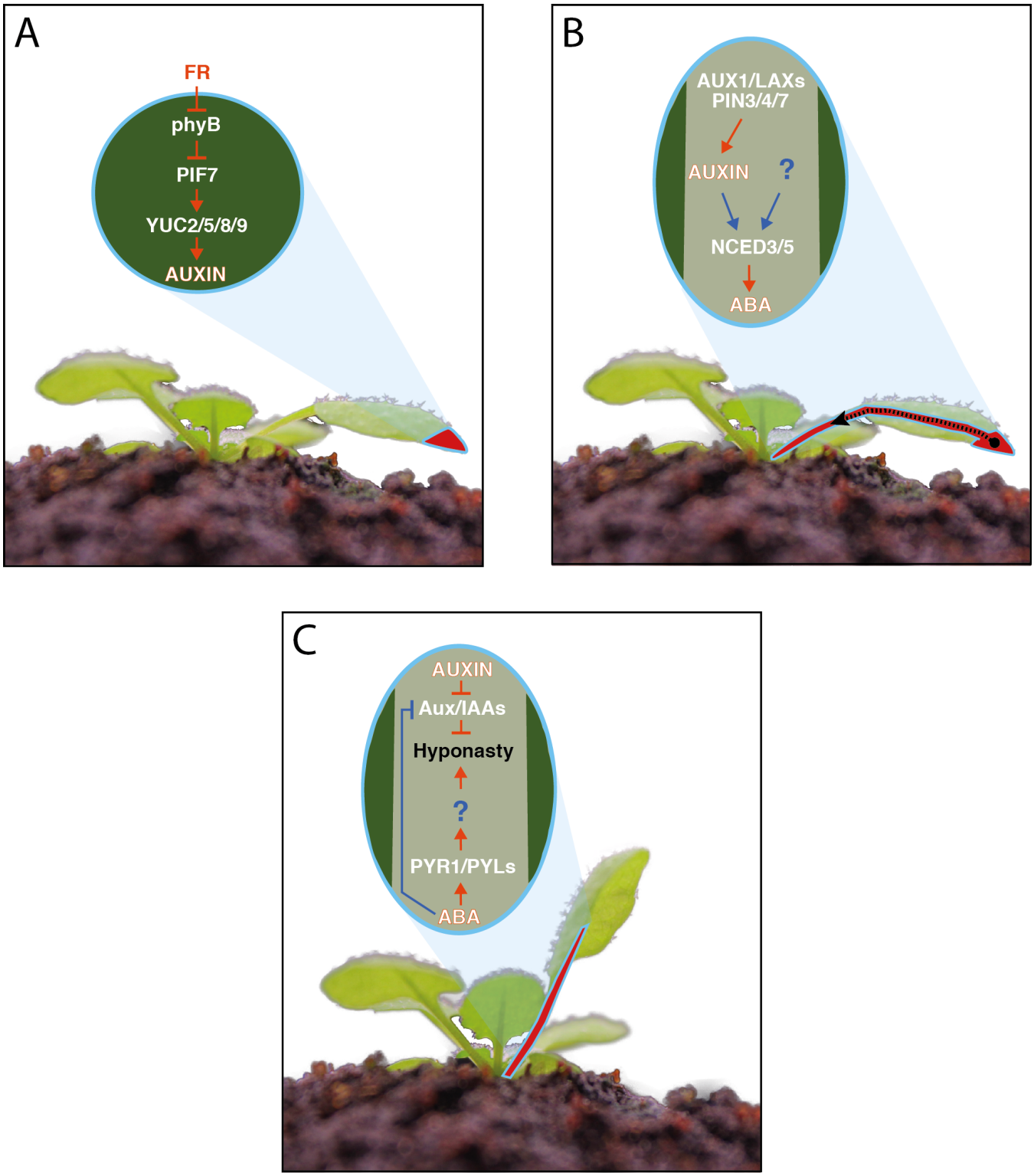
A
FR
phyB
PIF7
YUC2/5/8/9
AUXIN
B
AUX1/LAXs
PIN3/4/7
AUXIN
?
NCED3/5
ABA
C
AUXIN
Aux/IAAs
Hyponasty
?
PYR1/PYLs
ABA

Figure 1. Experimental model of leaf hyponasty in response to local neighbor detection.

(A) FR signals reflected from neighbors are sensed at the leaf tip where it leads to the inactivation of phyB and the consecutive release of PIFs activity (PIF4, PIF5, PIF7). PIFs (especially PIF7) in turn induce expression of four *YUCCAs* (*YUC2*, *YUC5*, *YUC8*, *YUC9*) thereby triggering a burst in auxin biosynthesis at leaf tip. **(B)** Newly produced auxin is transported mainly along leaf vasculature from leaf tip downwards to the leaf petiole through AUX1/LAXs importers (AUX1, LAX1, LAX2, LAX3) and PIN exporters (PIN3, PIN4, PIN7). On its way down through the vascular tissues, auxin potentially induces expression of *NCEDs* (*NCED3*, *NCED5*) thereby resulting in an increase in ABA levels. Besides auxin, PIFs may also directly regulate *NCED* expression through their binding to *NCED* promoter regions. **(C)** In the petiole, auxin inhibits the activity of the negative Aux/IAAs regulators and positively impacts on the hyponastic response. In parallel, perception of ABA through the receptors of the PYR/PYL/RCAR family triggers downstream signaling events leading to the leaf hyponastic response. ABA may also play a positive role in the response through its putative inhibition of the Aux/IAAs thereby potentiating the effects of auxin on leaf hyponasty. **(A-C)** Red and blue arrow-/bar-headed lines indicate established and putative relationships, respectively, between two entities.

Future perspectives

Based on our experimental model, follow-up experiments should first allow to get a better understanding of the signaling cascade taking place from shade perception to the upregulation of *NCEDs*. One should start by analyzing *NCED* expression as well as quantifying auxin and ABA levels in petiole and blade organs of typical shade-avoidance mutants such as *pif*, *yucca*, *msg2* and *pin* mutants. This would help in knowing which steps, if any, of the auxin pathway (biosynthesis, transport, signaling) do interfere with *NCED* expression and in which organs it happens. In addition, performing such experiments in plants treated with auxin at leaf tip would constitute a complementary approach. In case shade-induced *NCED* expression rather depends on auxin-independent pathways, ChIP-qPCR experiments would help to discover potential direct interactions between PIF transcription factors and *NCED* promoter regions.

Later, one should perform experiments aiming at deciphering how and where ABA perception takes place in the plant and ultimately triggers the shade-induced leaf hyponastic response. For this, one could for instance analyze the expression of ABA reporters at the whole plant level as well as in petiole cross sections. Also, testing the effects on leaf movement of applications of ABA and ABA inhibitors (265) at specific sites may lead to interesting results. In case one finds that applying ABA in a certain way would lead to hyponasty, we could then perform such an experiment with auxin defective *msg2* mutants to see if exogenous ABA is sufficient to rescue the defects in shade-induced hyponasty in such mutants. Based on the work of Park *et al.* (2015) and Barberon *et al.* (2016), one should also analyze shade-induced leaf hyponasty in lines triggering or inhibiting ABA responses in targeted leaf tissues (266, 267).

On a longer term, our phenotyping pipeline could be exploited for a large screening of ethyl methanesulfonate (EMS) mutagenized plants in order to find new loci involved in leaf hyponasty. Genome-wide association studies (GWAS) based on phenotypic data from a range of Arabidopsis accessions could also lead to the identification of variants underlying shade-induced leaf hyponasty.

References

1. Ballare CL, Sanchez RA, Scopel AL, Casal JJ, & Ghersa CM (1987) Early Detection of Neighbor Plants by Phytochrome Perception of Spectral Changes in Reflected Sunlight. *Plant Cell and Environment* 10(7):551-557.
2. Stitt M & Zeeman SC (2012) Starch turnover: pathways, regulation and role in growth. *Curr Opin Plant Biol* 15(3):282-292.
3. Valladares F & Pugnaire FI (1999) Tradeoffs Between Irradiance Capture and Avoidance in Semi-arid Environments Assessed with a Crown Architecture Model. *Annals of Botany* 83:459-469.
4. Smith H (1982) Light Quality, Photoperception, and Plant Strategy. *Annual Review of Plant Physiology and Plant Molecular Biology* 33:481-518.
5. Rizzini L*, et al.* (2011) Perception of UV-B by the Arabidopsis UVR8 protein. *Science* 332(6025):103-106.
6. Jenkins GI (2014) The UV-B photoreceptor UVR8: from structure to physiology. *Plant Cell* 26(1):21-37.
7. Tossi V, Lamattina L, Jenkins GI, & Cassia RO (2014) Ultraviolet-B-induced stomatal closure in Arabidopsis is regulated by the UV RESISTANCE LOCUS8 photoreceptor in a nitric oxide-dependent mechanism. *Plant Physiol* 164(4):2220-2230.
8. Vandenbussche F*, et al.* (2014) Photoreceptor-mediated bending towards UV-B in Arabidopsis. *Mol Plant* 7(6):1041-1052.
9. Song YH, Smith RW, To BJ, Millar AJ, & Imaizumi T (2012) FKF1 conveys timing information for CONSTANS stabilization in photoperiodic flowering. *Science* 336(6084):1045-1049.
10. Demarsy E & Fankhauser C (2009) Higher plants use LOV to perceive blue light. *Curr Opin Plant Biol* 12(1):69-74.
11. Christie JM, Blackwood L, Petersen J, & Sullivan S (2015) Plant flavoprotein photoreceptors. *Plant Cell Physiol* 56(3):401-413.
12. Inoue S, Kinoshita T, Takemiya A, Doi M, & Shimazaki K (2008) Leaf positioning of Arabidopsis in response to blue light. *Mol Plant* 1(1):15-26.
13. Inoue S, Kinoshita T, & Shimazaki K (2005) Possible involvement of phototropins in leaf movement of kidney bean in response to blue light. *Plant Physiol* 138(4):1994-2004.
14. Takemiya A*, et al.* (2013) Phosphorylation of BLUS1 kinase by phototropins is a primary step in stomatal opening. *Nat Commun* 4:2094.
15. Christie JM*, et al.* (2011) phot1 inhibition of ABCB19 primes lateral auxin fluxes in the shoot apex required for phototropism. *PLoS Biol* 9(6):e1001076.
16. Liu H, Liu B, Zhao C, Pepper M, & Lin C (2011) The action mechanisms of plant cryptochromes. *Trends Plant Sci* 16(12):684-691.
17. Chaves I*, et al.* (2011) The cryptochromes: blue light photoreceptors in plants and animals. *Annu Rev Plant Biol* 62:335-364.
18. de Wit M*, et al.* (2016) Integration of Phytochrome and Cryptochrome Signals Determines Plant Growth during Competition for Light. *Curr Biol* 26(24):3320-3326.
19. Keuskamp DH*, et al.* (2011) Blue-light-mediated shade avoidance requires combined auxin and brassinosteroid action in Arabidopsis seedlings. *Plant J* 67(2):208-217.

20. Pedmale UV*, et al.* (2016) Cryptochromes Interact Directly with PIFs to Control Plant Growth in Limiting Blue Light. *Cell* 164(1-2):233-245.
21. Keller MM*, et al.* (2011) Cryptochrome 1 and phytochrome B control shade-avoidance responses in Arabidopsis via partially independent hormonal cascades. *Plant J* 67(2):195-207.
22. Ballare CL & Pierik R (2017) The shade-avoidance syndrome: multiple signals and ecological consequences. *Plant Cell Environ*.
23. Li J, Li G, Wang H, & Wang Deng X (2011) Phytochrome signaling mechanisms. *Arabidopsis Book* 9:e0148.
24. Galvao VC & Fankhauser C (2015) Sensing the light environment in plants: photoreceptors and early signaling steps. *Curr Opin Neurobiol* 34:46-53.
25. Franklin KA*, et al.* (2003) Phytochromes B, D, and E act redundantly to control multiple physiological responses in Arabidopsis. *Plant Physiol* 131(3):1340-1346.
26. Roig-Villanova I & Martinez-Garcia JF (2016) Plant Responses to Vegetation Proximity: A Whole Life Avoiding Shade. *Front Plant Sci* 7:236.
27. Casal JJ (2012) Shade avoidance. *Arabidopsis Book* 10:e0157.
28. Keuskamp DH, Keller MM, Ballare CL, & Pierik R (2012) Blue light regulated shade avoidance. *Plant Signal Behav* 7(4):514-517.
29. Goyal A*, et al.* (2016) Shade Promotes Phototropism through Phytochrome B-Controlled Auxin Production. *Curr Biol* 26(24):3280-3287.
30. Sellaro R, Yanovsky MJ, & Casal JJ (2011) Repression of shade-avoidance reactions by sunfleck induction of HY5 expression in Arabidopsis. *Plant J* 68(5):919-928.
31. Hayes S, Velanis CN, Jenkins GI, & Franklin KA (2014) UV-B detected by the UVR8 photoreceptor antagonizes auxin signaling and plant shade avoidance. *Proc Natl Acad Sci U S A* 111(32):11894-11899.
32. Mazza CA & Ballare CL (2015) Photoreceptors UVR8 and phytochrome B cooperate to optimize plant growth and defense in patchy canopies. *New Phytol* 207(1):4-9.
33. Crepy MA & Casal JJ (2015) Photoreceptor-mediated kin recognition in plants. *New Phytol* 205(1):329-338.
34. Nito K*, et al.* (2015) Spatial Regulation of the Gene Expression Response to Shade in Arabidopsis Seedlings. *Plant Cell Physiol* 56(7):1306-1319.
35. van Gelderen K*, et al.* (2018) Far-red Light Detection in the Shoot Regulates Lateral Root Development through the HY5 Transcription Factor. *Plant Cell*.
36. Izaguirre MM, Mazza CA, Astigueta MS, Ciarla AM, & Ballare CL (2013) No time for candy: passionfruit (Passiflora edulis) plants down-regulate damage-induced extra floral nectar production in response to light signals of competition. *Oecologia* 173(1):213-221.
37. Valladares F & Niinemets Ü (2008) Shade Tolerance, a Key Plant Feature of Complex Nature and Consequences. *Annual Review of Ecology, Evolution, and Systematics* 39(1):237-257.
38. Ballare CL & Pierik R (2017) The shade-avoidance syndrome: multiple signals and ecological consequences. *Plant Cell Environ* 40(11):2530-2543.
39. Schmitt J, McCormac AC, & Smith H (1995) A test of the adaptive plasticity hypothesis using transgenic and mutant plants disabled in phytochrome-mediated elongation responses to neighbors. *Am Nat* 146(6):937-953.
40. Ballare CL (2014) Light regulation of plant defense. *Annu Rev Plant Biol* 65:335-363.

41. Smith H (1995) Physiological and Ecological Function within the Phytochrome Family. *Annual Review of Plant Physiology and Plant Molecular Biology* 46:289-315.
42. Leivar P & Quail PH (2011) PIFs: pivotal components in a cellular signaling hub. *Trends Plant Sci* 16(1):19-28.
43. Li L*, et al.* (2012) Linking photoreceptor excitation to changes in plant architecture. *Genes Dev* 26(8):785-790.
44. Hornitschek P*, et al.* (2012) Phytochrome interacting factors 4 and 5 control seedling growth in changing light conditions by directly controlling auxin signaling. *Plant J* 71(5):699-711.
45. Kohnen MV*, et al.* (2016) Neighbor Detection Induces Organ-Specific Transcriptomes, Revealing Patterns Underlying Hypocotyl-Specific Growth. *Plant Cell* 28(12):2889-2904.
46. Lorrain S, Allen T, Duek PD, Whitelam GC, & Fankhauser C (2008) Phytochrome-mediated inhibition of shade avoidance involves degradation of growth-promoting bHLH transcription factors. *Plant J* 53(2):312-323.
47. Hornitschek P, Lorrain S, Zoete V, Michielin O, & Fankhauser C (2009) Inhibition of the shade avoidance response by formation of non-DNA binding bHLH heterodimers. *EMBO J* 28(24):3893-3902.
48. Keuskamp DH, Pollmann S, Voesenek LACJ, Peeters AJM, & Pierik R (2010) Auxin transport through PIN-FORMED 3 (PIN3) controls shade avoidance and fitness during competition. *Proceedings of the National Academy of Sciences of the United States of America* 107(52):22740-22744.
49. Tao Y*, et al.* (2008) Rapid synthesis of auxin via a new tryptophan-dependent pathway is required for shade avoidance in plants. *Cell* 133(1):164-176.
50. Aloni R, Schwalm K, Langhans M, & Ullrich CI (2003) Gradual shifts in sites of free-auxin production during leaf-primordium development and their role in vascular differentiation and leaf morphogenesis in Arabidopsis. *Planta* 216(5):841-853.
51. de Wit M, Ljung K, & Fankhauser C (2015) Contrasting growth responses in lamina and petiole during neighbor detection depend on differential auxin responsiveness rather than different auxin levels. *New Phytol* 208(1):198-209.
52. Bou-Torrent J*, et al.* (2014) Plant proximity perception dynamically modulates hormone levels and sensitivity in Arabidopsis. *J Exp Bot* 65(11):2937-2947.
53. Won C*, et al.* (2011) Conversion of tryptophan to indole-3-acetic acid by TRYPTOPHAN AMINOTRANSFERASES OF ARABIDOPSIS and YUCCAs in Arabidopsis. *Proc Natl Acad Sci U S A* 108(45):18518-18523.
54. Muller-Moule P*, et al.* (2016) YUCCA auxin biosynthetic genes are required for Arabidopsis shade avoidance. *PeerJ* 4:e2574.
55. Chapman EJ*, et al.* (2012) Hypocotyl transcriptome reveals auxin regulation of growth-promoting genes through GA-dependent and -independent pathways. *PLoS One* 7(5):e36210.
56. Hersch M*, et al.* (2014) Light intensity modulates the regulatory network of the shade avoidance response in Arabidopsis. *Proc Natl Acad Sci U S A* 111(17):6515-6520.
57. Ge Y*, et al.* (2017) SHADE AVOIDANCE 4 Is Required for Proper Auxin Distribution in the Hypocotyl. *Plant Physiol* 173(1):788-800.

58. Kozuka T*, et al.* (2010) Involvement of auxin and brassinosteroid in the regulation of petiole elongation under the shade. *Plant Physiol* 153(4):1608-1618.
59. Morelli G & Ruberti I (2000) Shade avoidance responses. Driving auxin along lateral routes. *Plant Physiol* 122(3):621-626.
60. Grones P & Friml J (2015) Auxin transporters and binding proteins at a glance. *J Cell Sci* 128(1):1-7.
61. Peret B*, et al.* (2012) AUX/LAX genes encode a family of auxin influx transporters that perform distinct functions during Arabidopsis development. *Plant Cell* 24(7):2874-2885.
62. Bennett T*, et al.* (2016) Connective Auxin Transport in the Shoot Facilitates Communication between Shoot Apices. *PLoS Biol* 14(4):e1002446.
63. Sassi M, Wang J, Ruberti I, Vernoux T, & Xu J (2013) Shedding light on auxin movement: light-regulation of polar auxin transport in the photocontrol of plant development. *Plant Signal Behav* 8(3):e23355.
64. Galweiler L*, et al.* (1998) Regulation of polar auxin transport by AtPIN1 in Arabidopsis vascular tissue. *Science* 282(5397):2226-2230.
65. Goyal A, Szarzynska B, & Fankhauser C (2013) Phototropism: at the crossroads of light-signaling pathways. *Trends in Plant Science* 18(7):393-401.
66. Tanaka SI, Nakamura S, Mochizuki N, & Nagatani A (2002) Phytochrome in cotyledons regulates the expression of genes in the hypocotyl through auxin-dependent and -independent pathways. *Plant and Cell Physiology* 43(10):1171-1181.
67. Procko C, Crenshaw CM, Ljung K, Noel JP, & Chory J (2014) Cotyledon-Generated Auxin Is Required for Shade-Induced Hypocotyl Growth in Brassica rapa. *Plant Physiol* 165(3):1285-1301.
68. Zheng Z*, et al.* (2016) Local auxin metabolism regulates environment-induced hypocotyl elongation. *Nat Plants* 2:16025.
69. Chen X*, et al.* (2016) Shoot-to-Root Mobile Transcription Factor HY5 Coordinates Plant Carbon and Nitrogen Acquisition. *Curr Biol* 26(5):640-646.
70. Chapman EJ & Estelle M (2009) Mechanism of auxin-regulated gene expression in plants. *Annu Rev Genet* 43:265-285.
71. Goda H*, et al.* (2008) The AtGenExpress hormone and chemical treatment data set: experimental design, data evaluation, model data analysis and data access. *The Plant Journal* 55(3):526-542.
72. Paciorek T & Friml J (2006) Auxin signaling. *J Cell Sci* 119(Pt 7):1199-1202.
73. Devlin PF, Yanovsky MJ, & Kay SA (2003) A genomic analysis of the shade avoidance response in Arabidopsis. *Plant Physiol* 133(4):1617-1629.
74. Sasidharan R, Keuskamp DH, Kooke R, Voesenek LA, & Pierik R (2014) Interactions between auxin, microtubules and XTHs mediate green shade-induced petiole elongation in arabidopsis. *PLoS One* 9(3):e90587.
75. Sasidharan R*, et al.* (2010) Light Quality-Mediated Petiole Elongation in Arabidopsis during Shade Avoidance Involves Cell Wall Modification by Xyloglucan EndotransglucosylaseHydrolases. *Plant Physiology*.
76. Yu J*, et al.* (2015) Characterization of tub4(P287L) , a beta-tubulin mutant, revealed new aspects of microtubule regulation in shade. *J Integr Plant Biol* 57(9):757-769.
77. Dunser K & Kleine-Vehn J (2015) Differential growth regulation in plants--the acid growth balloon theory. *Curr Opin Plant Biol* 28:55-59.

78. Savaldi-Goldstein S, Peto C, & Chory J (2007) The epidermis both drives and restricts plant shoot growth. *Nature* 446(7132):199-202.
79. Procko C*, et al.* (2016) The epidermis coordinates auxin-induced stem growth in response to shade. *Genes & Development*.
80. Djakovic-Petrovic T, de Wit M, Voesenek LA, & Pierik R (2007) DELLA protein function in growth responses to canopy signals. *Plant J* 51(1):117-126.
81. de Lucas M*, et al.* (2008) A molecular framework for light and gibberellin control of cell elongation. *Nature* 451(7177):480-484.
82. Hisamatsu T, King RW, Helliwell CA, & Koshioka M (2005) The involvement of gibberellin 20-oxidase genes in phytochrome-regulated petiole elongation of Arabidopsis. *Plant Physiol* 138(2):1106-1116.
83. Pierik R, Djakovic-Petrovic T, Keuskamp DH, de Wit M, & Voesenek LA (2009) Auxin and ethylene regulate elongation responses to neighbor proximity signals independent of gibberellin and della proteins in Arabidopsis. *Plant Physiol* 149(4):1701-1712.
84. Vandenbussche F*, et al.* (2003) Ethylene and auxin control the Arabidopsis response to decreased light intensity. *Plant Physiol* 133(2):517-527.
85. Das D, St Onge KR, Voesenek LA, Pierik R, & Sasidharan R (2016) Ethylene- and Shade-Induced Hypocotyl Elongation Share Transcriptome Patterns and Functional Regulators. *Plant Physiol* 172(2):718-733.
86. Reddy SK, Holalu SV, Casal JJ, & Finlayson SA (2013) Abscisic acid regulates axillary bud outgrowth responses to the ratio of red to far-red light. *Plant Physiol* 163(2):1047-1058.
87. Kurepin LV, Emery RJ, Pharis RP, & Reid DM (2007) Uncoupling light quality from light irradiance effects in Helianthus annuus shoots: putative roles for plant hormones in leaf and internode growth. *J Exp Bot* 58(8):2145-2157.
88. Cagnola JI, Ploschuk E, Benech-Arnold T, Finlayson SA, & Casal JJ (2012) Stem transcriptome reveals mechanisms to reduce the energetic cost of shade-avoidance responses in tomato. *Plant Physiol* 160(2):1110-1119.
89. Holalu SV & Finlayson SA (2017) The ratio of red light to far red light alters Arabidopsis axillary bud growth and abscisic acid signalling before stem auxin changes. *J Exp Bot* 68(5):943-952.
90. Nambara E & Marion-Poll A (2005) Abscisic acid biosynthesis and catabolism. *Annu Rev Plant Biol* 56:165-185.
91. Belin C, Megies C, Hauserova E, & Lopez-Molina L (2009) Abscisic acid represses growth of the Arabidopsis embryonic axis after germination by enhancing auxin signaling. *Plant Cell* 21(8):2253-2268.
92. McClung CR (2006) Plant circadian rhythms. *Plant Cell* 18(4):792-803.
93. Dumais J & Forterre Y (2012) “Vegetable Dynamicks”: The Role of Water in Plant Movements.
94. Harmer SL & Brooks CJ (2017) Growth-mediated plant movements: hidden in plain sight. *Curr Opin Plant Biol* 41:89-94.
95. Zadnikova P, Smet D, Zhu Q, Van Der Straeten D, & Benkova E (2015) Strategies of seedlings to overcome their sessile nature: auxin in mobility control. *Front Plant Sci* 6:218.
96. Hangarter RP (1997) Gravity, light and plant form. *Plant Cell Environ* 20(6):796-800.
97. Mano E, Horiguchi G, & Tsukaya H (2006) Gravitropism in leaves of Arabidopsis thaliana (L.) Heynh. *Plant Cell Physiol* 47(2):217-223.

98. Evans ML, Ishikawa H, & Estelle MA (1994) Responses of Arabidopsis Roots to Auxin Studied with High Temporal Resolution - Comparison of Wild-Type and Auxin-Response Mutants. *Planta* 194(2):215-222.
99. Shkolnik D, Krieger G, Nuriel R, & Fromm H (2016) Hydrotropism: Root Bending Does Not Require Auxin Redistribution. *Mol Plant* 9(5):757-759.
100. Dietrich D*, et al.* (2017) Root hydrotropism is controlled via a cortex-specific growth mechanism. *Nat Plants* 3:17057.
101. Humplik JF, Bergougnoux V, & Van Volkenburgh E (2017) To Stimulate or Inhibit? That Is the Question for the Function of Abscisic Acid. *Trends Plant Sci*.
102. Barrero JM*, et al.* (2008) The ABA1 gene and carotenoid biosynthesis are required for late skotomorphogenic growth in Arabidopsis thaliana. *Plant Cell Environ* 31(2):227-234.
103. Watanabe H, Takahashi K, & Saigusa M (2001) Morphological and anatomical effects of abscisic acid (ABA) and fluridone (FLU) on the growth of rice mesocotyls. *Plant Growth Regulation* 34(3):273-275.
104. Pierik R, Tholen D, Poorter H, Visser EJ, & Voesenek LA (2006) The Janus face of ethylene: growth inhibition and stimulation. *Trends Plant Sci* 11(4):176-183.
105. Takahashi N, Goto N, Okada K, & Takahashi H (2002) Hydrotropism in abscisic acid, wavy, and gravitropic mutants of Arabidopsis thaliana. *Planta* 216(2):203-211.
106. Rayle DL & Cleland RE (1992) The Acid Growth Theory of Auxin-Induced Cell Elongation Is Alive and Well. *Plant Physiology* 99(4):1271-1274.
107. Hohm T*, et al.* (2014) Plasma membrane H(+) -ATPase regulation is required for auxin gradient formation preceding phototropic growth. *Mol Syst Biol* 10:751.
108. Fendrych M, Leung J, & Friml J (2016) TIR1/AFB-Aux/IAA auxin perception mediates rapid cell wall acidification and growth of Arabidopsis hypocotyls. *Elife* 5.
109. Barbez E, Dunser K, Gaidora A, Lendl T, & Busch W (2017) Auxin steers root cell expansion via apoplastic pH regulation in Arabidopsis thaliana. *Proc Natl Acad Sci U S A* 114(24):E4884-E4893.
110. Dornbusch T*, et al.* (2012) Measuring the diurnal pattern of leaf hyponasty and growth in Arabidopsis - a novel phenotyping approach using laser scanning. *Functional Plant Biology* 39(10-11):860-869.
111. Kawaguchi M (2003) SLEEPLESS, a gene conferring nyctinastic movement in legume. *J Plant Res* 116(2):151-154.
112. van Zanten M, Pons TL, Janssen JAM, Voesenek LA, & Peeters AJ (2010) On the Relevance and Control of Leaf Angle. *Critical Reviews in Plant Sciences*.
113. Uehlein N & Kaldenhoff R (2008) Aquaporins and plant leaf movements. *Ann Bot* 101(1):1-4.
114. Moshelion M*, et al.* (2002) Plasma membrane aquaporins in the motor cells of Samanea saman: diurnal and circadian regulation. *Plant Cell* 14(3):727-739.
115. Forterre Y (2013) Slow, fast and furious: understanding the physics of plant movements. *J Exp Bot* 64(15):4745-4760.
116. Moran N (2007) Osmoregulation of leaf motor cells. *FEBS Lett* 581(12):2337-2347.

117. van Zanten M*, et al.* (2010) Ethylene-induced hyponastic growth in Arabidopsis thaliana is controlled by ERECTA. *Plant J* 61(1):83-95.
118. Rauf M*, et al.* (2013) NAC transcription factor speedy hyponastic growth regulates flooding-induced leaf movement in Arabidopsis. *Plant Cell* 25(12):4941-4955.
119. Millenaar FF*, et al.* (2005) Ethylene-induced differential growth of petioles in Arabidopsis. Analyzing natural variation, response kinetics, and regulation. *Plant Physiol* 137(3):998-1008.
120. Polko JK*, et al.* (2012) Ethylene-induced differential petiole growth in Arabidopsis thaliana involves local microtubule reorientation and cell expansion. *New Phytol* 193(2):339-348.
121. Johnsson A, Solheim BG, & Iversen TH (2009) Gravity amplifies and microgravity decreases circumnutations in Arabidopsis thaliana stems: results from a space experiment. *New Phytol* 182(3):621-629.
122. Hatakeda Y*, et al.* (2003) Gravitropic response plays an important role in the nutational movements of the shoots of Pharbitis nil and Arabidopsis thaliana. *Physiologia Plantarum* 118(3):464-473.
123. Kitazawa D*, et al.* (2005) Shoot circumnutation and winding movements require gravisensing cells. *Proc Natl Acad Sci U S A* 102(51):18742-18747.
124. Baskin TI (2007) *Ultradian Growth Oscillations in Organs: Physiological Signal or Noise?*
125. Someya N, Niinuma K, Kimura M, Yamaguchi I, & Hamamoto H (2006) Circumnutation of Arabidopsis thaliana inflorescence stems. *Biologia Plantarum* 50(2):287-290.
126. Farre EM (2012) The regulation of plant growth by the circadian clock. *Plant Biol (Stuttg)* 14(3):401-410.
127. Crawford AJ, McLachlan DH, Hetherington AM, & Franklin KA (2012) High temperature exposure increases plant cooling capacity. *Curr Biol* 22(10):R396-397.
128. Mantilla-Perez MB & Salas Fernandez MG (2017) Differential manipulation of leaf angle throughout the canopy: current status and prospects. *J Exp Bot*.
129. Mullen JL, Weinig C, & Hangarter RP (2006) Shade avoidance and the regulation of leaf inclination in Arabidopsis. *Plant Cell Environ* 29(6):1099-1106.
130. Martín G*, et al.* (2018) Circadian Waves of Transcriptional Repression Shape PIF-Regulated Photoperiod-Responsive Growth in Arabidopsis. *Current Biology*.
131. Covington MF & Harmer SL (2007) The circadian clock regulates auxin signaling and responses in Arabidopsis. *PLoS Biol* 5(8):e222.
132. Koini MA*, et al.* (2009) High temperature-mediated adaptations in plant architecture require the bHLH transcription factor PIF4. *Curr Biol* 19(5):408-413.
133. Polko JK, Voesenek LA, Peeters AJ, & Pierik R (2011) Petiole hyponasty: an ethylene-driven, adaptive response to changes in the environment. *AoB Plants* 2011:plr031.
134. Voesenek LACJ*, et al.* (2003) Interactions between plant hormones regulate submergence-induced shoot elongation in the flooding-tolerant dicot Rumex palustris. *Annals of Botany* 91(2):205-211.

135. Cox MC, Millenaar FF, Van Berkel YE, Peeters AJ, & Voesenek LA (2003) Plant movement. Submergence-induced petiole elongation in Rumex palustris depends on hyponastic growth. *Plant Physiol* 132(1):282-291.
136. Cox MC*, et al.* (2004) The roles of ethylene, auxin, abscisic acid, and gibberellin in the hyponastic growth of submerged Rumex palustris petioles. *Plant Physiol* 136(2):2948-2960; discussion 3001.
137. Heydarian Z*, et al.* (2010) A kinetic analysis of hyponastic growth and petiole elongation upon ethylene exposure in Rumex palustris. *Ann Bot* 106(3):429-435.
138. van Zanten M*, et al.* (2009) Auxin perception and polar auxin transport are not always a prerequisite for differential growth. *Plant Signal Behav*.
139. Benschop JJ*, et al.* (2005) Contrasting interactions between ethylene and abscisic acid in Rumex species differing in submergence tolerance. *Plant J* 44(5):756-768.
140. Benschop JJ*, et al.* (2007) Abscisic acid antagonizes ethylene-induced hyponastic growth in Arabidopsis. *Plant Physiol* 143(2):1013-1023.
141. Polko JK*, et al.* (2013) Ethylene promotes hyponastic growth through interaction with ROTUNDIFOLIA3/CYP90C1 in Arabidopsis. *J Exp Bot* 64(2):613-624.
142. van Zanten M*, et al.* (2010) ERECTA controls low light intensity-induced differential petiole growth independent of phytochrome B and cryptochrome 2 action in Arabidopsis thaliana. *Plant Signal Behav* 5(3):284-286.
143. Mizoi J, Shinozaki K, & Yamaguchi-Shinozaki K (2012) AP2/ERF family transcription factors in plant abiotic stress responses. *Biochim Biophys Acta* 1819(2):86-96.
144. Chen MK & Shpak ED (2014) ERECTA family genes regulate development of cotyledons during embryogenesis. *FEBS Lett* 588(21):3912-3917.
145. Nuruzzaman M, Sharoni AM, & Kikuchi S (2013) Roles of NAC transcription factors in the regulation of biotic and abiotic stress responses in plants. *Front Microbiol* 4:248.
146. Vreeburg RA*, et al.* (2005) Ethylene regulates fast apoplastic acidification and expansin A transcription during submergence-induced petiole elongation in Rumex palustris. *Plant J* 43(4):597-610.
147. van Zanten M, Voesenek LA, Peeters AJ, & Millenaar FF (2009) Hormone- and light-mediated regulation of heat-induced differential petiole growth in Arabidopsis. *Plant Physiol* 151(3):1446-1458.
148. Legris M, Nieto C, Sellaro R, Prat S, & Casal JJ (2017) Perception and signalling of light and temperature cues in plants. *Plant J* 90(4):683-697.
149. Jung JH*, et al.* (2016) Phytochromes function as thermosensors in Arabidopsis. *Science* 354(6314):886-889.
150. Faigon-Soverna A*, et al.* (2006) A constitutive shade-avoidance mutant implicates TIR-NBS-LRR proteins in Arabidopsis photomorphogenic development. *Plant Cell* 18(11):2919-2928.
151. Ballare CL & Scopel AL (1997) Phytochrome signalling in plant canopies: Testing its population-level implications with photoreceptor mutants of Arabidopsis. *Functional Ecology* 11(4):441-450.
152. Millenaar FF*, et al.* (2009) Differential petiole growth in Arabidopsis thaliana: photocontrol and hormonal regulation. *New Phytol* 184(1):141-152.

153. de Carbonnel M*, et al.* (2010) The Arabidopsis PHYTOCHROME KINASE SUBSTRATE2 protein is a phototropin signaling element that regulates leaf flattening and leaf positioning. *Plant Physiol* 152(3):1391-1405.
154. Pierik R, Whitelam GC, Voesenek LA, de Kroon H, & Visser EJ (2004) Canopy studies on ethylene-insensitive tobacco identify ethylene as a novel element in blue light and plant-plant signalling. *Plant J* 38(2):310-319.
155. van Zanten M (2009) Control of differential petiole growth in Arabidopsis thaliana. *Utrecht University Thesis Repository*.
156. Pantin F, Simonneau T, & Muller B (2012) Coming of leaf age: control of growth by hydraulics and metabolics during leaf ontogeny. *New Phytol* 196(2):349-366.
157. Yaaran A & Moshelion M (2016) Role of Aquaporins in a Composite Model of Water Transport in the Leaf. *Int J Mol Sci* 17(7).
158. Sack L & Holbrook NM (2006) Leaf hydraulics. *Annu Rev Plant Biol* 57:361-381.
159. Shatil-Cohen A, Attia Z, & Moshelion M (2011) Bundle-sheath cell regulation of xylem-mesophyll water transport via aquaporins under drought stress: a target of xylem-borne ABA? *Plant J* 67(1):72-80.
160. Shatil-Cohen A & Moshelion M (2012) Smart Pipes: The bundle sheath role as xylem-mesophyll barrier. *Plant Signal Behav*.
161. Ache P*, et al.* (2010) Stomatal action directly feeds back on leaf turgor: new insights into the regulation of the plant water status from non-invasive pressure probe measurements. *Plant J* 62(6):1072-1082.
162. Lersten NR (1997) Occurence of Endodermis with a Casparian Strip in Stem and Leaf. *The Botanical Review*.
163. Steudle E (2001) The Cohesion-Tension Mechanism and the Acquisition of Water by Plant Roots. *Annu Rev Plant Physiol Plant Mol Biol* 52:847-875.
164. Canny M (2012) Water loss from leaf mesophyll stripped of the epidermis. *Functional Plant Biology* 39(5).
165. Lee KH*, et al.* (2006) Activation of glucosidase via stress-induced polymerization rapidly increases active pools of abscisic acid. *Cell* 126(6):1109-1120.
166. Tardieu F, Simonneau T, & Parent B (2015) Modelling the coordination of the controls of stomatal aperture, transpiration, leaf growth, and abscisic acid: update and extension of the Tardieu-Davies model. *J Exp Bot* 66(8):2227-2237.
167. Prado K & Maurel C (2013) Regulation of leaf hydraulics: from molecular to whole plant levels. *Front Plant Sci* 4:255.
168. Caringella MA, Bongers FJ, & Sack L (2015) Leaf hydraulic conductance varies with vein anatomy across Arabidopsis thaliana wild-type and leaf vein mutants. *Plant Cell Environ* 38(12):2735-2746.
169. Jia W & Davies WJ (2007) Modification of leaf apoplastic pH in relation to stomatal sensitivity to root-sourced abscisic acid signals. *Plant Physiol* 143(1):68-77.
170. Wigoda N*, et al.* (2017) Bundle-sheath cells are leaf "water valves" controlled via xylem acidification by H+-ATPase. *BioXriv*.
171. Haruta M*, et al.* (2010) Molecular characterization of mutant Arabidopsis plants with reduced plasma membrane proton pump activity. *J Biol Chem* 285(23):17918-17929.

172. Fuglsang AT*, et al.* (2007) Arabidopsis protein kinase PKS5 inhibits the plasma membrane H+ -ATPase by preventing interaction with 14-3-3 protein. *Plant Cell* 19(5):1617-1634.
173. Moshelion M, Halperin O, Wallach R, Oren R, & Way DA (2015) Role of aquaporins in determining transpiration and photosynthesis in water-stressed plants: crop water-use efficiency, growth and yield. *Plant Cell Environ* 38(9):1785-1793.
174. Pantin F*, et al.* (2013) The dual effect of abscisic acid on stomata. *New Phytol* 197(1):65-72.
175. Sade N*, et al.* (2014) The role of plasma membrane aquaporins in regulating the bundle sheath-mesophyll continuum and leaf hydraulics. *Plant Physiol* 166(3):1609-1620.
176. Postaire O*, et al.* (2010) A PIP1 aquaporin contributes to hydrostatic pressure-induced water transport in both the root and rosette of Arabidopsis. *Plant Physiol* 152(3):1418-1430.
177. Maurel C, Verdoucq L, Luu DT, & Santoni V (2008) Plant aquaporins: membrane channels with multiple integrated functions. *Annu Rev Plant Biol* 59:595-624.
178. Boursiac Y*, et al.* (2005) Early effects of salinity on water transport in Arabidopsis roots. Molecular and cellular features of aquaporin expression. *Plant Physiol* 139(2):790-805.
179. Monneuse JM*, et al.* (2011) Towards the profiling of the Arabidopsis thaliana plasma membrane transportome by targeted proteomics. *Proteomics* 11(9):1789-1797.
180. Alexandersson E*, et al.* (2005) Whole gene family expression and drought stress regulation of aquaporins. *Plant Mol Biol* 59(3):469-484.
181. Li G, Santoni V, & Maurel C (2014) Plant aquaporins: roles in plant physiology. *Biochim Biophys Acta* 1840(5):1574-1582.
182. Tournaire-Roux C*, et al.* (2003) Cytosolic pH regulates root water transport during anoxic stress through gating of aquaporins. *Nature* 425(6956):393-397.
183. Da Ines O*, et al.* (2010) Kinetic analyses of plant water relocation using deuterium as tracer - reduced water flux of Arabidopsis pip2 aquaporin knockout mutants. *Plant Biol (Stuttg)* 12 Suppl 1:129-139.
184. Prado K*, et al.* (2013) Regulation of Arabidopsis leaf hydraulics involves light-dependent phosphorylation of aquaporins in veins. *Plant Cell* 25(3):1029-1039.
185. Tardieu F & Simonneau T (1998) Variability among species of stomatal control under fluctuating soil water status and evaporative demand: modelling isohydric and anisohydric behaviours. *Journal of Experimental Botany* 49:419-432.
186. Galle A*, et al.* (2013) Isohydric and anisohydric strategies of wheat genotypes under osmotic stress: biosynthesis and function of ABA in stress responses. *J Plant Physiol* 170(16):1389-1399.
187. Brodribb TJ & McAdam SA (2013) Abscisic acid mediates a divergence in the drought response of two conifers. *Plant Physiol* 162(3):1370-1377.
188. Cochard H*, et al.* (2007) Putative role of aquaporins in variable hydraulic conductance of leaves in response to light. *Plant Physiol* 143(1):122-133.

189. Boursiac Y*, et al.* (2008) Stimulus-induced downregulation of root water transport involves reactive oxygen species-activated cell signalling and plasma membrane intrinsic protein internalization. *Plant J* 56(2):207-218.
190. Baaziz KB*, et al.* (2012) Light-mediated K(leaf) induction and contribution of both the PIP1s and PIP2s aquaporins in five tree species: walnut (Juglans regia) case study. *Tree Physiol* 32(4):423-434.
191. Scoffoni C, Pou A, Aasamaa K, & Sack L (2008) The rapid light response of leaf hydraulic conductance: new evidence from two experimental methods. *Plant Cell Environ* 31(12):1803-1812.
192. Chaumont F & Tyerman SD (2014) Aquaporins: highly regulated channels controlling plant water relations. *Plant Physiol* 164(4):1600-1618.
193. Caldeira CF, Jeanguenin L, Chaumont F, & Tardieu F (2014) Circadian rhythms of hydraulic conductance and growth are enhanced by drought and improve plant performance. *Nat Commun* 5:5365.
194. Takase T*, et al.* (2011) The circadian clock modulates water dynamics and aquaporin expression in Arabidopsis roots. *Plant Cell Physiol* 52(2):373-383.
195. Lopez F*, et al.* (2003) Diurnal regulation of water transport and aquaporin gene expression in maize roots: contribution of PIP2 proteins. *Plant Cell Physiol* 44(12):1384-1395.
196. Savvides A, Fanourakis D, & van Ieperen W (2012) Co-ordination of hydraulic and stomatal conductances across light qualities in cucumber leaves. *J Exp Bot* 63(3):1135-1143.
197. Sellin A, Sack L, Ounapuu E, & Karusion A (2011) Impact of light quality on leaf and shoot hydraulic properties: a case study in silver birch (Betula pendula). *Plant Cell Environ* 34(7):1079-1087.
198. Casson SA*, et al.* (2009) phytochrome B and PIF4 regulate stomatal development in response to light quantity. *Curr Biol* 19(3):229-234.
199. Boccalandro HE*, et al.* (2009) Phytochrome B enhances photosynthesis at the expense of water-use efficiency in Arabidopsis. *Plant Physiol* 150(2):1083-1092.
200. Hartung W, Radin JW, & Hendrix DL (1988) Abscisic-Acid Movement into the Apoplastic Solution of Water-Stressed Cotton Leaves - Role of Apoplastic Ph. *Plant Physiology* 86(3):908-913.
201. Timergalina LN, Vysotskaya LB, Veselov SY, & Kudoyarova GR (2007) Effect of increased irradiance on the hormone content, water relations, and leaf elongation in wheat seedlings. *Russian Journal of Plant Physiology* 54(5):633-638.
202. Thompson AJ*, et al.* (2007) Overproduction of abscisic acid in tomato increases transpiration efficiency and root hydraulic conductivity and influences leaf expansion. *Plant Physiol* 143(4):1905-1917.
203. Galvez-Valdivieso G*, et al.* (2009) The high light response in Arabidopsis involves ABA signaling between vascular and bundle sheath cells. *Plant Cell* 21(7):2143-2162.
204. McAdam SA & Brodribb TJ (2016) Linking Turgor with ABA Biosynthesis: Implications for Stomatal Responses to Vapor Pressure Deficit across Land Plants. *Plant Physiol* 171(3):2008-2016.
205. Christmann A, Weiler EW, Steudle E, & Grill E (2007) A hydraulic signal in root-to-shoot signalling of water shortage. *Plant J* 52(1):167-174.

206. Sussmilch FC, Brodribb TJ, & McAdam SAM (2017) Up-regulation of NCED3 and ABA biosynthesis occur within minutes of a decrease in leaf turgor but AHK1 is not required. *J Exp Bot* 68(11):2913-2918.
207. Endo A*, et al.* (2008) Drought induction of Arabidopsis 9-cis-epoxycarotenoid dioxygenase occurs in vascular parenchyma cells. *Plant Physiol* 147(4):1984-1993.
208. Bauer H*, et al.* (2013) The stomatal response to reduced relative humidity requires guard cell-autonomous ABA synthesis. *Curr Biol* 23(1):53-57.
209. Ha JH*, et al.* (2018) Shoot phytochrome B modulates root ROS homeostasis via abscisic acid signaling in Arabidopsis. *Plant J*.
210. Hartung W, Sauter A, & Hose E (2002) Abscisic acid in the xylem: where does it come from, where does it go to? *J Exp Bot* 53(366):27-32.
211. Kudoyarova G*, et al.* (2011) Involvement of root ABA and hydraulic conductivity in the control of water relations in wheat plants exposed to increased evaporative demand. *Planta* 233(1):87-94.
212. Christmann A, Hoffmann T, Teplova I, Grill E, & Muller A (2005) Generation of active pools of abscisic acid revealed by in vivo imaging of water-stressed Arabidopsis. *Plant Physiol* 137(1):209-219.
213. Dodd IC (2013) Abscisic acid and stomatal closure: a hydraulic conductance conundrum? *New Phytol* 197(1):6-8.
214. Kaldenhoff R*, et al.* (1995) The Blue Light-Responsive Athh2 Gene of Arabidopsis-Thaliana Is Primarily Expressed in Expanding as Well as in Differentiating Cells and Encodes a Putative Channel Protein of the Plasmalemma. *Plant Journal* 7(1):87-95.
215. Kline KG, Barrett-Wilt GA, & Sussman MR (2010) In planta changes in protein phosphorylation induced by the plant hormone abscisic acid. *Proc Natl Acad Sci U S A* 107(36):15986-15991.
216. Jang JY, Kim DG, Kim YO, Kim JS, & Kang H (2004) An expression analysis of a gene family encoding plasma membrane aquaporins in response to abiotic stresses in Arabidopsis thaliana. *Plant Mol Biol* 54(5):713-725.
217. Grondin A*, et al.* (2015) Aquaporins Contribute to ABA-Triggered Stomatal Closure through OST1-Mediated Phosphorylation. *Plant Cell* 27(7):1945-1954.
218. Peret B*, et al.* (2012) Auxin regulates aquaporin function to facilitate lateral root emergence. *Nat Cell Biol* 14(10):991-998.
219. Vandeleur RK*, et al.* (2014) Rapid shoot-to-root signalling regulates root hydraulic conductance via aquaporins. *Plant Cell Environ* 37(2):520-538.
220. Miyamoto N, Ookawa T, Takahashi H, & Hirasawa T (2002) Water uptake and hydraulic properties of elongating cells in hydrotropically bending roots of Pisum sativum L. *Plant Cell Physiol* 43(4):393-401.
221. Moshelion M*, et al.* (2002) Diurnal and circadian regulation of putative potassium channels in a leaf moving organ. *Plant Physiol* 128(2):634-642.
222. Wood WML (1953) Thermonasty in Tulip and Crocus Flowers. *Journal of Experimental Botany* 4(10):65-77.
223. Azad AK, Sawa Y, Ishikawa T, & Shibata H (2004) Phosphorylation of plasma membrane aquaporin regulates temperature-dependent opening of tulip petals. *Plant Cell Physiol* 45(5):608-617.
224. Siefritz F, Otto B, Bienert GP, van der Krol A, & Kaldenhoff R (2004) The plasma membrane aquaporin NtAQP1 is a key component of the leaf unfolding mechanism in tobacco. *Plant Journal* 37(2):147-155.

225. Dornbusch T, Michaud O, Xenarios I, & Fankhauser C (2014) Differentially phased leaf growth and movements in Arabidopsis depend on coordinated circadian and light regulation. *Plant Cell* 26(10):3911-3921.
226. Hofmann NR (2014) Simultaneous monitoring of leaf growth and leaf movement. *Plant Cell* 26(10):3828.
227. Michaud O, Fiorucci AS, Xenarios I, & Fankhauser C (2017) *Local auxin production underlies a spatially restricted neighbor-detection response in Arabidopsis* 2017/06/28 Ed.
228. Zhao Y (2018) Essential Roles of Local Auxin Biosynthesis in Plant Development and in Adaptation to Environmental Changes. *Annual Review of Plant Biology*.
229. Simon S*, et al.* (2013) Defining the selectivity of processes along the auxin response chain: a study using auxin analogues. *New Phytologist* 200(4):1034-1048.
230. Pantazopoulou CK*, et al.* (2017) Neighbor detection at the leaf tip adaptively regulates upward leaf movement through spatial auxin dynamics. *Proc Natl Acad Sci U S A*.
231. Finkelstein R (2013) Abscisic Acid synthesis and response. *Arabidopsis Book* 11:e0166.
232. Koornneef M, Jorna ML, Brinkhorst-van der Swan DL, & Karssen CM (1982) The isolation of abscisic acid (ABA) deficient mutants by selection of induced revertants in non-germinating gibberellin sensitive lines of Arabidopsis thaliana (L.) heynh. *Theor Appl Genet* 61(4):385-393.
233. Iuchi S, Kobayashi M, Yamaguchi-Shinozaki K, & Shinozaki K (2000) A stress-inducible gene for 9-cis-epoxycarotenoid dioxygenase involved in abscisic acid biosynthesis under water stress in drought-tolerant cowpea. *Plant Physiol* 123(2):553-562.
234. Tan BC*, et al.* (2003) Molecular characterization of the Arabidopsis 9-cis epoxycarotenoid dioxygenase gene family. *Plant J* 35(1):44-56.
235. Okamoto M*, et al.* (2006) CYP707A1 and CYP707A2, which encode abscisic acid 8'-hydroxylases, are indispensable for proper control of seed dormancy and germination in Arabidopsis. *Plant Physiol* 141(1):97-107.
236. Koiwai H*, et al.* (2004) Tissue-specific localization of an abscisic acid biosynthetic enzyme, AAO3, in Arabidopsis. *Plant Physiol* 134(4):1697-1707.
237. Ikegami K, Okamoto M, Seo M, & Koshiba T (2009) Activation of abscisic acid biosynthesis in the leaves of Arabidopsis thaliana in response to water deficit. *J Plant Res* 122(2):235-243.
238. Kuromori T, Sugimoto E, & Shinozaki K (2014) Intertissue signal transfer of abscisic acid from vascular cells to guard cells. *Plant Physiol* 164(4):1587-1592.
239. Grundy J, Stoker C, & Carre IA (2015) Circadian regulation of abiotic stress tolerance in plants. *Front Plant Sci* 6:648.
240. Covington MF, Maloof JN, Straume M, Kay SA, & Harmer SL (2008) Global transcriptome analysis reveals circadian regulation of key pathways in plant growth and development. *Genome Biol* 9(8):R130.
241. Frey A*, et al.* (2012) Epoxycarotenoid cleavage by NCED5 fine-tunes ABA accumulation and affects seed dormancy and drought tolerance with other NCED family members. *Plant J* 70(3):501-512.

242. Holalu SV & Finlayson SA (2016) The ratio of red light to far red light alters Arabidopsis axillary bud growth and abscisic acid signalling before stem auxin changes. *Journal of Experimental Botany*.
243. Raghavan C, Ong EK, Dalling MJ, & Stevenson TW (2005) Effect of herbicidal application of 2,4-dichlorophenoxyacetic acid in Arabidopsis. *Funct Integr Genomics* 5(1):4-17.
244. Kuromori T*, et al.* (2010) ABC transporter AtABCG25 is involved in abscisic acid transport and responses. *Proc Natl Acad Sci U S A* 107(5):2361-2366.
245. Kang J*, et al.* (2010) PDR-type ABC transporter mediates cellular uptake of the phytohormone abscisic acid. *Proc Natl Acad Sci U S A* 107(5):2355-2360.
246. Kanno Y*, et al.* (2012) Identification of an abscisic acid transporter by functional screening using the receptor complex as a sensor. *Proc Natl Acad Sci U S A* 109(24):9653-9658.
247. Cutler SR, Rodriguez PL, Finkelstein RR, & Abrams SR (2010) Abscisic acid: emergence of a core signaling network. *Annu Rev Plant Biol* 61:651-679.
248. Gonzalez-Guzman M*, et al.* (2012) Arabidopsis PYR/PYL/RCAR receptors play a major role in quantitative regulation of stomatal aperture and transcriptional response to abscisic acid. *Plant Cell* 24(6):2483-2496.
249. LeonKloosterziel KM*, et al.* (1996) Isolation and characterization of abscisic acid-deficient Arabidopsis mutants at two new loci. *Plant Journal* 10(4):655-661.
250. Park SY*, et al.* (2009) Abscisic acid inhibits type 2C protein phosphatases via the PYR/PYL family of START proteins. *Science* 324(5930):1068-1071.
251. Nozue K*, et al.* (2015) Shade avoidance components and pathways in adult plants revealed by phenotypic profiling. *PLoS Genet* 11(4):e1004953.
252. Glauser G, Vallat A, & Balmer D (2014) Hormone profiling. *Methods Mol Biol* 1062:597-608.
253. Kraft M, Kuglitsch R, Kwiatkowski J, Frank M, & Grossmann K (2007) Indole-3-acetic acid and auxin herbicides up-regulate 9-cis-epoxycarotenoid dioxygenase gene expression and abscisic acid accumulation in cleavers (Galium aparine): interaction with ethylene. *J Exp Bot* 58(6):1497-1503.
254. Fiorucci AS & Fankhauser C (2017) Plant Strategies for Enhancing Access to Sunlight. *Curr Biol* 27(17):R931-R940.
255. Arend D*, et al.* (2016) Quantitative monitoring of Arabidopsis thaliana growth and development using high-throughput plant phenotyping. *Sci Data* 3:160055.
256. Bours R, Muthuraman M, Bouwmeester H, & van der Krol A (2012) OSCILLATOR: A system for analysis of diurnal leaf growth using infrared photography combined with wavelet transformation. *Plant Methods* 8(1):29.
257. Dobrescu A, Scorza LCT, Tsaftaris SA, & McCormick AJ (2017) A "Do-It-Yourself" phenotyping system: measuring growth and morphology throughout the diel cycle in rosette shaped plants. *Plant Methods* 13:95.
258. Wagner L, Schmal C, Staiger D, & Danisman S (2017) The plant leaf movement analyzer (PALMA): a simple tool for the analysis of periodic cotyledon and leaf movement in Arabidopsis thaliana. *Plant Methods* 13:2.
259. Apelt F, Breuer D, Nikoloski Z, Stitt M, & Kragler F (2015) Phytotyping(4D) : a light-field imaging system for non-invasive and accurate monitoring of spatio-temporal plant growth. *Plant J* 82(4):693-706.

260. Cerrudo I*, et al.* (2017) Exploring growth-defence trade-offs in Arabidopsis: phytochrome B inactivation requires JAZ10 to suppress plant immunity but not to trigger shade-avoidance responses. *Plant Cell Environ* 40(5):635-644.
261. Gonzalez CV, Ibarra SE, Piccoli PN, Botto JF, & Boccalandro HE (2012) Phytochrome B increases drought tolerance by enhancing ABA sensitivity in Arabidopsis thaliana. *Plant Cell Environ* 35(11):1958-1968.
262. Oh E, Zhu JY, & Wang ZY (2012) Interaction between BZR1 and PIF4 integrates brassinosteroid and environmental responses. *Nat Cell Biol* 14(8):802-809.
263. Christmann A, Grill E, & Huang J (2013) Hydraulic signals in long-distance signaling. *Curr Opin Plant Biol* 16(3):293-300.
264. Nozue K, Harmer SL, & Maloof JN (2011) Genomic analysis of circadian clock-, light-, and growth-correlated genes reveals PHYTOCHROME-INTERACTING FACTOR5 as a modulator of auxin signaling in Arabidopsis. *Plant Physiol* 156(1):357-372.
265. Ye YJ*, et al.* (2017) A novel chemical inhibitor of ABA signaling targets all ABA receptors. *Plant Physiol*.
266. Park SY*, et al.* (2015) Agrochemical control of plant water use using engineered abscisic acid receptors. *Nature* 520(7548):545-548.
267. Barberon M*, et al.* (2016) Adaptation of Root Function by Nutrient-Induced Plasticity of Endodermal Differentiation. *Cell* 164(3):447-459.